

FACULTY OF AGRICULTURAL SCIENCES

Institute of Plant Production and Agroecology in the Tropics and Subtropics

University of Hohenheim

Field: Food security and coastal protection

Prof. Dr. Georg Cadisch



Modeling the influence of coastal vegetation on the 2004 tsunami wave impact

Dissertation

Submitted in fulfillment of the requirements for the degree
“Doktor der Agrarwissenschaften”
(Dr.sc.agr. / Ph.D. in Agricultural Sciences)

to the
Faculty of Agricultural Sciences

presented by:
Juan Carlos Laso Bayas
born in:
Quito, Ecuador

submitted on : June 2012

Date of oral examination:	10.04.2013
Examination committee:	
Supervisor and reviewer:	Prof. Dr. Georg Cadisch
Co-reviewer:	Prof. Dr. Torsten Müller
Additional examiner:	Prof. Dr. Joachim Müller
Vice-dean of studies and head of the committee:	Prof. Dr. Markus Rodehutscord

I confirm that the present work is my own except where indicated and that I did not use any other than the stated resources. I have completed the dissertation independently, according to the doctoral regulations of the University of Hohenheim, § 8.2.2.

Juan Carlos Laso Bayas | Stuttgart, March, 2014

Dedicated to Valentina, wherever you may be

Acknowledgements

After finishing my M. Sc. it was my goal to continue my studies and obtain a Ph.D. degree. As the time passed I realized more and more that the goal was less and less important. I realized that the important part was going through the process of becoming a trained independent researcher. I have enjoyed the journey, the places I've seen and the people I've met, and the journey has enriched my life.

First of all I thank my family, my parents Jorge and Carmen and my brother Jose Luis. Without their support and love nothing would have been possible. At the same time I want to thank my uncles and my grandparents who always supported my education, giving me the basic tools required to continue achieving my goals.

In Hohenheim I want to thank my supervisor Prof. Georg Cadisch, who has enabled me to be independent in my research and through his guiding style has encouraged me to give the best out of me. I also want to thank Dr. Carsten Marohn for his continuous support and critical appraisal of my work, Dr. Thomas Hilger for his continuous support during my studies as well as to all my colleagues at the Institute of Plant Production and Agroecology for the Tropics and Subtropics. To both I am deeply grateful.

I would not have been able to enter into the tsunami research if it would not have been for Dr. Gerd Dercon. Gerd is, simply put, an extra-ordinary man. Optimistic and dreamer, he encouraged me to aim high and not give up. For his friendship and support I will always be indebted to him.

I am very grateful to Germany its people and institutions. In particular I am grateful to the late Senator Dr. Hermann Eiselen and his legacy guided by Dr. Andrea Fadani from the Fiat Panis foundation that supported not only my M.Sc. studies but also part of my PhD research through financial contributions and prizes like the Hans H. Ruthenberg award. Germany has also supported me through the program BEAF-GIZ Small Grants that enabled most of my research in Indonesia and the Seychelles. Additionally I am grateful to the University of Hohenheim through the Institute of Bioinformatics, especially to Prof. Dr. Hans-Peter Piepho, who has not only contributed to the success of the main research but also has believed in my potential and supported the last part of my Ph.D. I am very grateful to him and all that I have learned in the process.

When I traveled to Indonesia I was expecting to find a very exotic culture, perhaps quite a shock compared to mine. I was delighted to discover, besides beautiful landscapes, the warmth of its people. In Meulaboh, Banda Aceh, Pulau Weh, Medan, Bogor, Jakarta, Yogyakarta, Bali, Lombok, it did not matter where I was, I always found nice people to whom I related very easily. It was like being in my own country! I am grateful specially to my field assistants Aulia Firdaus, Yuli Astuti, Dewi Herlita, Wahyu Ankasa and the staff at the World Agroforestry Centre, ICRAF-Bogor, ICRAF-Meulaboh and ICRAF-Chalang as well as the Alam Bahasa language school staff who contributed greatly to the research. I am very grateful to Dr. Sonya Dewi my local supervisor in Indonesia, Dr. Meine van Noordwijk, Dr. Atiek Widayati, Dr. Laxman Joshi, Betha Lusiana, Andree

Ekadinata and Ery Nugraha. All of them have shared their insights, encouragement and support and they all have provided me with lots of wisdom. I am also grateful to many people from the Center for International Forestry Research (CIFOR-Bogor) who also contributed to the research and the overall journey

In the same way, I am very grateful to the people in the Seychelles in particular to my field assistant France Sophola and all the staff of the Department of Risk and Disaster Management and the Ministry of Environment and the GIS Unit at the Ministry of Land Use and Habitat who provided me with all the facilities to carry on my research. The research there would not have been possible without the encouragement of Dr. Lucy Rist and the support of Dr. Dennis Matatiken, Dr. Christopher Kaiser and Dr. Nancy Bunbury.

I want to acknowledge also the support from the German Aerospace Center and the Pacific Disaster Center for providing satellite imagery and support; the Rehabilitation and Reconstruction Agency (BRR-Indonesia), Red Cross International and BPS-Statistics Indonesia for secondary damage information in Indonesia; the Federal Institute for Geosciences and Natural Resources, Hannover, Germany for GIS support;

A deep note of appreciation goes to the inhabitants of the populations in the study for their participation in the research and their warmth and simplicity. Perhaps is from them from who I have learned the most; more than anything else in the Ph.D. I trust that the findings can be effectively applied and be of benefit to their communities and others like them.

Thanks be given to Kefyalew Sahle for his support on my last article and to Judith Zimmerman for her translation of my summary to German.

Thanks of course have to be given to my friends and closest ones: Victor and Susanne Rueda Richt and my godchild Toa who has filled us all with light; Germán Calberto, Manuel Narjes, Scott and Anna Demyan, Daniela Núñez, Martina Keller, Tim Loos, Judith Zimmerman, Irene Chukwumah, Betha Lusiana, Juan Guillermo Cobo, Petra Schmitter and all those that I am omitting here not because of lack of care but because of lack of able neurons at this point. You know that without your support, love, friendship and all that you have given to me this would not have been possible!

Thank you my dear Hanne, for being always by my side.

Table of contents

Acknowledgements

Table of contents

List of abbreviations

CHAPTER 1 General introduction and description

1.1. The Sumatra-Andaman seaquake and its effects

1.2. Tsunami impact factors

1.3. Coastal vegetation and its disputed role on tsunami events

1.4. Building a roughness coefficient: Coastal vegetation resistance against the wave

1.5. Statistical approaches

1.6. Justification

1.7. Hypotheses

1.8. Goals and objectives

1.9. Outline of the study

CHAPTER 2 Influence of coastal vegetation on the 2004 tsunami wave impact in west Aceh

CHAPTER 3 Tsunami in the Seychelles: Assessing mitigation mechanisms

CHAPTER 4 Comparison of land cover roughness coefficients derived from different imagery sources using tsunami impact models from west Aceh, Indonesia

CHAPTER 5 General discussion

5.1. Is coastal vegetation protecting communities?

5.2. How is the effect of coastal vegetation acknowledged?

5.3. What is the effect of coastal vegetation under different tsunami intensities?

5.4. What are the most important factors influencing the damages made by a tsunami?

5.5. Do images with higher resolution and/or closest to the tsunami event provide a more accurate vegetation resistance approximation?

5.6. What are the advantages and disadvantages of the current developed approaches?

5.7. Planning effective tsunami impact mitigation measures

CHAPTER 6 References

Summary

Zusammenfassung

Resumen

Appendix A

Figure A1

Figure A2

Table A1

Table A2

Table A3

Table A4

Appendix B

Figure B1

Figure B2

Figure B3

Figure B4

List of abbreviations

A = transect Area (ha)

AIC = Akaike information criterion

CASU= casualties (%)

D = distance from the settlement to the shoreline (m)

DEM = digital elevation model

DN = vegetation immobilized sand dunes (4 categories: non existing, less than a meter high, between 1 and 2 meters high, more than 2 meters high)

DRDM = Department for risk and disaster management, Seychelles

E = elevation (m a.s.l.)

GIS = geographic Information System

GLIMMIX= generalized linear mixed models

IWH = initial water height at shoreline (m)

LCR_{B5}= weighted average land cover roughness coefficient (up to 500 m behind the settlement)

LCR_{B20} = weighted average land cover roughness coefficient (up to 20 m behind the

LCR_F = weighted average land cover roughness from the settlement to the shoreline settlement)

LCRs = land cover roughness coefficients

LCR_T = weighted average land cover roughness in the transect (up to maximum flood distance)

LS = Landsat satellite imagery (30 x 30 m resolution)

LUGR= land use green roughness

ML= maximum likelihood

MD = maximum flood distance (m)

MOE = Ministry of Environment, Seychelles

REML= restricted maximum likelihood

SP = SPOT satellite imagery (10 x 10 m resolution)

SP3+ = combination of all transects from SPOT 2003 plus additional ones from SPOT 2004

STD = structural damage (%)

T = transects (number of observations)

VR = vegetation resistance coefficient ($\text{m}^3 \text{ha}^{-1}$)

WL = seawalls (4 categories: non existing, less than a meter high, between 1 and 2 meters high, more than 2 meters high)

X^2/Df = chi square / degrees of freedom

ΣLCR = cumulative land cover roughness

CHAPTER 1. General introduction and description

The measurements and models developed after the event also revealed interesting facts regarding how a tsunami propagates. For example, wave amplitudes besides being widely dissimilar, were also not equally distributed according to their distance from the epicenter: Places like Cocos Islands, only 1700 km from the event, registered smaller tsunami amplitudes than Halifax, Nova Scotia. To put this in perspective, in order for the tsunami waves to reach there, they had to propagate west across 24.000 km on the Indian Ocean and then north across the entire length of the Atlantic Ocean (Titov *et al.* 2005). This was due to the nature the tsunami propagated across the ocean, being the seafloor topography and specially the mid-ocean ridges the factors channeling and modifying the tsunami energy (Titov *et al.* 2005) (Figure 1.1).

In terms of wave characteristics, the tsunami displayed different types of waves depending on the affected zone. While in some parts it arrived as a breaking wave (many visual examples being evident in videos taken by tourists in Thailand), in other countries such as the Seychelles, the tsunami arrived as a bore, raising the water level and flooding everything on its path (Hagan *et al.* 2007). Overall, once the tsunami was inland it became a bore crashing against different land uses and carrying their debris. This particular characteristic has made determination of its effects, especially on structures, a seemingly difficult task to model and describe (Synolakis and Bernard 2006).

Regarding tsunami recurrence, the past two centuries provided no evidence of a similar event occurring in the Indian Ocean (Dominey-Howes *et al.* 2007), but according to some studies, the predecessor of the 2004 tsunami happened around 550 to 770 years ago (Jankaew *et al.* 2008; Monecke *et al.* 2008). This meant that the forces building between the two plates (Indo-Australian and southeastern Eurasian) were steadily increasing over a large period of time, releasing consequently the huge amount of energy that the 2004 event contained, causing the destruction seen on the populations living closest to the sea.

Coastal areas in the world are home for over one sixth of the total human population being three times more densely populated than the world average (Small and Nicholls 2003). The 2004 tsunami effects were felt by many of these populations in countries located along the Indian Ocean basin. Amongst these countries, the most affected were Indonesia, Thailand, Sri Lanka and India (Menke *et al.* 2006). Nevertheless almost all the countries of the Indian Ocean basin were affected directly or indirectly, including the Maldives, the Seychelles, Somalia and Yemen (UNEP 2005).

Upon the arrival of the tsunami waves to the shore, their speed decreased and their height rose by the effect of wave shoaling. Communities close to the sea shore suffered widespread destruction, especially those closer to the epicenter. The province of Aceh, closest to the tsunami epicenter, is the clearest example: Over 150.000 people died only in this province and at least half a million lost their homes. The overall cost of the tsunami in terms of human lives was over 250.000 casualties (UNEP 2005). The well-established agricultural and tree crop systems that were the main source of income and subsistence were also affected: large parts of coconut plantations were destroyed and rubber agroforests were severely damaged, in particular at sites close to the coast line (Szcucinski *et al.* 2006). Prior to the tsunami, as much as 40-60% of peoples' income

was generated from tree crops such as coconut, rubber, coffee, cacao and oil palm (Joshi 2006) and therefore people's livelihoods were greatly dependent on them.

1.2. Tsunami impact factors

The tragic amount of casualties that the 2004 tsunami caused on coastal settlements close to the seaquake was due mainly to the lack of a warning system as well as the poor or limited knowledge existing regarding how to react in the event of an incoming tsunami. Few communities knew how to behave upon such an event. An example was the people from the island of Simeulue, 50 km away from the fault line. Here the tsunami arrived in less than 10 minutes but, despite the terrible damage to infrastructure, only 7 people died (McAdoo *et al.* 2006). Thousands were saved by the combination of two factors: existing hills and especially the oral traditions passed on by generations regarding on how to act when tsunami signs are evident (McAdoo *et al.* 2006). This was not the case for the population in Aceh where the tsunami reached also minutes after the seaquake.

In the Pacific Ocean, the existence of warning systems was triggered by the also tragic events of the 1960 Chilean tsunami that affected several areas, including Hawaii and even Japan on the opposite side of the ocean. Nevertheless, in the Indian Ocean no such system was installed. Perhaps, since no event of such magnitude was registered before, being its predecessor centuries ago (Monecke *et al.* 2008), no urgent need of such a system was seen. Also, the tsunami of 2004 was generated from a fault zone previously not thought as a possible candidate to produce such a big event (Geist *et al.* 2006) (Figure 1.2), adding this fact to the lack of preparedness.

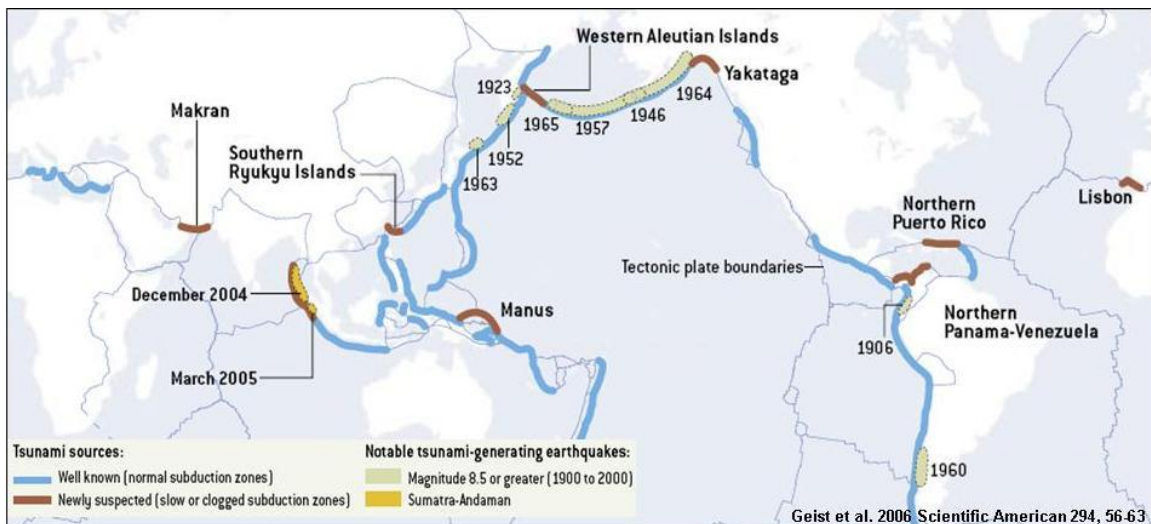


Figure 1.2. Most notable tsunamis of the past century, showing “well known” and “newly suspected” tsunami generating areas. (Adapted from Geist *et al.* 2006)

With regards to factors determining the tsunami impacts, wave energy at the shoreline is the main driving force. The intensity of the waves when they reached shoreline is determined by the seaquake magnitude, the distance from the specific shoreline to the

epicenter and the sea floor or bathymetric characteristics, including proximal slopes (Chatenoux and Peduzzi 2007). On farther sites however, much of where the tsunami waves focused was determined by sea floor characteristics, specially the existence of mid-ocean ridges (Titov *et al.* 2005). Other factors like presence of reefs and or granitic rock shelves over which several island nations were located changed the patterns of the waves by reflection and refraction (Jackson *et al.* 2005).

In general, once the tsunami is inland, the forces interacting against the advance of the wave are gravity and friction (Shuto 1987). According to this relationship, topographical changes and obstacles on the path of waves should be considered when acknowledging the possible effects a tsunami may inflict on coastal populations and their infrastructure. A consequence of this force interaction is that, due to its loss of energy as the water advances inland, the farther a community is from the shoreline, the lower the chances it will be damaged by the waves. Nevertheless, many of the coastal communities depend on their shoreline location directly, e.g. fisheries, coconut plantations or indirectly, i.e. tourism. Furthermore, it is important to consider that from those settlements that are relatively close to the shoreline, the areas that are positioned on higher grounds have an advantage compared to those located on lower lands as was the case from the island of Simeulue, mentioned before (McAdoo *et al.* 2006).

Additional factors reducing the energy of a tsunami are physical barriers. Usually, coastlines prone to strong effects of storms or more vulnerable to tsunamis, e.g. east coast of Japan, have invested strongly on these methods building seawalls and wave-breakers. These barriers reduce the energy carried by the waves creating also under normal conditions a relatively calm environment for ports and beaches. Despite this, as tragically demonstrated by the latest tsunami event of March 2011 in Japan and its effects on the Fukushima nuclear plant, sometimes not even those barriers are enough. Nevertheless, naturally occurring physical structures such as sand dunes have also been mentioned by some studies as important features reducing the impact of storms but also of tsunami waves (Chandrasekar *et al.* 2007; Kathiresan and Rajendran 2005). These barriers have usually been poorly understood and appreciated, leading in some cases to their destruction in order to obtain profit, e.g. bulldozing sand dunes in order to provide better views for a hotel (Keys *et al.* 2006).

A last but perhaps also misunderstood and sometimes misused factor influencing tsunami effects inland is coastal vegetation, becoming part of the friction opposing resistance to the advance of the water. This resistance could be exerted directly by becoming an obstacle to the water advance or indirectly by creating and/or maintaining physical barriers such as sand dunes. Nevertheless, the possible effects of coastal vegetation are still a controversial issue.

1.3. Coastal vegetation and its disputed role in tsunami events

Coastal vegetation has been a topic of intense discussion regarding its possible effects as a possible provider of mitigation against tsunami impact effects. Some proven effects of

coastal vegetation include protection against erosion, salt effects and in general stabilization of beach and slope areas (Paul and Rahman 2006; Devall 1992). Several studies advocated the protection of coastal vegetation against the effects of a tsunami given their effects reducing damages and impacts to the communities and the area affected (Danielsen *et al.* 2005; Tanaka *et al.* 2007; Olwig *et al.* 2007; Kathiresan and Rajendran 2005). Mapping assessment (Borrero *et al.* 2006) indicated that along the coastline of Sumatra (Indonesia) major changes in land cover occurred, indicating a reducing effect of the coastal vegetation on tsunami impact. Many programs were started on the affected coasts of several countries such as Indonesia leading to a planting “boom” of shelterbelts of trees along the coast line, such as the ones seen on Figure 1.3.



Figure 1.3. Coastal barriers planted on the west coast of Aceh, close to Meulaboh (Source: Prof. Georg Cadisch)

Nevertheless, this boom has been criticized by other authors (Kerr and Baird 2007; Young, 2006) who mentioned that no real proof for this mitigation effect exists and green barriers therefore may be giving a false sense of security. In general most of the studies were referring to the use of mangroves as a first line of defense against the incoming wave. Nevertheless very little or nothing had been mentioned regarding coastal vegetation that excludes mangroves but formed part of local livelihoods. It is mostly this type of vegetation that became the main focus of the present Ph.D. study. Forests and tree based crops such as rubber plantations as well as agro-forestry systems that included fruit producing perennial species (e.g. coffee and mango) and annual crops (e.g. corn and vegetables) but also grasslands and paddy rice production were all land uses included in the study. Additionally, on places like the Seychelles, species found on beach berms and dunes such as Vouloutye (*Scaevola sericea*), beach morning glories/Patatan (*Ipomoea pes-caprae*) and Bwa Matlo (*Suriana maritima*) were considered due to effects retaining sand and maintaining dunes as coastal protection.

1.4. Building a roughness coefficient: Coastal vegetation resistance against the wave

Shuto (1987) stated that the resistance offered to the advance of a wave was based on two forces: Gravity and friction. In the present study, transects from the shoreline up the maximum flooded area were used in order to extract land cover and topography. Digital elevation models were used to extract topographical data (elevation above sea level),

representing gravity and land cover maps from before the tsunami were used as the base from which to extract resistance by friction. Nevertheless, since these land uses were very diverse, a unique way of transforming their resistance against the wave had to be developed.

The previously existing approaches used a multi factorial mechanistic approach, which was usually quite precise but highly data demanding (Latief *et al.* 2007; Freeman *et al.* 2000; Järvelä 2004). Mostly, these approaches consist on determining several drag coefficients and mainly rely on the determination of the Manning's n coefficient. A simplified approach (Järvelä 2004) requires the determination of segments on the analyzed trees or vegetation as well as average diameters for each segment, although the research applies only to floodplains and with partially submerged vegetation.

Flow resistance of shrubs and other types of plants such as woody vegetation was described by Freeman *et al.* (2000). The authors employed models considering parameters such as the Darcy Weisbach friction factor, drag force, Chezy resistance coefficient, and Manning's n resistance coefficient. The models were deemed as quite accurate in terms of representing all the forces interacting on an incoming flood but also highly demanding on data and processing time. Additionally these were not used on tsunami events but mainly on lab experiments and flood events.

For the current research a combination of field measured plant characteristics, i.e. stand height, stems diameter, and planting density was required in order to relate coastal vegetation and resistance against incoming forces. Peltola *et al.* (2000) stated that the combination of tree trunks height and their diameter was highly correlated to their modulus of elasticity, a measurement of resistance against a pulling/pushing force. The approach was adapted to a landscape level by multiplying this coefficient with the planting density of the vegetation being considered.

1.5. Statistical approaches

Tsunami studies trying to relate impacts to coastal vegetation have usually been criticized due to the procedures applied to analyze the data. Some of the studies employed usually univariate methods (Kathiresan and Rajendran 2005) or did not control for the spatial proximity of analytical units or distance to the shoreline (Das and Vincent 2009). Also some studies did not include important factors like topography (Danielsen *et al.* 2005). Several critics have mentioned these facts (Kerr and Baird 2007; Young 2006; Baird and Kerr 2008; Baird *et al.* 2009) and have suggested the use of multivariate models that acknowledge the factors affecting a tsunami impact and their spatial interaction.

For data collected from the coastline, e.g. through the use of semi-structures interviews, several characteristics should be considered: Indications of a linearity or non-linear tendency of the data; the use of percentages or derived from counts may result in data distributions that do not follow normality or present different distributions, e.g. binomial response. Additionally, given the nature of how the data is collected, e.g. transects laid alongside each other, spatial autocorrelation has to be considered.

One of the approaches considered and finally employed for the current models in the present study was the use of Generalized Linear Mixed Models (GLIMMIX). Being an “expanded” family of the mixed models, the procedure allows the fitting of fixed and random effects, i.e. in this case direct predictors of damage plus effects that are part of the variance of the overall model. A generalized procedure means that it can fit several families of distributions for the variable that is being predicted. Through the use of random factors, these models allow for the fitting of variance-covariance matrices of different types, including those that can acknowledge lack of independence between observations. This means the procedure can produce linear models acknowledging serial correlations (time) but also spatial autocorrelation existing between observational units close to each other (Schabenberger 2005). In order to check for the acknowledgment of such spatial autocorrelations, empirical semi-variograms can be used. These could be plotted after each model in order to test possible remaining spatial auto-correlation. In the current study these techniques provided a good frame to acknowledge the spatial location of the study units. Given that the observational units were close to each other, i.e. side by side transects along the coastline, spatial autocorrelation amongst observations close to each other is higher than between those farther.

As mentioned, GLIMMIX works with data presenting different types of frequency distribution, including data showing a binomial distribution. This type of distribution of the predicted variable is entered through the use of the logit link function. The results of these models provide an output that measures the probability of occurrence of the desired variable. In the current study the structural damage model results used this framework. Maximum flood distance and casualties’ relationships were modeled under standard regression assumptions of normality, therefore using the normal link function.

An additional feature of GLIMMIX is the use of the Akaike Information Criterion (AIC) as discriminator for model selection (Burnham and Anderson 2002). Models using AIC as a measure of goodness of fit were selected using the Maximum Likelihood technique. In order to discriminate, δAIC larger than 2 points was the benchmark to measure a better fitted model. For binomial models, e.g. structural damage, the one closest to a value of 1 on the indicator chi squared over degrees of freedom (X^2/DF) can be chosen as a better model.

1.6. Justification

The damages caused by the tsunami event of December 2004 were felt in several countries across the Indian Ocean. Many of the survivors of the catastrophe provided information regarding people that were saved by trees, or were behind an area protected by coastal vegetation hence their survival. These stories were quickly spread and initial studies regarding the possible effects of coastal vegetation protecting from an incoming tsunami were developed.

Some of these studies argued for the protective role of different types of coastal vegetation, being mangrove the most common, decreasing the impact the tsunami had on local communities (Danielsen *et al.* 2005; Tanaka *et al.* 2007; Olwig *et al.* 2007; Kathiresan and Rajendran 2005; Latief *et al.* 2007). Soon after the tsunami, afforestation programs were developed and executed in order to establish “green belts” protecting vulnerable coastal areas and populations against future natural events.

In the meantime, other authors argued that the studies supporting the establishment of such plantations had no empirical evidence to support these “protective” claims. These studies mentioned that the relationships and analysis on which these conclusions were based excluded some important parameters or confounded factors (Baird and Kerr 2008; Young 2006; Baird *et al.* 2009). These authors argued that such plantations could be dangerous by providing a false sense of security.

Most of the studies developed analyzed the suitability or not of mangrove forests to protect the affected areas (Baird *et al.* 2009; Kathiresan and Rajendran 2005) but local vegetation existing between settlements and the seashore were not considered. Additionally, some of the survivors from the 2004 event reported that coarse vegetation types behind their settlements and the debris formed by these hampered their escape. Overall the effects of coastal vegetation remained a controversial topic (Iverson and Prasad 2007a; Kaplan *et al.* 2009).

In order to understand what possible effects coastal vegetation might have exerted over the damages inflicted by the tsunami event of 2004, parts of the west coast of Aceh were selected as the initial research area. This area was one of the closest to the seaquake epicenter receiving what was probably the largest tsunami impact. The selected study area presented a mostly regular coastline, with towns along the coast connected to each other through the “national road”. Given the regular geomorphology of this area, the road ran basically parallel along the shoreline, one of the reasons why after the event it was completely obliterated. Few ruins of this road and the small towns along the coast remain on the most affected areas (Fig 1.4). Under this scenario, we tested the effects of coastal vegetation on the affected area along more than 100 km of coastline. Additionally, in order to understand the effects of coastal vegetation on sites with a lower tsunami impact, the Seychelles archipelago was selected as a second area of interest; more specifically, the coasts of the islands Mahé, Praslin and La Digue were analyzed. On the Seychelles, the tsunami arrived not as breaking wave but more as bore (Jackson *et al.* 2005), raising its level and pushing everything on its path, destroying infrastructure in the process. The Seychelles case provided a good scenario to test direct as well as indirect effects of vegetation seen by the formation and maintenance of sand dunes. Additionally, many parts of these islands included seawalls, sturdy barriers fulfilling a defensive role usually against high tides or simply protecting areas of land gained to the sea.



Figure 1.4. Damages to the coastal “national” road. Above: leftover asphalt and lacking bridge. Below: Road ends on a broken bridge over what before used to be a creek of small watery area. Close to the previously existing villages of Suak Ulue and Suak Sireen (Source: author).

In order to develop a vegetation resistance coefficient, land cover from before the tsunami event had to be determined. In the case of Aceh, the source for this were land cover maps based on mid resolution remote sensing imagery (Landsat® 2002, 30 m resolution). In the Seychelles, visual determination using Google Earth® high resolution imagery from 2004 as well as on site verification and comparison against old pictures from many sites were the methods used in order to determine and extract the land cover existing when the tsunami occurred. An additional attempt to improve the accuracy of the land cover maps for Aceh was done via the classification and extraction of land cover from higher resolution images, i.e. SPOT® 2003 and 2004 as well as from mid resolution imagery closer to the tsunami event, i.e. Landsat® 2003 and 2004. In this case, the hypothesis behind the use of these new land cover maps was that pictures closer to the event and/or coming from higher resolution satellite imagery should provide a more vegetation resistance coefficient and therefore provide a more accurate model linking the effect of coastal vegetation regarding the tsunami event of 2004.

1.7. Hypotheses

The main hypotheses analyzed on the study are:

Coastal vegetation reduced tsunami inland damages caused by the 2004 event, i.e. structural damage, casualties and maximum flood distance.

Coastal vegetation provides more protection in a high intensity area, i.e. west coast of Aceh, versus a low intensity area, i.e. Seychelles

Vegetation resistance coefficients obtained through the use of satellite imagery acquired on a date closer to the tsunami event and/or from a higher resolution sensor provide improved resistance coefficients, therefore improving the overall fit of the tsunami mitigation models.

1.8. Goals and objectives

The present study analyzed data collected from different field locations using multivariate spatially acknowledging statistical methods in order to determine the factors that may have affected the outcome of the 2004 tsunami with regards to its effects inland, i.e. structural damage, casualties and maximum flood distance. Of particular interest for the study was coastal vegetation, in order to determine if there was any measurable effect with regards to these damages. The study tried to allocate a proportional combined resistance factor based on field measurable factors, i.e. stem diameter, stem height and planting density.

The goal of the study was to determine and fine tune the possible effects that coastal vegetation might have had on the tsunami event of 2004 in two scenarios, i.e. on 100 km over the west coast of Aceh as well as in three islands from the Seychelles archipelago. Specific objectives included:

To develop a land cover roughness coefficient representing the proportional resistance that different types of vegetation may offer against an incoming force, e.g. a tsunami wave.

To incorporate the land cover roughness coefficient, the effect of topography, as well as other factors such as the initial tsunami strength and the distance of a settlement to the shoreline in a statistical model, acknowledging possible spatial autocorrelation issues through a spatial variance-covariance matrix.

To test the developed models using field collected data from two sites, i.e. Aceh (high intensity event) and Seychelles (low intensity event) in order to determine the factors affecting the tsunami damages inland.

To test the models developed for the case of Aceh through the use of vegetation resistance coefficients obtained from imagery acquired on a date closer to the tsunami event and/or from a higher resolution sensor.

1.9. Outline of the study

The study is based on a paper published in a high impact journal (Laso Bayas *et al.* 2011, PNAS) shown on Chapter 2, and two additional submitted papers (Chapters 3 and 4). Chapter 1 gives an overview of the thesis introducing the tsunami event of 2004 and its effects as well as the controversy regarding the effects of coastal vegetation on such event and the development of models capable of considering all factors affecting the tsunami effects inland in an spatially acknowledging manner. Chapter 2 analyzes data collected in west Aceh and develops a model explaining the effects of coastal vegetation on tsunami damages. Chapter 3 applies and adapts the previously developed model on a low intensity tsunami scenario, describing also possible indirect effects of coastal vegetation in the 2004 tsunami event in the Seychelles. Chapter 4 attempts to fine tune the models developed for the case of Aceh by obtaining vegetation resistance coefficients from satellite imagery acquired on dates closer to the tsunami event and/or from a higher resolution sensor. The thesis continues in Chapter 5 with an overall discussion of the models, the scenarios tested and the attempts of model improvement as well as practical recommendations. Chapter 6 is the references section. Summaries in English, German and Spanish are included as well as additional information as appendices.

**CHAPTER 2. Influence of coastal vegetation on the 2004 tsunami wave
impact in west Aceh**

Chapter 2. Influence of coastal vegetation on the 2004 tsunami wave impact in West Aceh¹

Juan Carlos Laso Bayas¹, Carsten Marohn¹, Gerd Dercon^{1†}, Sonya Dewi², Hans P. Piepho³, Laxman Joshi², Meine van Noordwijk², Georg Cadisch¹

¹ *Institute of Plant Production and Agroecology in the Tropics and Subtropics, University of Hohenheim, 70593 Stuttgart, Germany*

² *World Agroforestry Centre (ICRAF), Southeast Asia Regional Program, P.O. Box 161, Bogor 16001, Indonesia*

³ *Institute of Crop Science, University of Hohenheim, 70593 Stuttgart, Germany*

[†] *Current address: The Joint FAO/IAEA Division of Nuclear Techniques in Food and Agriculture, Department of Nuclear Sciences and Applications, International Atomic Energy Agency, Wagramerstrasse 5, 1400 Vienna, Austria*

2.1. Abstract

In a tsunami event human casualties and infrastructure damage are determined predominantly by seaquake intensity and offshore properties. On land, wave energy is attenuated by gravitation (elevation) and friction (land cover). Tree belts have been promoted as ‘bio-shields’ against wave impact. However, given the lack of quantitative evidence of their performance in such extreme events, tree belts have been criticized for creating a false sense of security. This study used 180 transects perpendicular to over 100 km on the west coast of Aceh, Indonesia to analyze the influence of coastal vegetation, particularly cultivated trees, on the impact of the 2004 tsunami. Satellite imagery, land cover maps, land use characteristics, stem diameter, height, and planting density, and a literature review were used to develop a land cover roughness coefficient accounting for the resistance offered by different land uses to the wave advance. Applying a spatial generalized linear mixed model, we found that while distance to coast was the dominant determinant of impact (casualties and infrastructure damage), the existing coastal vegetation in front of settlements also significantly reduced casualties by an average of 5%. In contrast, dense vegetation behind villages endangered human lives and increased structural damage. Debris carried by the backwash may have contributed to these dissimilar effects of land cover. For sustainable and effective coastal risk management, location of settlements is essential while the protective potential of coastal vegetation, as determined by its spatial arrangement, should be regarded as an important livelihood provider rather than just as a bio-shield.

2.2. Keywords

Glimmix, tsunami mitigation, vegetation effects, food security

¹ **A version of this chapter is published as:**

Laso Bayas, J.C., Marohn, C., Dercon, G., Dewi, S., Piepho, H.P., Joshi, L., van Noordwijk, M., Cadisch, G., 2011. Influence of coastal vegetation on the 2004 tsunami wave impact in west Aceh. *Proceedings of the National Academy of Sciences, USA* 108, 18612-18617. The original publication is available at <http://www.pnas.org/content/108/46/18612.full>.

2.3. Introduction

On December 26, 2004, a rupture in the fault line between the Indo-Australian and southeastern Eurasian tectonic plates 150 km off the coast of West Aceh, Indonesia, triggered one of the largest seismic events in the last four decades (Stein and Okal 2005). The seaquake generated a tsunami with disastrous consequences in the region.

Soon after the 2004 event, the possible effects of coastal vegetation regarding the impact caused by tsunamis (mitigating or aggravating) was researched, especially under scenarios with initial water heights below 10 m (Danielsen *et al.* 2005; Tanaka *et al.* 2007; Olwig *et al.* 2007; Kathiresan and Rajendran 2005). In Sri Lanka and India, coastal communities located behind tree cover were reported to be less affected than those directly exposed to the sea (Danielsen *et al.* 2005; Tanaka *et al.* 2007; Latief *et al.* 2007). Parameters such as stem diameter and height as well as a 'bio-shield' width were identified as key vegetation characteristics with a bearing on impact mitigation (Latief *et al.* 2007). However, several studies advocating bio-shields have been criticized for lacking empirical evidence to support the protective function of vegetation, some even suggesting that bio-shields may give a false sense of security to coastal populations (Kerr and Baird 2007; Baird *et al.* 2009; Baird and Kerr 2008; Young 2006). The role of vegetation in tsunami impact mitigation still remains a controversial issue (Geist *et al.* 2006; Iverson and Prasad 2007a; Kaplan *et al.* 2009). In the coastal regions of western Aceh in 2004, the potential for mitigating tsunami impacts appeared limited as a result of the massive energy released by waves with heights exceeding 20 m (Geist *et al.* 2006). Mangroves along this coastline were naturally scarce since this is a high energy coastline in contrast to locations in Thailand and Sri Lanka. Dense natural vegetation had been replaced by cultivated (tree and annual) crops, being rubber agroforests the most forest-like. Nevertheless, soon after the tsunami, afforestation programmes were launched to reduce the impact of possible future tsunami flood events (Iverson and Prasad 2007b). Many of these plans overlooked local needs and acceptance of such solutions, therefore compromising their future maintenance.

This study assessed the effectiveness of coastal vegetation in mitigating the wave impact caused by the tsunami event of 2004 in part of the west coast of Aceh. The role of vegetation behind villages, which had been previously reported as relevant by local informants, was particularly considered.

2.4. General description of the study

The intensity of damage caused by a tsunami depends not only on the strength of the seaquake and offshore properties but also on landscape characteristics such as coastal geomorphology, topography, and land cover (Kurian *et al.* 2006, Chada *et al.* 2005). Once a tsunami wave-train arrives inland, its energy is dissipated by gravitational forces and friction (Shuto 1987). The remaining wave energy determines the effects experienced inland, i.e., maximum flood distance, human casualties and structural damage to buildings. Therefore, the utility of initial water height at shoreline (as proxy for wave

energy), elevation at point of impact (gravity) and land cover roughness (including vegetation friction) (Danielsen *et al.* 2005; Dahdouh-Guebas *et al.* 2005) as predictors of inland damage was assessed using spatially explicit statistical models.

On the west coast of Aceh sample sites were identified using satellite imagery (Fig. 2.1). Differences in observed initial water height pointed to offshore factors affecting the wave energy arriving at the shore. Consequently, initial water height at the shoreline (IWH), was used to represent initial wave energy. Topography was represented by elevation (E); the area is a relatively homogeneous coastal plain with gentle slopes between 0.2 and 4.5%. Information on IWH, land cover changes and damage indicators was collected on site during interviews with over 200 groups of eye witnesses, a literature review, and from satellite images (details see Methods). Such data was correspondingly allocated to each of the 180 transects perpendicular to the coastline, used as study units. The different land covers present in the transects were afterwards transformed to a vegetation resistance index, i.e. land over roughness (LCR).

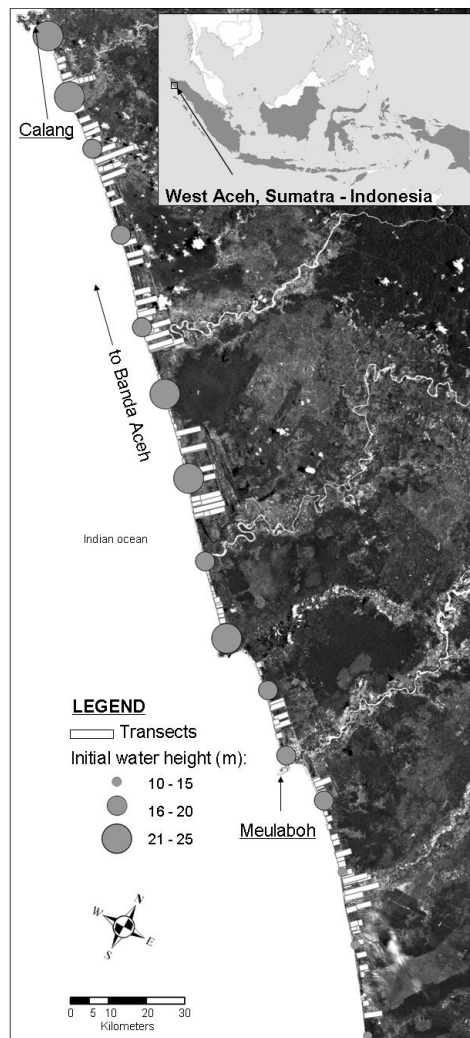


Figure 2.1. Study area: transects and initial water height along the coast (Landsat® ETM).

Multi-factorial approaches describing resistance of vegetation to a flow (Latief *et al.* 2007; Freeman *et al.* 2000; Järvelä 2004) are usually highly data demanding. Consequently, a set of characteristics were identified which were not only comparatively easy to quantify on site but also able to sufficiently represent the resistance of specific land uses. The maximum bending moment, a measure of resistance, is highly correlated with tree height, diameter at breast height, and with the material specific ‘Modulus of Elasticity’ (Peltola *et al.* 2000). Empirically, the main force that different types of trees (vegetation) oppose to water mass flows could therefore be approximated by combining information on stem diameter and stand height. By including planting density, the vegetation resistance coefficient (VR in m³ ha⁻¹) at stand level can be defined as:

$$VR = H \times SD^2 \times d \quad , \quad (2.1)$$

where H= vegetation height (m), SD= stem diameter at breast height (trees) or at ground level (non-tree vegetation) (m) and d= planting density (number of individuals per area).

Height, stem diameter and planting density were measured in the field on corresponding land uses of comparable age class and characteristics as the ones affected by the tsunami (details see Methods).

The sum of vegetation resistance coefficients per land use type multiplied by their respective area in each transect (Fig. 2.1) i.e. the cumulative land cover roughness ($\sum LCR$, in m³) was then calculated as:

$$\sum LCR = VR_1 \times A_1 + VR_2 \times A_2 + \dots + VR_n \times A_n \quad , \quad (2.2)$$

where VR_(1→n)= specific resistance coefficient for any given land use (m³ ha⁻¹), A_(1→n)= area (ha) covered by the respective land use in a transect.

$\sum LCR$ includes distance and because distance from the shoreline has commonly been reported to influence tsunami impacts, land cover roughness was normalized by division over total transect area. The resulting weighted average land cover roughness coefficient (LCR) was used for all models:

$$LCR = [VR_1 \times A_1 + VR_2 \times A_2 + \dots + VR_n \times A_n] \times A_T^{-1} \quad , \quad (2.3)$$

where A_T= total transect area.

A description of land cover types identified in the study area as well as their respective coefficients is given in Table 2.1. Community members reported that the vegetation directly behind a settlement influenced the tsunami impact they experienced. Thus, land cover roughness of the first 500 m behind the settlement was evaluated and added as a further predictor (LCR_{B5}) in the impact models (Eq. 2.5 and 2.6).

Table 2.1. Land cover types, area covered in the study transects, estimated planting densities and vegetation resistance coefficients (VR), west coast of Aceh (from Calang to south of Meulaboh). (Obtained from Landsat® ETM 2002 land cover classification). Ordered by VR.

Land-cover type	Area covered (%)	Estimated planting density (stems ha ⁻¹)	VR (m ³ ha ⁻¹)*
Cleared land: Areas with no vegetation	0.63	0	0
River: Water areas including ponds and estuaries	3.33	0	0
Agriculture: Various crops, mostly vegetable plantations	0.03	31,250	13
Grass: Grasses growing on previously cleared areas or used for animal feed e.g. <i>Imperata spp.</i>	8.34	2,000,000	15
Rice field: Plantations of <i>Oriza sativa</i> , usually paddies	19.04	2,000,000	15
Shrub: Natural vegetation of 1 to 2 m height	0.01	4,445	150
Cocoa: Plantations of <i>Theobroma cacao</i>	1.99	1,111	156
Coconut: Plantations of <i>Cocos nucifera</i>	20.46	156	281
Oil palm: Plantations of <i>Elaeis guineensis</i>	4.45	156	366
Agroforest: Combination of different plant species with canopies at various levels e.g. mango (<i>Mangifera indica</i>), coffee (<i>Coffea arabica</i>), sugar cane (<i>Saccharum spp.</i>) and vegetables	6.34	625	844
Rubber: <i>Hevea brasiliensis</i> , mostly extensive jungle rubber	16.72	494	1,343
Forest: Local timber and non timber species on protected and non-protected areas	0.24	494	2,099
Settlements	17.11	N/A	3,538 [†]

Note: Around 1% of the area was non-identifiable on satellite imagery (classified either as cloud, shadow or no data).

* ‘m³ ha⁻¹’ refers to volume of plants (stems) resisting the force of water advancing per hectare. See Eq. (2.4) and (2.5).

[†] For the land-cover ‘settlements’ values of Modulus of Elasticity (MOE) of wood, concrete and grasses reported in several studies (Peltola *et al.* 2000; Chan *et al.* 1999; Oladokun 2006; Toledo and Rincón 1997; Tomosawa and Noguchi 1993; Boen 2006) were compared. A ‘VR’ value was then derived based on the transformed values for concrete Compressive Strength (CE) of the buildings in Aceh. Before the tsunami, buildings in Aceh had a CE of around 10 to 12.5 MPa (Boen 2006) (MOE ~ 17 GPa). In practical terms this meant buildings in Aceh were offering a resistance to the flow of roughly 1.7 times higher than forests.

Distribution of structural damage data was non-homogenous, i.e. mainly split into two categories: ‘destroyed’ or ‘not significantly affected’ (Fig. A2-C). Therefore, all values bigger than ‘0’ were transformed to 1, creating a binomial response variable ‘STDB’. Additionally, values of the predicted variable CASU and MD were transformed from a scale of 0 to 100 to a scale of 0 to 1 (CASU01 and MD01, respectively). Finally, all predictors in each model were standardized to mean 0 and variance 1. Therefore, the three tsunami impact models, each using a total of 180 observations, were:

$$MD01 = f(IWH-s, E_{T-s}, \sum LCR_{T-s}) \quad , \quad (2.4)$$

$$CASU01 = f(IWH-s, D-s, E_{F-s}, LCR_{F-s}, LCR_{B5-s}) \quad , \quad (2.5)$$

and

$$STDB = f(IWH-s, D-s, E_{F-s}, LCR_{F-s}, LCR_{B5-s}) \quad , \quad (2.6)$$

where suffix -s= standardized, MD01= maximum flood distance (0 to 1), CASU01= casualties (0 to 1), STDB= structural damage (binomial), IWH-s= initial water height at shoreline (m), E_T -s= maximum elevation over the whole transect (m a.s.l.), $\sum LCR_T$ -s= cumulative land cover roughness in the transect up to the maximum flood distance, D-s= distance from the settlement to the shoreline (m), E_F -s= maximum elevation at the settlement level (m a.s.l.), LCR_F -s= weighted average land cover roughness from the settlement to the shoreline and LCR_{B5} -s= weighted average land cover roughness from the settlement up to 500 m behind.

Variables description and summary statistics are shown in Table 2.2 and a schematic representation of model parameters can be seen in Fig. 2.2.

Table 2.2. Variables (not transformed) used in the models and their descriptive statistics. N=180.

Variable	Mean	Std Dev.	Min.	Max.
MD - Maximum flood distance (m)	2250	850	950	4450
STD - Structural damage (%)	78	39	0	100
CASU - Casualties (%)	34	31	0	95
IWH - Initial water height at shoreline (m)	20	5	10	25
D - Distance from the shoreline to the settlement (m)	1200	950	50	4400
E_F - Maximum elevation in front of the settlement (m a.s.l.)	14	5	6	47
E_T - Maximum elevation over the whole transect (m a.s.l.)	19	8	12	74
LCR_F - Weighted average land cover roughness in front of the settlement	1165	640	71	3538
LCR_{B5} - Weighted average land cover roughness from the settlement up to 500 m behind	914	694	0	3444
LCR_T - Weighted average land cover roughness in the transect	987	311	141	1899

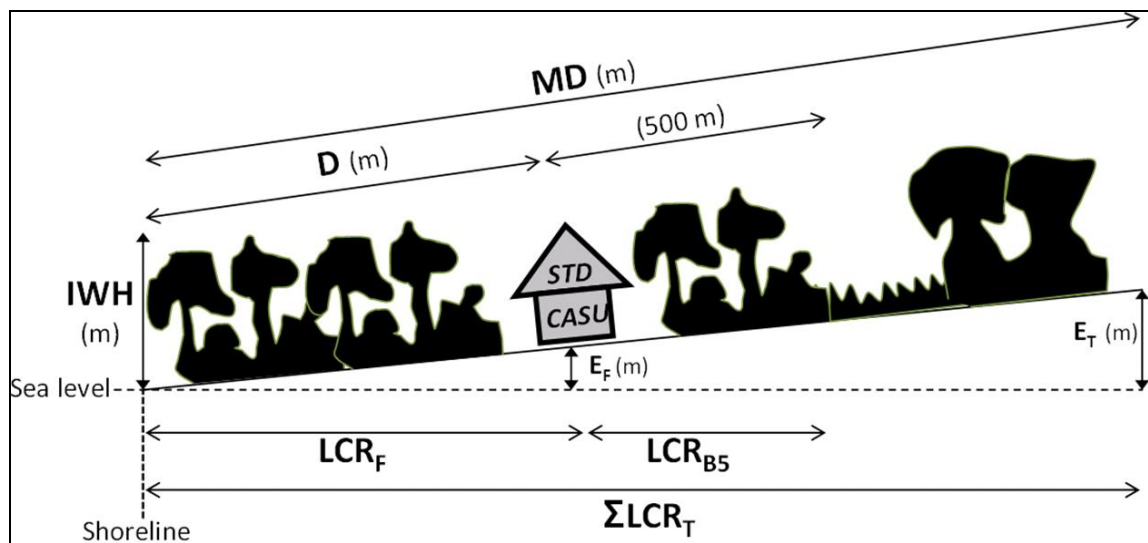


Figure 2.2. Schematic transect showing the variables used in the models. MD = maximum flood distance (m), CASU = casualties (%), STD = structural damage (%), IWH = initial water height (m), D = distance from the shoreline to the settlement (m) E_T = maximum elevation over the whole transect (m a.s.l.), E_F = maximum elevation at the

settlement level (m a.s.l.), LCR_T = weighted average land cover roughness in the transect (up to the maximum flood distance), LCR_F = weighted average land cover roughness in front of the settlement and LCR_{B5} = weighted average land cover roughness from the settlement up to 500 m behind.

Data were expected to be spatially correlated because of dense sampling along the coastline. Also, some response variables violated the usual assumptions of normality and homoscedasticity (See appendix A, Figs. A1-B and A1-C). In order to account for these factors, we fitted spatial Generalized Linear Mixed Models (GLMM) by maximum and pseudo-likelihood methods (Schabenberger 2005). The Akaike Information Criterion (AIC) was used as a measure of goodness of fit for the maximum flood distance and casualty models. In the binomial GLMM for structural damage, Pearson's chi-squared statistic divided by the degrees of freedom was used as a measure of model fit. Pearson residuals from spatial GLMMs for structural damage, casualties, and maximum flood distance were checked for remaining spatial dependencies. Moran's test I ($I=0.02$; Z score = 0.1) and empirical semivariograms (Appendix A, Fig. A2) showed no indication of such spatial relationships.

2.5. Methods

Maximum flood distance (m), casualties (%), and structural damage (%) were used as proxies for tsunami energy and tsunami damage indicators. Impact data were collected in the districts of Aceh Barat, Nagan Raya, and Aceh Jaya, along more than 110 km of shoreline south of the city of Calang. Settlements where damage was registered were georeferenced. Semi-structured interviews in 49 coastal communities were carried out to gather primary information on damage indicators and land cover changes. Structural damage was calculated from the number of buildings left standing after the tsunami. Maximum water height was determined by measuring references mentioned during the interviews (e.g. houses, palm trees or overland electricity lines) with a clinometer.

To assign pre-tsunami plant parameters of different land uses, vegetation density, stem diameter (at breast height for tree-type vegetation or ground level for smaller types), and height were measured using a clinometer and measuring tape and then averaged for each land use type. The assessment was done in 2008/9 on corresponding plots adjacent to the tsunami affected zone. Two high resolution pre-tsunami images (Quick Bird®, 2.5m) were compared to post-tsunami imagery in order to identify similar land uses inside and adjacent to tsunami affected areas. According to interviews and satellite imagery, the plantation techniques and designs for major tree crops as well as food crops followed a standard pattern in the investigated region. Additionally, for the tree crops such as coconut and rubber, plant parameters were measured on 0.5 ha plots for each land cover type with comparable age classes as before the tsunami. A transect across each plot was used and all trees in at least 2 subplots of 10x10 m were measured and averaged. Pre-tsunami land cover classification of the area was based on a 2002 Landsat® imagery and identified 13 types of land use. The area was covered by a mosaic of tree-crop plantations, agroforests (home gardens), and rice fields. Approximately half of the study

area was covered by trees including coconut (20%), rubber (17%), agroforests and forests (7%) and oil palm plantations (6%) (Table 2.1).

The initial impact data were collected in 2007 (24 communities, approximately 60 km of shoreline) and expanded following the same methodology during a second campaign (25 communities, over 50 km of shoreline) in 2008. Post-tsunami satellite imagery (Quickbird® 5 m resolution, 2004) and data from different agencies were used to cross-check field information. Navigation charts were used to visually verify homogeneity of coastal geomorphology and factors such as absence of reefs. Similar near-shore bathymetrical variability along the studied coast was also observed. For each observation point where damage indicators were determined in a village, transects 550 m wide extending from the shoreline through the settlement location to the maximum flooded area were superimposed (Fig. 1.1). Measurements of distance to the shoreline, elevation (Digital Elevation Model – Shuttle Radar Topographic Mission <http://www2.jpl.nasa.gov/srtm/>) and land cover friction coefficients in front of and behind settlements were allocated to these transects (N=180).

Generalized linear mixed models allowed fitting the spatial autocorrelation of observations distributed along the coastline. The coordinates of each observation were used to fit a spatial variance-covariance model across all observations using a spherical covariance structure for all the models. The procedure was also run as a logit link/binomial and an identity link/normal model for binary and quantitative responses, respectively. Spatial covariance was entered via a random effect in the linear predictor (Schabenberger 2005).

The normal model was fitted using Maximum Likelihood (ML) in order to compare models of the same dependent variable with different fixed effects by AIC (Burnham and Anderson 2002). Models explaining the respective damage indicators were defined by equations (2.4), (2.5) and (2.6). Explanatory variables considered were: initial water height (IWH) representing initial tsunami magnitude and energy at shoreline given by offshore characteristics; elevation above sea level (E) representing gravity and weighted average land cover roughness coefficient (LCR) representing wave resistance by vegetation. Distance from the settlement to the shoreline (D) was entered as an additional predictor to test for the effects correlated to other predictors where LCR_F and LCR_{B5} were used.

Response variables representing the damage caused by the waves were casualties (CASU), structural damage (STD), and maximum flood distance (MD). A stepwise procedure was used to test the improvement of the model by sequentially introducing the terms LCR_F and LCR_{B5} in the corresponding models (Appendix A, Tables A1-A2). Final equations are shown in Table 2.3. Comparison of different model approaches showed that the fit of individual (single) predictor models (Appendix A, Tables A3-A4) was poorer than that for models including all variables (Table 2.3). Pearson pairwise correlation tests run amongst all predictors yielded only weak correlations.

Normality of the residuals for the casualties and maximum flood distance models was checked using q-q plots. GIS and statistical analyses were carried out using a combination of the packages Open Jump 1.2, ArcGIS 9.2, ArcView 3.2, SAS 9.2 (PROC GLIMMIX) and Sigmaplot 10.0. Data was collected and geo-referenced in the field with a GPS Garmin® GPSMAP 76CSx.

Table 2.3. Selected models for maximum flood distance (MD), casualties (CASU) and structural damage (STD) showing standardized regression coefficients and their corresponding p values. Generalized linear mixed model using a spatial variance-covariance model fitted by a random term. Estimation technique for ‘MD’ and ‘CASU’: Maximum Likelihood (ML). Estimation technique for ‘STD’: Pseudo Likelihood (PL). N=180.

Model	Intercept	IWH-s	E _T -s	E _F -s	D-s	LCR _T -s	LCR _F -s	LCR _{B5} -s	AIC*	X ² /Df [†]
MD	0.53 ± 0.05 ($p<0.001$)	0.62 ± 0.31 ($p=0.044$)	-0.32 ± 0.09 ($p=0.001$)			0.06 ± 0.06 ($p=0.351$)			-503.0	
CASU	0.38 ± 0.04 ($p<0.001$)	1.14 ± 0.46 ($p=0.018$)		-0.19 ± 0.21 ($p=0.368$)	-2.40 ± 0.36 ($p<0.001$)		-0.38 ± 0.21 ($p=0.067$)	0.28 ± 0.17 ($p=0.101$)	-117.3	
STD	2.66 ± 0.41 ($p<0.001$)	3.45 ± 3.73 ($p=0.358$)		-4.95 ± 3.35 ($p=0.143$)	-22.42 ± 4.40 ($p<0.001$)		0.13 ± 5.14 ($p=0.981$)	6.90 ± 3.62 ($p=0.061$)		1.07

Notes: Independent variables used in the models were standardized (suffix ‘-s’) to variance=1, mean=0.

IWH-s = initial water height (standardized), **E_T-s** = maximum elevation over the whole transect (standardized), **E_F-s** = maximum elevation at the settlement level (standardized), **D-s** = distance from the shoreline to the settlement (standardized), **LCR_T-s** = weighted average land cover roughness in the transect (up to the maximum flood distance) (standardized), **LCR_F-s** = weighted average land cover roughness in front of the settlement (standardized) and **LCR_{B5}-s** = weighted average land cover roughness from the settlement up to 500 m behind (standardized).

*= Akaike Information Criterion †= Chi square / degrees of freedom

2.5. Results and Discussion

The developed models (Table 2.3) revealed that distance from the shoreline to the settlement (D) was the main factor significantly reducing the number of casualties and structural damage ($p<0.001$). Nevertheless, vegetation in front of the settlement (LCR_F), and particularly vegetation with a high land cover roughness coefficient, (Table 2.1) also significantly helped to reduce fatalities ($p=0.067$). Estimates, based on our casualty model (Table 2.3) with local land cover conditions (Table 2.1), suggested that having a forest in front of a settlement would have resulted in an average 8% reduction of casualties whereas rubber plantations and agroforestry would have reduced casualties by 5% and 3%, respectively. In contrast, thick vegetation behind settlements (LCR_{B5}) resulted in adverse effects, increasing structural damage ($p=0.061$) as well as casualties ($p=0.101$). Corresponding model estimates suggest that casualties increased on average

by 3% given the mean LCR_{B5} observed in the study (Table 2.1). Having a dense forest directly behind a village would have increased casualties by 6% compared to losses in cases with non vegetated fields behind villages. These latter effects, although statistically not very strong, could be the result of debris created by the initial wave, trapped in dense forest vegetation and returned by the backwash, as reported by many witnesses. There was no significant effect of coastal vegetation in front of the settlement regarding structural damage ($p=0.981$).

The importance of distance and the interplay of land use allocation for tsunami related coastal planning could be demonstrated using the casualties model (Table 2.3). Given the mean tsunami intensity in 2004 (Table 2.2) and existing land use (Table 2.1), locating settlements about 3.5 km away from the shoreline apparently could have avoided most casualties. Scenarios comparing hypothetical areas with different agricultural vegetation types in front/behind settlements, e.g. Grass-Rice/Rubber vs. Rubber/Grass-Rice (Fig. 2.3) showed that inverted LCR_F/LCR_{B5} relationships resulted in up to 10% difference in casualty estimates. Consequently, critical distances from the shoreline to the settlement, i.e. distance where no casualties occur, can vary by up to 500 m. Best/worst case scenarios comparing high and low vegetation roughness behind the settlement (LCR_{B5}) (Fig. 2.4) resulted in up to 30% difference in probability of occurrence of structural damage. Nevertheless, at very short and long distances from the shore such differences between vegetation types are overridden by the influence of wave energy.

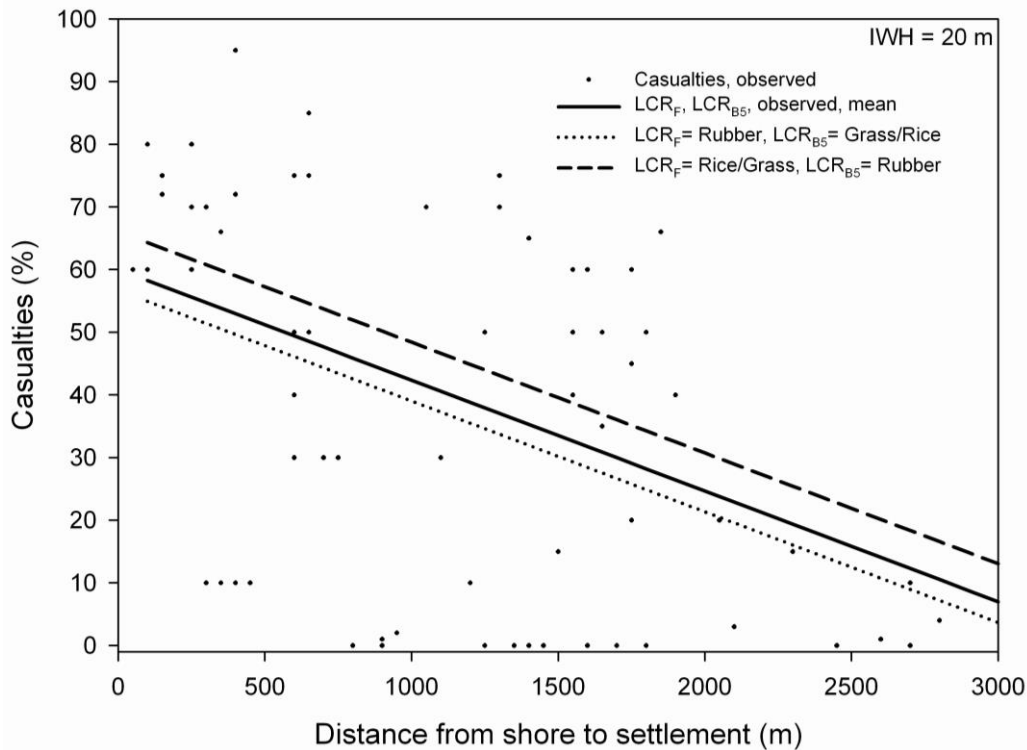


Figure 2.3. Predicted (lines, CASU model, Table 2.3) and observed (symbols) change in percentage of casualties with distance from shoreline to settlement (D) at average initial water height (IWH) of 20m. Three model scenarios of weighted average land cover

roughness in front of the settlement (LCR_F) and weighted average land cover roughness from the settlement up to 500 m behind (LCR_{B5}) were used.

Offshore conditions (IWH) were positively related to maximum flood distance ($p=0.044$) and casualties ($p=0.018$) (Table 2.3). Higher IWH significantly increased flood extension and number of casualties. However, no significant effect of IWH on structural damage was detected ($p=0.358$). This was most likely due to the extreme force of the waves in West Aceh, being only 150 km away from the epicenter with wave heights up to 25 m. In contrast to other areas (2, 4), even the reported minimum IWH (10 m) was sufficient to cause total damage to structures close to the shore. While buildings were fully exposed to the force of the waves, peoples' chances to escape increased at lower wave height.

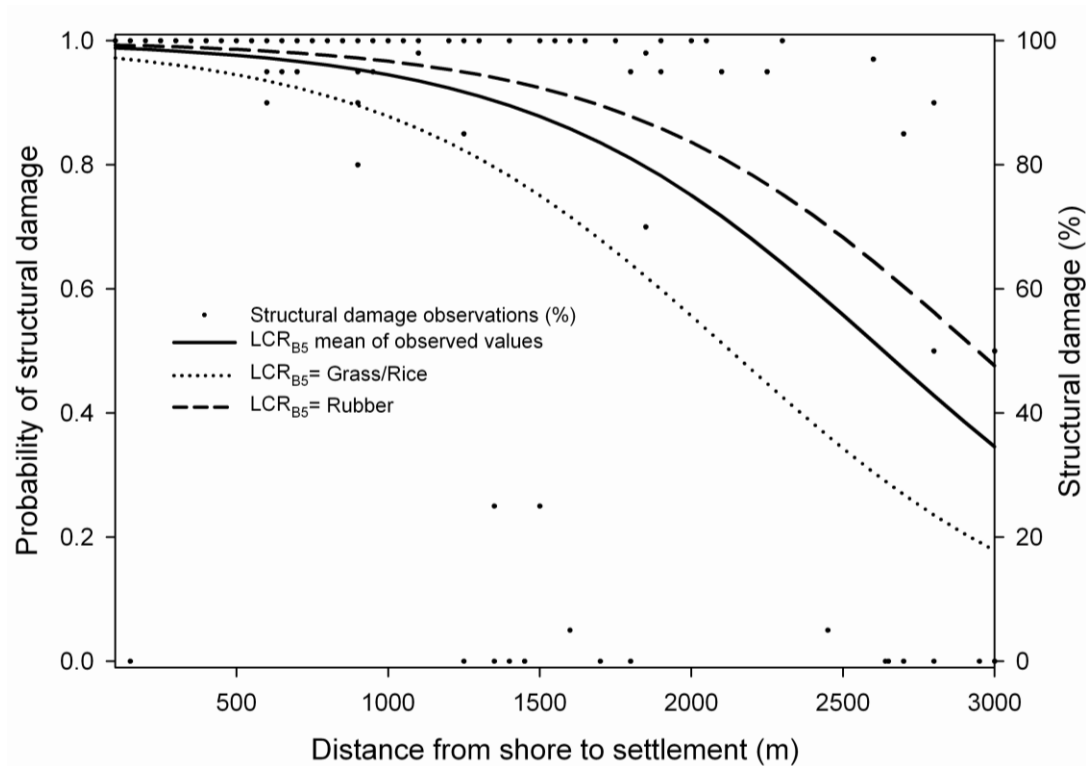


Figure 2.4. Probability of structural damage with distance from shoreline to settlement (D) (lines, STD model, Table 2.3) over all initial water height (IWH) values. Three scenarios of weighted average land cover roughness from the settlement up to 500 m behind (LCR_{B5}) were employed. Symbols represent observed structural damage (%).

The lack of significance of topography (E_F) in the casualties ($p=0.368$) and structural damage ($p=0.143$) models (Table 2.3) might have been due to the small elevation changes on site (Table 2.2). A different result was shown for the maximum flood distance model where elevation changes were more relevant ($p=0.001$) together with IWH (Table 2.3). LCR_T showed no significant impact on flood distance. This suggested that a tsunami wave travels as far as the elevation bounds, but may go slower if there are obstacles set by vegetation.

Claims of vegetation helping people to escape have also been documented in other studies (Tanaka *et al.* 2007; Tanaka 2009; Dengler and Preuss 2003), including the concept of ‘soft landing’ (Tanaka 2009). A moderate positive impact of vegetation on the chances of saving human lives was confirmed in our study but only with respect to land cover in front of settlements. Nevertheless, the current study also showed that an increase in land cover roughness behind a settlement (LCR_{B5}) was positively related to an increase in casualties, indicating an adverse effect (Table 2.3). This relationship may also indicate that people washed into forested areas, either against trees or places with high LCR, had lower survival chances (ca. -3%, based on our mean model estimates for the study area) than those washed into places with low LCR or open areas. These results are in agreement with observations by other studies mentioning that vegetation in Thailand may have created fatal barriers between the shoreline and higher ground hindering people ability to escape (Cochard *et al.* 2008).

Thus, vegetation can induce different impacts depending on its occurrence and shape in front and behind villages. Hence, the difference in data distribution between LCR_F and LCR_{B5} (Fig. 2.5) explains why an overall decrease in casualties in the study area was possible given the higher weighted average roughness in front of settlements against a relatively lower one behind. In terms of future coastal planning this would suggest that it is preferential to plant productive agroforests in front of communities while cropping fields would be allocated behind villages.

Observations along the coast of Kerala, India, showed that not even concrete walls protected the coast from the 2004 tsunami impact (Kurian *et al.* 2006), yet at the same time bio-shields were recommended for tsunami hazard mitigation. Our research suggests that, under extreme conditions as in West Aceh and without mangrove forests, coastal vegetation between the shoreline and a settlement reduced casualties, probably diminishing water speed and allowing people to escape, which would explain why such effect was not observed for structural damage.

Earlier assessments also included land and vegetation effects on water flows, especially floods (Latief *et al.* 2007; Freeman *et al.* 2000; Järvelä 2004), but their procedures to quantify such effects were more complex and data demanding. Our approach accounts for the resistance of vegetation opposing flow, expressed in volumetric units (diameter, height, density) as a vegetation resistance coefficient (VR). Once VR was combined with different land covers and their areas, the LCR coefficient allowed a landscape level assessment. This approach enabled grouping land covers such as ‘forest’ and ‘rubber’, which have similar height and density but differ due to the typically higher average diameter of forest stems than rubber. A more comprehensive resistance factor might include elements such as Manning’s resistance coefficient and the Darcy-Weisbach friction factor as well as differences in flow speed and resistance of submerged and non-submerged vegetation (Freeman *et al.* 2000; Järvelä 2004). Although the use of such characteristics may produce a more mechanistic model, the approach proposed here provides an assessment that facilitates coastal planning based on readily available data. Despite our measurements of height, stem diameter, and planting density being made in

post-tsunami conditions using similar land cover types, albeit not affected by the tsunami, we believe the values were an adequate representation of pre-tsunami conditions.

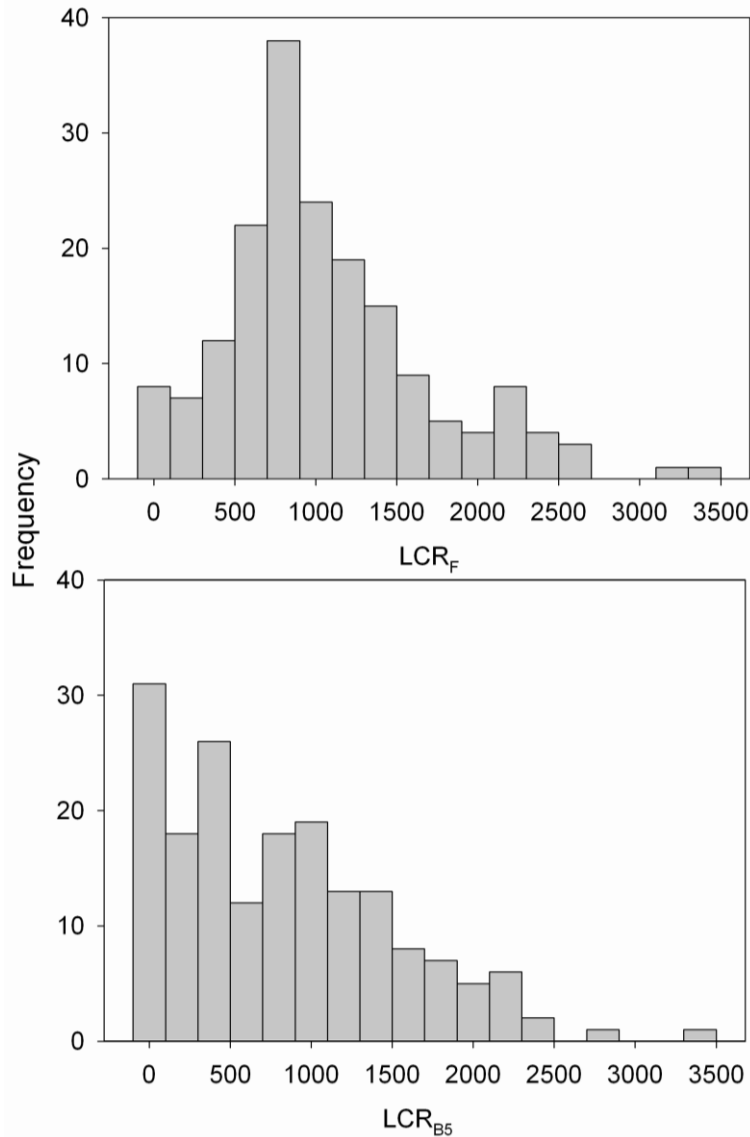


Figure 2.5. Histogram comparison for weighted average land cover roughness in front of the settlement (LCR_F) and weighted average land cover roughness up to 500 m behind the settlement (LCR_{B5}).

The present damage evaluation focused on casualties and structural damage, similar to other studies (Danielsen *et al.* 2005; Olwig *et al.* 2007; Kathiresan and Rajendran 2005), but considered criticism that some of these had received (Dahdouh-Guebas *et al.* 2005; Kerr and Baird 2007; Baird *et al.* 2009; Baird and Kerr 2008; Young 2006). Issues regarding spatial autocorrelation in assessment methods were addressed through the use of a spatially explicit statistical model. Factors discarded by other authors, such as topographic changes (Kaplan *et al.* 2009), were included. Offshore factors such as bathymetry, distance to epicenter and slope of the island (proximal and distal) were represented through IWH. The multivariate models allowed us to focus specifically on

inland factors and filter out vegetation effects. Despite distance being the overall factor determining damage, the effects of land cover roughness in the models was statistically confirmed at $\alpha=0.1$.

Tsunamis of a magnitude like the 2004 event are relatively rare (Monecke *et al.* 2008). Nevertheless, recent events such as the one in Japan on March 2011 and the February 2010 earthquake in Chile show that these threats are real and require preparedness and adequate policy responses. Unsubstantiated statements regarding protection provided by coastal vegetation can be obstructive and even dangerous. More critical investigation, including spatial multivariate approaches must be encouraged in order to determine criteria for successful mitigation measures, including debris effects.

Our main conclusion that distance to the shoreline (D) most effectively reduced casualties and structural damage (Table 2.3) implies that settlements should be preferentially located away from the shoreline and at an elevated position (although in the case of the study area there was limited scope to chose higher elevated areas close to the shoreline). However, in practical terms, a coastal planning strategy that aims only to locate settlements away from coastlines is likely to fail. For local villagers, closeness to the sea not only represents danger but also potential income generation opportunities and food security. Thus coastal planning must consider additional attenuating and mitigation effects of coastal vegetation such as the demonstrated reduction of casualties provided by agroforests in front of settlements having a large vegetation roughness coefficient (LCR_F). Because of the only moderate effectiveness and associated uncertainties of coastal vegetation against tsunami effects, its composition must be based upon its wider livelihood context not only its mitigation role (e.g. bio-shields). Allocation of more dense agroforests in between sea and communities (i.e. cacao, rubber and multi-layered home gardens) yielding tangible benefits for farmers should be an important spatial planning measure. Additionally, cropping fields that do not trap people while they try to escape i.e. rice, agriculture, should be located behind settlements. These interventions should consider local ecological niches and customs.

In order to reduce vulnerability and to have lasting benefits, strategic planning thus must consider strengthening livelihoods via satisfaction of local needs, and preferences (Ziegler *et al.* 2009) as well as provision of environmental goods and services. Economically valuable tree crops such as rubber and agroforests can potentially satisfy these requirements. Risk management planning thus must consider adequate distribution of settlements but also of productive areas, and it must take into account the potential negative impact of dense vegetation behind communities. Because of the limited effectiveness of vegetation towards large tsunamis, additionally appropriate risk mitigation actions such as early warning systems need to be implemented (Cochard *et al.* 2008). Only a combination of these measures will provide hazard reduction and mitigation as well as food security and sustainable development opportunities.

CHAPTER 3. Tsunami in the Seychelles: Assessing mitigation mechanisms

Chapter 3. Tsunami in the Seychelles: Assessing mitigation mechanisms²

Juan Carlos Laso Bayas, Carsten Marohn , Georg Cadisch

*Institute of Plant Production and Agroecology in the Tropics and Subtropics,
University of Hohenheim, 70593 Stuttgart, Germany*

3.1. Abstract

A spatial statistical model determining the possible tsunami impact mitigation by coastal vegetation developed after the December 2004 earthquake event for Aceh, Indonesia, was adapted and tested under the conditions of the Seychelles in the western Indian Ocean to find out whether comparable protective effects of vegetation existed. The waves generated at the three main populated islands, Mahé, Praslin and La Digue averaged less than 2 meters at the shoreline allowing assessment of effects of vegetation in mitigating impact of a low intensity tsunami event. Semi structured interviews with local witnesses of the event, field measurements of local features, as well as secondary data sources provided information on wave height at the shoreline, landscape characteristics as well as tsunami impacts inland, i.e. structural damage and maximum flood distance. Observation points at maximum flood distance and where damage occurred were geo-located and entered into a GIS. Vegetation density and resistance coefficients were determined on site and their spatial distribution through visual interpretation of Google Earth® pre tsunami imagery. Data was analyzed using a generalized linear mixed model, acknowledging the spatial distribution of data. As for Aceh, the results indicated that distance from the settlement to the shoreline was the most important factor to avoid adverse tsunami effects. In contrast to Aceh, a direct effect of coastal vegetation was not observed ($p > 0.05$). A significant protective effect, however, was apparent through sand dunes, stabilized by vegetation, reducing damage to buildings by up to 30% where initial water height at shoreline was 3 m. Maximum flood distance was not affected by sand dunes but was reduced ($p = 0.013$) by existing sea walls. A coastal planning that encompasses the promotion and protection of multi-use coastal vegetation, i.e. generating income through tourism, providing food products and protecting natural physical barriers is encouraged in order to enhance local resilience against natural wave events such as those of the 2004 tsunami.

3.2. Keywords

Tsunami, Seychelles, GLIMMIX, coastal vegetation, dunes

²A version of this chapter is published as:

Laso Bayas J.C., Marohn C., Cadisch G., 2013. Tsunami in the Seychelles: Assessing mitigation mechanisms. *Ocean and Coastal Management*. Volume 86, Pages 42–52. The original publication is available at <http://www.sciencedirect.com/science/article/pii/S0964569113002329>.

3.3. Introduction

The tsunami event of 2004 was one of the biggest events of the last 40 years (Lay *et al.* 2005), affecting several countries across the Indian Ocean. It generated historically unexpected damage in countries very distant to the epicenter like India, Sri Lanka and Somalia (Okal and Synolakis 2008). The Republic of Seychelles (herein referred to as the Seychelles) was one of the countries on the path of the waves. The tsunami in the Seychelles arrived not as a breaking wave but as a bore (Hagan *et al.* 2007), a surge of water pushing materials, fences and everything in its way, flooding the coastal areas. The human casualties due to the tsunami in the Seychelles, where 2 people died, were fortunately low compared to the over 160,000 casualties in Aceh, Sumatra (Tsuji *et al.* 2006). There were a number of specific interactions which probably reduced the impact of the 2004 tsunami in the Seychelles.

On one hand, several off-shore factors reduced wave force. The tsunami wave height was only slightly above average than the normal tidal variation (Obura 2006), but also the peak waves reached the islands during low tide (Jackson *et al.* 2005). Additionally, since many of the coastal areas were protected by reefs (Cazes-Duvat 2001), damage was not as severe as in other countries that were further in distance to the epicenter, e.g. Somalia (Fritz and Borrero 2006). The rock shelf on which the archipelago is located refracted and changed the patterns of the waves and further reduced the wave impact inland (Jackson *et al.* 2005).

Shoreline and inland factors, such as coastal vegetation, seawalls and dunes also influenced the impact of the tsunami in the Seychelles. Coastal vegetation effects on a tsunami event have been controversially discussed in previous studies, some affirming that coastal vegetation reduced impact on coastal communities inland (Danielsen *et al.* 2005, Tanaka *et al.* 2007), whilst others doubting such effects (Kerr and Baird 2007, Baird and Kerr 2008, Baird *et al.* 2009, Young 2009).

A previously developed set of models (Laso Bayas *et al.*, 2011) based on data from the coastal communities of Aceh, Indonesia, where the 2004 tsunami impact was very high, indicated that coastal vegetation may play opposite roles depending on the type and location of vegetation present in the area. Coastal vegetation with a high resistance coefficient located in between the settlement and the sea shore reduced casualties from 3 to 8 % but when such vegetation was located directly behind settlements, casualties and damages to buildings increased 3% on average. The 2004 tsunami also caused damages in the Seychelles but under different initial conditions, i.e. tsunami intensity was much lower when compared to the situation in Aceh. The contrasting circumstances in the Seychelles provided hence an opportunity to test the previously developed models. This was at the same time deemed a more applied use of the models since smaller tectonic movements producing small tsunamis are more frequent events than larger tsunamis (Monecke *et al.* 2008).

Additionally, the Seychelles presented a different set of characteristics with regards to their land use. The main populated islands have, besides natural coastal vegetation, seawalls built to protect roads, land, and houses from common tides. Besides this man-made protection, there were additional naturally occurring sand dunes along parts of the coastlines. Most of these dunes were maintained by the presence of coastal vegetation such as *Ipomoea pes-caprae* with its sand binding properties

(Devall 1992). In general, roots and vines of dune-colonizing plants stabilize dunes and reduce dune abrasion due to wind erosion (Seliskar 2006). When the tsunami occurred, dunes could have offered some degree of protection as they do under regular storm waves and high tides. Protective effects of dunes have been reported in other studies where they reduced inundation distance (Chandrasekar *et al.* 2007), or decreased the speed of the waves, thus diminishing casualties (Kathiresan and Rajendran 2005).

The objective of the present study was therefore to adapt and apply the previously developed tsunami models (Laso Bayas *et al.*, 2011) in order to determine if coastal vegetation had an effect on structural damage and flooding distance in the Seychelles. Additional features, such as seawalls and dunes stabilized by coastal vegetation, allowed expansion of the previous models, relating direct and indirect effects (sand dune immobilization) of coastal vegetation to the impact of the 2004 tsunami waves under the conditions of the main islands of the Seychelles: Mahé, Praslin and La Digue.

3.4. Materials and Methods

3.4.1. Model development

The basis for the current models describing impact indicators, i.e. structural damage (damage to buildings and roads affected in a village in percentage), and maximum flood extension from the shore (meters advanced by the flood), were the models developed by Laso Bayas *et al.* (2011) in Aceh, Indonesia. These models were based on the concept established by Shuto (1987), stating that the two forces that diminish the energy of the water once it arrived at the shoreline are gravity (represented by elevation) and friction (land cover resistance). The impact indicators were functions of the wave force at the shoreline shaped by offshore factors (IWH) as well as elevation and land cover resistance to the flow. Friction exerted by land cover was approximated by its characteristics, more specifically by the combination of stem diameter (SD), stem height (H), and planting density (d). However, inland differences between Aceh and the Seychelles included not only different land uses, but in the Seychelles seawalls and dunes were additional features resisting the force of the waves. These features occurred on many of the visited sites, seawalls prominently on built areas closer to the sea or in areas where dunes did not exist. In the current study, these structures were present on three quarters of the areas analyzed. The current study extends the previous models to include these two types of structures.

The existence and sizes of dunes at the time of the tsunami were corroborated with local key informants as well as personnel from the Department for Risk and Disaster Management (DRDM) and the Ministry of Environment (MOE) from the Seychelles and cross checked with 2004 pre-tsunami Google Earth® imagery. The dunes observed on the study were covered by vegetation stabilizing them. As previously reported by other studies (Seliskar 1995, Devall 1992, Koske and Polson 1984) dune-plants colonize the existing sand dunes, and given favorable conditions, e.g. absence of extreme slopes, maintain the dunes by preventing wind erosion. Colonizing vegetation additionally increases dune height and width (Adriani and Terwindt 1974).

With regards to data collection, the field campaign was carried out from March until April 2009. For data collection, the current study used transects perpendicular to the coastline in order to determine elevation changes and assess the areas covered by different land uses in front of and behind villages, as well as presence and size of seawalls and dunes. The size of the transects (N=219) was adapted accordingly to the area exposed, being on average 75 m wide, extending from the shoreline to the affected settlement (n=128: Mahé=78, Praslin=44, La Digue=6) or to the maximum flooded distance, whenever such information was available (n=104, Mahé=51, Praslin=39, La Digue=14). The sites where transects were overlaid are shown in Figure 3.1.

To assess the land cover present along each of the transects and develop resistance coefficients, we combined on site specific vegetation assessment (vegetation inventory) and visual imagery comparison (pre-tsunami Google Earth® imagery). The resistance that different land uses offered to the tsunami advance was calculated as suggested by Laso Bayas *et al.* (2011) using the relationships stated by Peltola *et al.* (2000). The vegetation resistance coefficient (VR), a measure of the resistance offered by the different land cover types to the advance of a flow was obtained by the multiplication of stand height, density of plantation, and squared stem diameter. To obtain the data needed in order to develop this factor, a combination of two approaches was used: 1) on site assessment of vegetation characteristics including type of land-cover, stem diameter (m), heights (m), and plant density (stems ha⁻¹) on representative areas selected from high resolution satellite imagery dated from before the tsunami event (2004), available in Google Earth®; and 2) comparison between pictures taken from the affected sites and visual determination using the above mentioned satellite imagery.

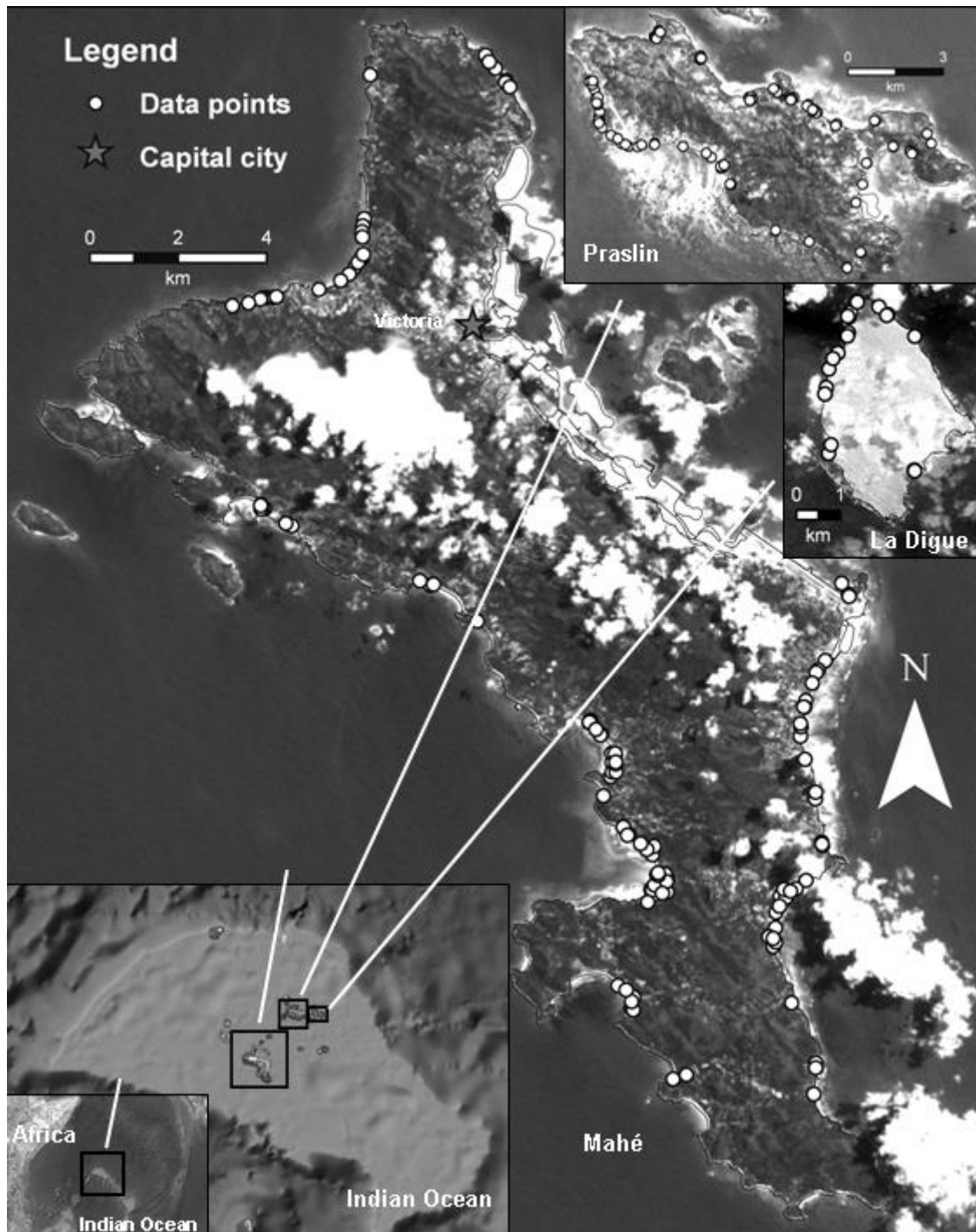


Figure 3.1. Study area: Data collection points distributed along the coasts of the islands of Mahé, Praslin, and La Digue. Transects and data overlaid on Landsat® TM imagery. Shoreline borders including reclaimed land (mostly present on the east coast of Mahé) provided by GIS unit, Ministry of Land Use and Habitat, Seychelles. Lower left corner images obtained from Google Earth® (© 2011 Google, Data SIO, NOAA, U.S. Navy, NGA, GEBCO; © 2012 Cnes/Spot Image).

Under the 2004 tsunami conditions of the Seychelles, the area affected was relatively small and existing land cover maps were too coarse for a detailed analysis. The visual classification of dominant land cover types, i.e. trees (except coconut), grassland, settlement, coconut palms, and bush-type vegetation (e.g. non-tree, tall vegetation)

was carried out using the previously mentioned Google Earth® imagery. This percentage was multiplied by the total area of the transect to obtain the cumulative land cover roughness ΣLCR (eq. 2.2). The correspondent area corrected LCR was calculated dividing ΣLCR by total transect area (eq. 2.3).

In order to test the effects of vegetation behind the settlements, the variable weighted average land-cover roughness behind the settlement (LCR_{B20}) was included. In the Seychelles the average advance distance reached by the water was around 50 m inland. LCR_{B20} included vegetation up to 20 meters behind an observation point. In contrast to Aceh, the LCRs used for the Seychelles were flexible and not fixed, i.e. specific to each transect according to its vegetation density. Table 3.1 summarizes land cover types in front and behind the settlements as recorded in the field and observed on the Google Earth® imagery. Given the small area affected in the Seychelles two additional and more localized barriers were detected and consequently introduced in the models: seawalls and dunes.

Table 3.1. Overview of land cover types present in the study area. Corresponding average estimated land cover roughness in front (LCR_F) and up to 20 m behind (LCR_{B20}) the observation point.

Land use	Area in front of settlements (%)	LCR_F	Area behind settlements (%)	LCR_{B20}
Cleared land	1	0 ± 0	7	0 ± 0
Sand	8	0 ± 0	12	0 ± 0
Grass	10	8 ± 6	13	19 ± 28
Coconut	27	55 ± 36	11	40 ± 31
Bush	18	63 ± 42	3	150 ± 26
Trees	31	120 ± 102	31	106 ± 94
Settlement ^a	5	2628 ± 863	23	1525 ± 445

Notes: Weighted average roughness coefficients (including densities) were calculated individually for each transect in front and behind the settlement. Settlement resistance values were considered similar to Aceh (Laso Bayas et al., 2011). ^a Settlement=constructed area in front or behind the main settlement

Damage indicators estimated in the field were structural damage (STD) and maximum flood distance (MD). STD was adapted to the transects according to the description given by local key informants and cross checked with personnel from DRDM and MOE. Criteria were the total collapse of the buildings on the area was corresponding to 100% damage whereas toppled fences and cracked house-walls amounted to 5% and 10% of damage, respectively. Tsunami energy at the shoreline was influenced by offshore conditions, e.g. bathymetry, reefs, proximal and distal slope and represented in the models by initial water height at shoreline (IWH). The effect of gravity was given by the changes in elevation (E) whereas friction was represented by the weighted land cover roughness coefficients (LCR_T , LCR_F and LCR_{B20}), seawalls (WL) and dunes (DN). For the structural damage model, distance (D) from an affected building to the shoreline was an additional variable. A representation of the tsunami interactions is shown in Figure 3.2 and its outreach and effects on structures were estimated using the following two equations:

$$MD = f(IWH, E, LCR_T, WL, DN) \quad (3.3)$$

and

$$STD = f(IWH, E, D, LCR_F, LCR_{B20}, WL, DN) \quad (3.4)$$

where MD= maximum flood distance (m), STD= structural damage (%), IWH= initial water height at shoreline (m), E= elevation (m a.s.l.), D= distance to the shoreline (m), LCR_T = weighted average land cover roughness throughout the transect, LCR_F = weighted average land cover roughness in front of the settlement, LCR_{B20} = weighted average land cover roughness from a settlement up to 20 m behind, WL= seawall, DN= vegetation immobilized sand dunes. WL and DN incorporated four categories: Non-existing, less than a meter high, between 1 and 2 meters high, more than 2 meters high. Categories were preferred to exact height measurements due to the time difference existing between the tsunami event and the field campaign. Proportional comparative resistance differences existing between transects and sites were thus maintained.

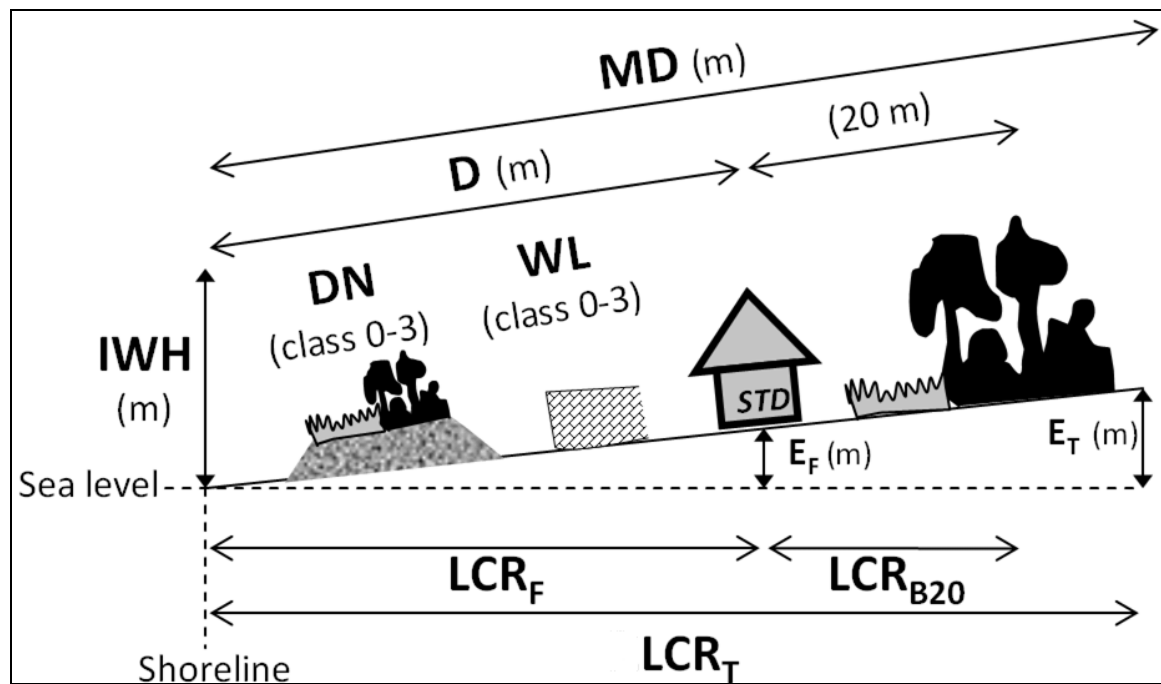


Figure 3.2. Transect schematic diagram showing the variables measured, calculated and used on the models. MD= maximum flood distance (m), STD= structural damage (%), IWH= initial water height at shoreline (m), D= distance from the shoreline to the community (m) E_T = elevation at MD (m), E_F = elevation at the building location (m), LCR_T = Weighted average land cover roughness throughout the transect, LCR_F = Weighted average land cover roughness in front of the settlement, LCR_{B20} = Weighted average land cover roughness from the settlement up to 20 meters behind, DN= vegetation immobilized sand dunes (4 classes, values: 0-1-3-5) and WL= Seawalls (4 classes, values: 0-1-3-5).

3.4.2. Site characteristics and tsunami impact data collection

Jackson *et al.* (2005) reported 20 sites visited during their tsunami effects assessment in the Seychelles. Thirteen sites were located in Mahé and seven in Praslin. These sites were used as starting points for the present study to determine possible areas for data collection. With information and recommendations provided by the GIS unit at the Ministry of Land Use and Habitat and DRDM of the Seychelles, 29 additional research sites were added. Figure 3.1 shows the location of all the observation points.

Semi-structured interviews with over 200 inhabitants and key informants, e.g. district administrators from the affected areas, were carried out. Interviews were performed *in situ* at each of the affected areas in order to geo-reference information regarding tsunami characteristics and effects. Data provision from local inhabitants was anonymous and referred only to primary quantitative information on tsunami intensity, i.e. initial wave height (IWH, m); damage indicators, i.e. structural damage (STD, %) and maximum flood distance (MD, m); and land cover characteristics, i.e. presence and size category of vegetation immobilized sand dunes (DN, 0-3) and seawalls (WL, 0-3) when the tsunami occurred. Summaries of the data collected can be found in Tables 3.2 - 3.4. Information and support provided by the personnel of the DRDM and MOE of the Seychelles helped to cross-reference the data provided during the above mentioned interviews, e.g. maximum flood distance and structural damages (affected houses, broken bridges, demolished buildings). All the information was geo-referenced using a GPS (Garmin 76 csx).

Table 3.2. Variables used in the maximum flooded distance model and their descriptive statistics. N=104.

Variable	Mean / Mode ^a	Std Dev.	Min.	Max.
MD - Maximum flood distance (m)	63	64	5	355
IWH - Initial water height at shoreline (m)	1.6	0.8	0	3
E_T - Maximum elevation over the whole transect (m a.s.l.)	1.5	1.3	0	8.5
LCR_T – Weighted average land cover roughness throughout the transect	157	510	0	3184
DN - Dune (classes: 0-3)	0	1	0	3
WL - Seawall (classes: 0-3)	0	1	0	3

^a Mode is used instead of the mean for the class variables, i.e. dunes and seawalls 4 categories: 0='non existing', 1='less than a meter high', 2='in between 1 and 2 meters high' and 3='more than 2 meters high'.

Additionally, data collected by the Canadian Geological Service mission (Jackson *et al.* 2005) were used to cross check the data gathered in the field. Topographic data was extracted from digital elevation models (DEM) provided by the GIS unit of the Ministry of Land Use and Habitat. The DEM for the islands of La Digue and Praslin had 2 m vertical resolution whereas the one for the island of Mahé had a resolution of 10 m. Tables 3.2 and 3.3 show a summary of the elevation data used in each model in the study.

A general overview of a typical transect, showing the location of landscape features, including seawalls and vegetation stabilized sand dunes, can be seen in Figure 3.2. Data were collected along the coastline of the islands Mahé, Praslin and La Digue and transects were allocated to each of these data points. Examples of the data collected including the vegetation and sand dune arrangements are shown in the appendix B (Figures B1-B4).

Table 3.3. Variables used in the structural damage model and their descriptive statistics. N=128.

Variable	Mean / Mode^a	Std Dev.	Min.	Max.
STD - Structural damage (%)	2	3	0	10
IWH - Initial water height at shoreline (m)	1.7	0.8	0	3
E_F – Maximum elevation in front of the settlement (m a.s.l.)	1.2	1.0	0	4.9
D - Distance from the shoreline to the settlement (m)	42	46	5	285
LCR_F – Weighted average land cover roughness in front of the settlement	129	430	0	2830
LCR_{B20} – Weighted average land cover roughness from the settlement up to 20 meters behind	366	648	0	1769
DN - Dune (classes: 0-3)	0	1	0	3
WL - Seawall (classes: 0-3)	0	1	0	3

^a Mode is used instead of the mean for the class variables, i.e. dunes and seawalls 4 categories: 0='non existing', 1='less than a meter high', 2='in between 1 and 2 meters high' and 3='more than 2 meters high'.

Table 3.4. Comparison of parameter characteristics from the Aceh and Seychelles models.

Model Parameter	Mean/mode ^a		Range	
	Aceh	Seychelles	Aceh	Seychelles
STD - Structural Damage (%)	78	2	0-100	0-10
CASU - Casualties (%)	34	NA	0-95	NA
MD - Maximum flood distance (m)	2250	63	950-3500	5-355
IWH - Initial water height at shoreline (m)	20	1.7 ^b	10-25	0-3
E_F - Maximum elevation in front of the settlement (m a.s.l.)	14	1.2	6-47	0-4.9
E_T - Maximum elevation over the whole transect (m a.s.l.)	19	1.5	12-74	0-8.5
LCR_F - Weighted average land cover roughness in front of the settlement	1165	129	71-3538	0-2830
LCR_B - Weighted average land cover roughness from behind the settlement ^c	914	366	0-3444	0-1769
LCR_T - Weighted average land cover roughness throughout the transect	987	157	141-1899	0-3184
D - Distance from the shoreline to the settlement (m)	1200	42	50-4400	5-285
DN - Sand dunes (classes 0-3)	NA	0	NA	1-3
WL - Seawalls (classes 0-3)	NA	0	NA	1-3

^a Mode is used instead of the mean for the class variables, i.e. dunes and seawalls 4 categories: 0='non existing', 1='less than a meter high', 2='in between 1 and 2 meters high' and 3='more than 2 meters high'.

^b IWH Mean value for the MD model = 1.6 m (see Table 3.2). Range for this variable is the same on both models.

^c For the case of Aceh the coefficient represents vegetation roughness from the settlement up to 500 m behind whereas for Seychelles it represents vegetation roughness from the settlement up to 20 m behind.

3.4.3. Data Analysis

Skewed and categorical data distribution patterns were found for the impact indicators maximum flood distance (MD) and structural damage (STD), respectively (Fig. 3.3). Given these distribution patterns generalized linear mixed models (GLMM) were chosen in order to fit the models using the statistical software package SAS® v. 9.2. (SAS Institute Inc., Cary, N.C., U.S.A.). This procedure was employed because it can fit multivariate linear models with different data distributions while at the same time acknowledging spatial auto-correlation (Schabenberger 2005), e.g. the one existing amongst transects located side by side along the coast.

STD categorical data was transformed to a binomial response (STDB, 0/1) representing absence or presence of structural damage. A logistic regression using a logit link function was performed for this model. MD data was square root-

transformed (SQMD) (Fig. 3.3) and linear assumptions (homogeneity of variance, normality) were tested on the model residuals. To determine statistical independence, Pearson and Spearman correlations tests were performed amongst the predictor variables. For each model, predictors on appropriate scales (standardized to mean=0 and standard deviation=1, when required) were employed.

The multivariate models considered several fixed effects, i.e. tsunami intensity shaped by offshore conditions (represented by initial water height at shoreline), topography (elevation), and friction provided by land cover roughness in front of and behind settlements as well as by seawalls and dunes. Random effects, i.e. spatial distribution of the geographic coordinates of each observation were modeled using a spatial exponential/spherical variance-covariance matrix (Schabenberger 2005). Maximum flood distance used AIC as a measure of fit and model comparison (Burnham and Anderson 2002) and structural damage (binomial) used the ratio of chi square over degrees of freedom as measure of model performance. Tables 3.2 and 3.3 show the characteristics of the variables used in each model.

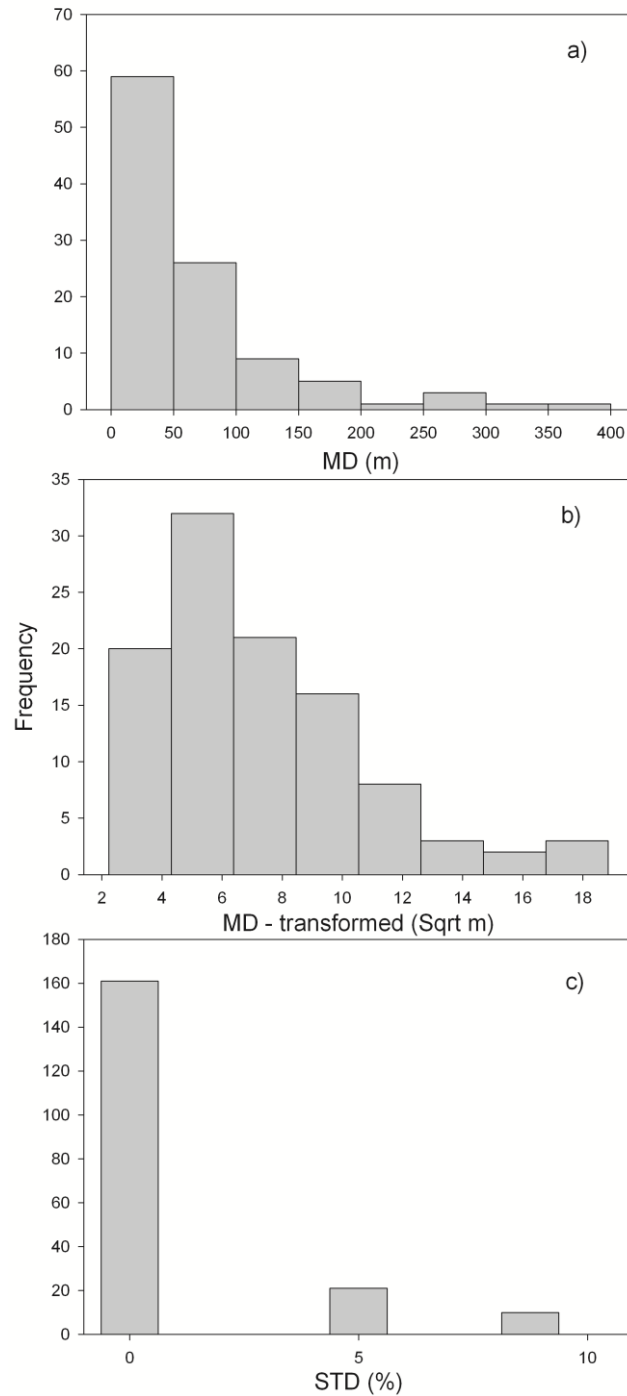


Figure 3.3. Data distribution for the dependent variables a) maximum flood distance (**MD**), b) square root transformed maximum flood distance (**MD transformed**) and c) structural damage (**STD**).

Empirical semi-variograms were used in order to test if spatial autocorrelation was properly acknowledged.

In Figure 3.4, the distribution per class of seawalls and dunes is documented. Barbier *et al.* (2008) mentioned that the resistance of such structures increases exponentially. Consequently, in order to determine an adequate way of representing the effects of these physical structures against the impact of incoming waves, three empirical numerical progressions showing an increasing resistance due to an increase of height were tested. The progressions were: 0-1-2-3, 0-1-3-5 and 0-1-5-25, each number

representing respectively: absence of the structure - structure less than 1 meter high - structure between 1 and 2 meters high - structure higher than 2 meters. Models employing each of these sequences were used to determine the progression that provided an adequate representation of resistance, i.e. the model with the best fit implied to have the most adequate progression. Models' goodness of fit selection was compared using AIC (lowest value) and closeness to best fit ($X^2/Df=1$) in the maximum flood distance and structural damage models, respectively.

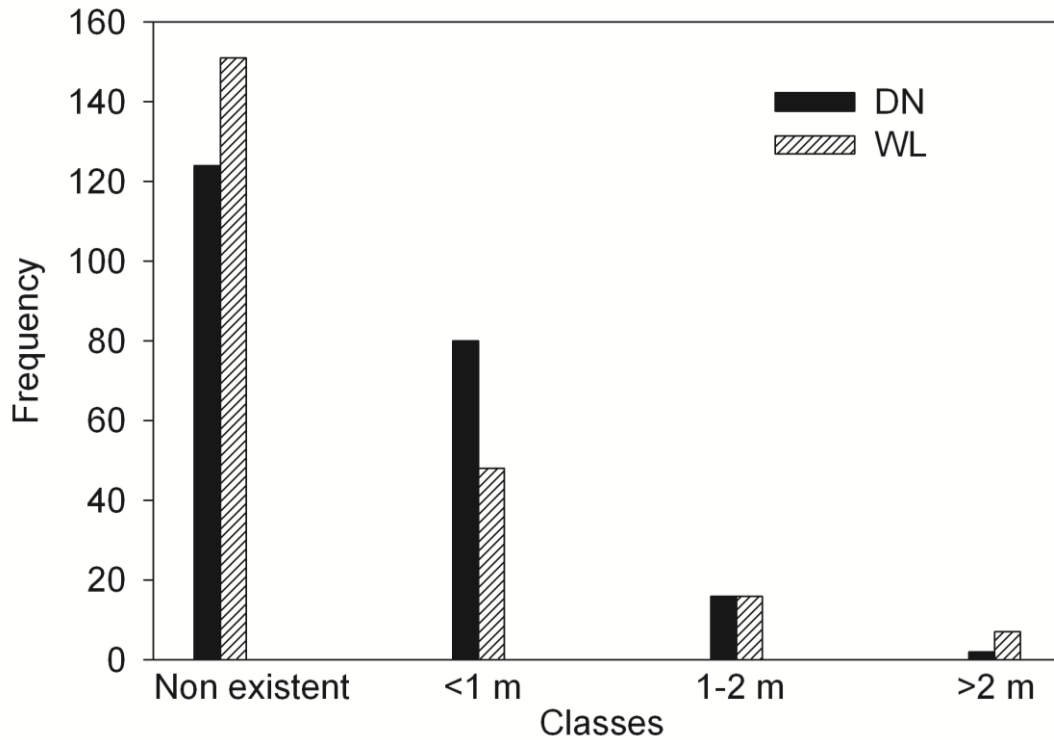


Figure 3.4. Data distribution for the independent variables vegetation immobilized sand dunes (**DN**) and seawalls (**WL**). Data corresponding to all the areas visited in the Islands of Mahé, Praslin and La Digue.

Empirical semi-variograms were used in order to test if spatial autocorrelation was properly acknowledged.

3.5. Results

3.5.1. Area, tsunami impact characteristics and model assumptions

When the 2004 tsunami reached the Seychelles it was a relatively low energy event. It arrived with waves reaching a height of up to 3 m, with an initial water height at shoreline in average less than two meters (Table 3.3). Nevertheless the impact caused damages to buildings, bridges and other structures, albeit only up to a maximum of 10% i.e. cracks to the walls of buildings or similar. Flooded distance extended up to a maximum of 355 m but with an average of only around 60 m (Table 3.4).

Three quarters of the affected coastal areas analyzed in this study presented either vegetation colonized sand dunes (33%) or sea-walls (45%). Only 2% of these areas presented both features at the same time. With regards to seawalls and sand dunes

colonized by vegetation, model fit suggested the sequence 0-1-3-5 as best representing the resistance provided by seawalls and dunes against the flow of water (Table 3.5).

Table 3.5. Comparison of full model fits (using all variables) given different progressions for the variables sand dunes and seawalls. Generalized linear mixed procedure using a spatial exponential (for **MD**) or spherical (for **STD**) covariance matrix as a random term. Estimation techniques: Maximum Likelihood (ML, N=104) for **MD** and Pseudo Likelihood (PL, N=128) for **STD**.

Dunes and seawalls progressions: 4 classes	AIC^a (MD)	X²/Df^b (STD)
0-1-2-3	-170.3	0.86
0-1-3-5	-170.7	0.89
0-1-5-25	-167.4	0.89

Notes:

^a Akaike Information Criterion: lower value = better fit.

^b Chi square / degrees of freedom: closest to 1 = better fit.

3.5.2. Vegetation characteristics

In the Seychelles, land cover including coconut and other trees made up almost 60% of the area in front of settlements and over 40% of the area behind the settlements (Table 3.1). Nevertheless, the individual estimation of planting densities obtained from the visual analysis of high resolution imagery yielded variable instead of fixed (as in the Aceh study) LCR coefficients per transect. The range of these coefficients is shown on Table 3.1.

Observations of the affected coastlines showed that Coconut (*Cocos nucifera*), Takamaka (*Calophyllum inophyllum*), and Bois Blanc (*Herrandia sinora*) were the most common tree species. These grew on top of beach berms and sand dunes. Additionally, species such as Vouloutye (*Scaevola sericea*), beach morning glories/Patatran (*Ipomoea pes-caprae*) and Bwa Matlo (*Suriana maritima*) were found covering sand dunes; Casuarina trees (*Casuarina equisetifolia*) as well as sea almond trees (*Terminalia catappa*) had also an important presence distributed on top of beach berms and sand dunes (Annex B, Figures B1-B4). Seliskar (2005) mentioned that dune colonizers perform two important functions: the first being to foster sand accumulation and the second that their below ground systems stabilize dunes. Devall (1992) mentioned that species such as *Ipomoea pes-caprae* have sand-binding properties, therefore allowing them to stabilize dunes. Dune stabilization is considered an important action to prevent beach erosion and therefore to also maintain coastal dune ecosystems and the services they provide. Consequently, many authors have discussed methods to promote plant-dune colonization as a method of dune immobilization (van der Meulen and Salman 1996, Wilcock and Carter 1977, Adriani and Terwindt 1974).

Mango trees (*Mangifera indica*) were usually found behind the beach berms or dunes. Papaya (*Carica papaya*) was also common behind dunes or walls and especially close to homes, though no particular link to sand dunes was observed. Mangroves such as *Avicennia marina*, *Rhizophora mangle*, and *Xylocarpus granatum* were mentioned by previous studies (Fleischmann *et al.* 2003, Obura and Abdulla 2005), but these were not present in the analyzed areas.

3.5.3. Model results

3.5.3.1. Maximum flood distance model

A summary of the maximum flood distances reached by the 2004 tsunami in the Seychelles is shown in Table 3.3. Comparative maximum flood data between Aceh and Seychelles can be seen in Table 3.4. The spatially explicit GLIMMIX model for maximum flood distance showed that offshore factors – subsumed as IWH – had an important effect increasing the distance the water reached inland ($p = 0.023$; Table 3.6 final model). No direct effect of vegetation (LCR_T) was found ($p = 0.251$). Vegetated sand dunes showed also no significant decrease on the distance reached by the flood ($p = 0.693$). However, in combination with seawalls they showed a significant effect ($p = 0.013$) reducing flood distance as well as improving model fit by $\delta\text{AIC} = 3.9$. When dunes were excluded from the model, fit did not improve considerably ($\delta\text{AIC} < 2$) therefore the final model included both factors.

Elevation had a significant positive relationship with maximum flood distance ($p = 0.008$, Table 3.6), showing the transects were mostly on a slope. An exclusion of bay areas and peninsulas as in Aceh was not possible in the Seychelles due to the irregular geomorphology of the coastline. Most of the settlements were located in such areas.

Table 3.6. Variables tested in the maximum flood distance model (**MD**-transformed values) showing standardized regression coefficients (\pm standard error) and their corresponding p values. Generalized linear mixed model using a spatial exponential covariance matrix as a random term. Estimation technique: Maximum Likelihood (ML). $N=104$.

Intercept	IWH-s	E_T-s	LCR_T-s	DN	WL	AIC^a
0.36 \pm 0.03 ($p < 0.001$)						-128.6
0.36 \pm 0.03 ($p < 0.001$)	0.21 \pm 0.16 ($p = 0.188$)	0.38 \pm 0.12 ($p = 0.001$)				-141.3
0.36 \pm 0.03 ($p < 0.001$)	0.24 \pm 0.16 ($p = 0.137$)	0.38 \pm 0.11 ($p = 0.001$)	0.09 \pm 0.09 ($p = 0.305$)			-140.4
0.35 \pm 0.03 ($p < 0.001$)	0.25 \pm 0.14 ($p = 0.073$)	0.29 \pm 0.10 ($p = 0.005$)	0.08 \pm 0.08 ($p = 0.320$)	0.17 \pm 0.10 ($p = 0.094$)		-166.6
0.36 \pm 0.03 ($p < 0.001$)	0.33 \pm 0.14 ($p = 0.018$)	0.26 \pm 0.10 ($p = 0.001$)	0.09 \pm 0.08 ($p = 0.305$)		-0.29 \pm 0.10 ($p = 0.003$)	-172.5
0.36 \pm 0.03 ($p < 0.001$)	0.32 \pm 0.14 ($p = 0.023$)	0.27 \pm 0.10 ($p = 0.008$)	0.09 \pm 0.08 ($p = 0.251$)	-0.04 \pm 0.11 ($p = 0.693$)	-0.27 \pm 0.11 ($p = 0.013$)	-170.7

Notes: Independent variables used in the models were standardized (suffix ‘-s’) to variance=1, mean=0.

IWH-s= initial water height (standardized), **E_T-s**= maximum elevation over the whole transect (standardized), **LCR_T**= Weighted average land cover roughness throughout the transect (standardized), **DN**= Sand dunes (4 classes: 0-1-3-5) and **WL**= Seawalls (4 classes: 0-1-3-5).

^a Akaike Information Criterion: lower value = better fit

3.5.3.2. Structural damage model

A summary of the structural damage observed on the area is shown on Table 3.3 and a comparison of damage between Aceh and Seychelles can be found on Table 3.4. The analysis of structural damage data revealed that IWH was the most important factor ($p < 0.001$) increasing damage to buildings and structures (Table 3.7). On land, distance

from the settlement to the shoreline was the most significant factor decreasing the likelihood of damage to buildings ($p = 0.039$). Coastal vegetation in front and behind the settlement showed no significant direct tsunami impact mitigation effect, neither increasing nor decreasing structural damage probability ($p = 0.491$ and $p = 0.193$ respectively). Vegetated dunes significantly decreased structural damage probability ($p = 0.084$), becoming effectively a factor with similar importance as the distance from the shoreline to the settlement. Elevation (topography) had no effect in the structural damage model ($p = 0.346$).

Table 3.7. Variables used for the structural damage model (STD) showing standardized regression coefficients (\pm standard error) and their corresponding p values. Generalized linear mixed model using an spatial spherical covariance matrix as a random term. Estimation technique: Pseudo Likelihood. N=128.

Intercept	IWH-s	E _F -s	D-s	LCR _F	LCR _{B2}	DN	WL	X ² / Df ^a
-1.73 \pm 0.31 ($p < 0.001$)	18.3 \pm 3.67 ($p < 0.001$)	-4.52 \pm 3.84 ($p = 0.243$)	-5.99 \pm 3.35 ($p = 0.079$)	1.90 \pm 2.52 ($p = 0.451$)	3.42 \pm 2.68 ($p = 0.203$)			0.90
-1.72 \pm 0.31 ($p < 0.001$)	17.7 \pm 3.58 ($p < 0.001$)	-3.69 \pm 3.89 ($p = 0.346$)	-7.74 \pm 3.67 ($p = 0.039$)	1.87 \pm 2.71 ($p = 0.491$)	3.66 \pm 2.80 ($p = 0.193$)	-7.46 \pm 4.29 ($p = 0.084$)	-3.21 \pm 3.45 ($p = 0.354$)	0.89

Notes: Independent variables used in the models were standardized (suffix ‘-s’) to variance=1, mean=0.

IWH-s= initial water height (standardized), **E_F-s**= maximum elevation in front of the settlement (standardized), **D-s**= distance from the shoreline to the community (standardized), **LCR_F**= Weighted average land cover roughness in front of the settlement, **LCR_{B2}**= Weighted average land cover roughness 20 meters behind the settlement, **DN**= Sand dunes (4 classes: 0-1-3-5) and **WL**= Seawalls (4 classes: 0-1-3-5).

^a Chi square / degrees of freedom: closest to 1 = better fit.

The empirical semi-variograms showed no signs of spatial autocorrelation (Fig. 3.5). Linear assumptions for the MD model were verified on the residuals. Pair-wise correlation tests between model predictors showed no strong associations.

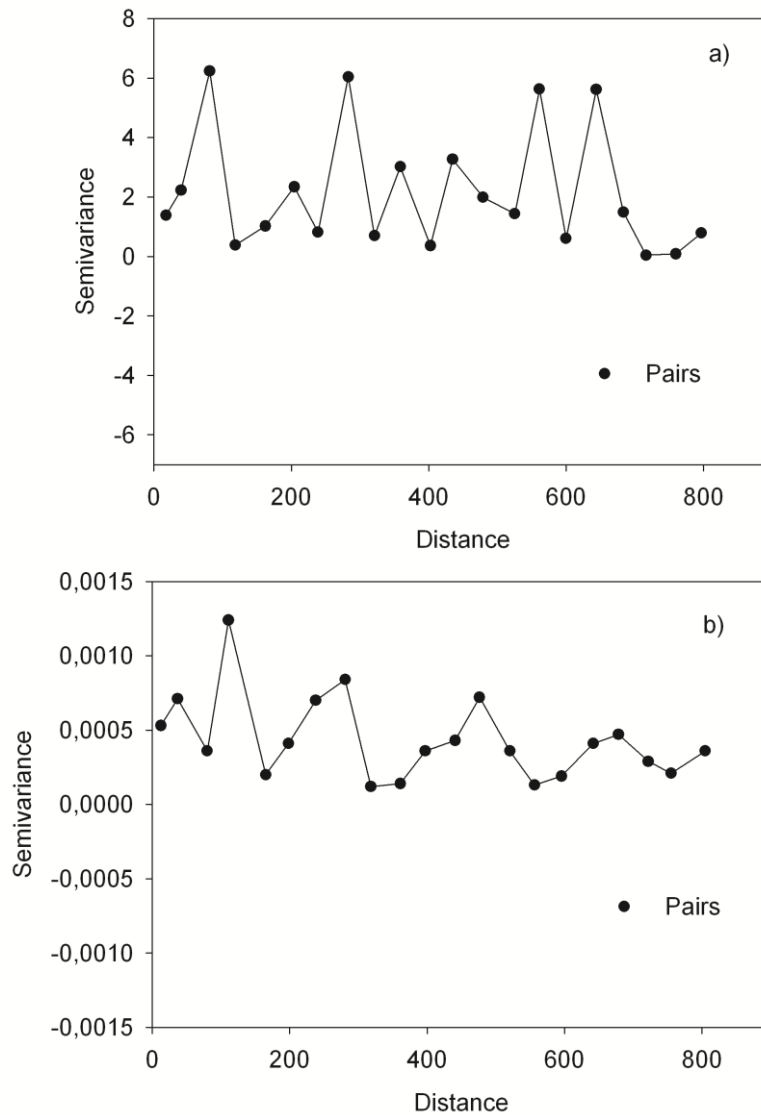


Figure 3.5. Empirical semi-variograms for the a) Structural Damage (**STD**) and b) Maximum Flood Distance (**MD**) models. Pairs > 30.

3.6. Discussion

In order to perform an appropriate analysis and evaluation of the coastal vegetation effects on the 2004 tsunami impact in the Seychelles as well as to extrapolate the conclusions reached, it was important to place the current research in context with the effects the same tsunami event caused in West Aceh, Indonesia. The differences between the Seychelles and Aceh in terms of tsunami intensity and land cover provided a good opportunity to adapt and test the models developed in West Aceh to small wave intensities. Special emphasis was made to understand the effects of dunes that were stabilized by coastal vegetation with regards to tsunami effects inland, since these structures opposed resistance to the wave advance. The progression selected to represent the resistance of seawalls and sand dunes of 0-1-3-5 was in agreement with an exponential increase of resistance mentioned by Barbier *et al.* (2008), representing

adequately the increase of resistance given an increase of height. The models we used have been previously recommended since they can simultaneously analyze several factors and their interactions, but also take possible spatial autocorrelation issues into consideration (Cochard 2011). Several studies criticized previous analysis of tsunami-vegetation interactions and recommended the use of multivariate spatial approaches such as GLMM (Kerr *et al.* 2006, Cochard *et al.* 2008) as those used in this study.

3.6.1. Lack of direct effect of vegetation on impact of low intensity tsunami: Seychelles vs. Aceh

The lack of significance of coastal vegetation effects (LCR) on the maximum flood distance and structural damage models in the Seychelles (Tables 3.6 and 3.7) is one of the main differences with the case of Aceh. It could be explained by two factors: 1) Initial water heights at shoreline (IWH) in the Seychelles were approximately ten times smaller than those found in Aceh (Table 3.4); 2) Compared to densities of coconut plantations and rubber trees in Aceh (150 and 494 trees ha⁻¹, respectively) the Seychelles had a comparatively low tree density. In the affected areas, tree densities in front of the settlements were between 25 and 150 trees per hectare (average of 110 trees ha⁻¹). From the settlement up to 20 meters behind, tree densities were between 10 and 150 trees per hectare (average of 75 trees ha⁻¹). These densities are due to the importance of a scenic value having open beaches for houses and hotels fronting shorelines. The observed lack of direct protection by coastal vegetation in the case of the Seychelles compared to the one observed in the case of Aceh, points towards the need for the adoption of different strategies under different tsunami scenarios. For example, at lower tsunami intensities, passive defenses like dunes can prevent larger damages to buildings whereas under higher wave intensities, thicker strong vegetation between the shoreline and the community allows people to escape reducing the number of casualties. A synergetic strategy that simultaneously considers the maintenance of passive defenses like dunes but at the same time promotes the spatial allocation of thicker robust vegetation between the communities and the sea-shore could be a better option.

While the basic procedure employed to acknowledge coastal vegetation effects considered resistance on a landscape level without requiring more than basic information on land uses, other studies used different methods to allocate resistance of vegetation and objects to an advancing flow (Freeman *et al.* 2000, Latief *et al.* 2007, Järvelä 2004, Järvelä 2005). For our research in Aceh as well as in our current study, these methodologies were deemed complex and highly data demanding. In contrast to our initial Aceh models, where each land cover obtained from the base land use map had, across all transects, a fixed LCR coefficient, the use of variable LCR coefficients on the current study constitutes one of the main differences. These flexible LCR coefficients allowed more precise allocation of the resistance that different types of vegetation opposed to the advance of the wave. The individual allocation of planting densities and consequently resistance of coefficients was a more time consuming process. Yet, since the impact area was limited, such a process was possible. In Aceh this process could not be easily achieved due to the large area (>40 km of coastline) affected.

Direct effects of coastal vegetation mitigating tsunami strength and impacts have been proposed in studies, referring to some of the plant species found in the Seychelles,

such as Casuarina trees (*Casuarina equisetifolia*) Sea almond trees (*Terminalia catappa*) and Coconut (*Cocos nucifera*) (Latief *et al.* 2007, Tanaka *et al.* 2007, Danielsen *et al.* 2005). Nevertheless, probably due to the low tsunami intensity in the Seychelles such direct effects were not observed in our study (Table 3.7). However, these species were used by locals and sometimes recommended by the Minister of Environment and the DRDM of the Seychelles in order to avoid beach erosion by immobilizing sand dunes. Additional effects of these species include esthetical value and promoting tourism which in turn generates revenue. Also, some of these species supported income sources by providing products and derivatives. In countries such as the Seychelles, due to its irregular topography, flat arable land is scarce and is usually relatively close to the coastline; therefore, a protection of income sources is indirectly also a provision of food security for the local population.

3.6.2. Mitigation of tsunami impact by vegetated sand dunes and seawalls

In the Seychelles, most of the affected places were open beaches and areas used for tourism, with relatively low vegetation density. This was reflected by the roughness coefficients (LCR), which were lower than the ones in Aceh (Table 3.4). Behind patches of open beach, vegetation with a very low planting density per area and sand dunes reinforced by vegetation became the only obstacles between the wave and the communities. As physical obstacles, sand dunes fulfill a defensive function by opposing resistance to the water advance (Dahdouh-Guebas *et al.* 2005).

The significant reduction of maximum flood distance by seawalls, but not by sand dunes could be explained due to low tsunami intensity in the Seychelles. According to information provided by DRDM, areas where seawalls existed were previously prone to flooding and susceptible to high tides. Consequently, these barriers erected to counteract those events, also fulfilled their protective function when the low intensity tsunami arrived.

The opposite effect observed for the structural damage model, i.e. vegetated sand dunes, but not seawalls, reducing the structural damage occurrence probability (Table 3.7) pointed also to low tsunami intensity. This meant that open beach areas, i.e. without seawalls, were naturally less susceptible to high tides and flooding. When the tsunami occurred, it affected not only susceptible areas but also open beaches. Nevertheless, those areas presenting the additional physical protection of an obstacle such as dunes fared better than those without them. It must be noted though, that these sand dunes reduced wave strength, reducing structural damage, but not its dispersal or how far the water reached.

Several authors (Tanaka 2009, Liu *et al.* 2005, Hart and Knight 2009) mentioned that gaps in barriers such as sand dunes may cause more damage inland. The present study included the class 'non-existing' for dunes and seawalls, which were corresponding to parts of coastal fronting beaches with no seawalls or permanent (plant immobilized) sand dunes. The existence of partially missing protective structures could be providing some additional supporting evidence to the importance of a continuous rather than a fragmented barrier as suggested by Tanaka (2009). Nevertheless, this hypothesis requires more testing on site for a specific spatial effect of such fragmented barriers.

According to several studies, coastal features such as sand dunes in general diminished the strength of tsunami waves, protecting the communities behind them (Chandrasekar *et al.* 2007, Hart and Knight 2009, Kathiresan and Rajendran 2005, Mascarenhas and Jayakumar 2008). Some of these studies used tsunami scenarios from the south coast of India. Such sites provided conditions where the initial wave force was stronger than in the Seychelles but weaker than in Aceh. Our study results are concurrent with the protective effect ascribed to dunes but with the difference that the barriers observed in our study were stabilized by coastal vegetation. For example, with a given IWH= 3m, the probability of damage to buildings fronting the sea (at the shoreline) with no protection whatsoever was around 35% (Fig. 3.6). This probability is reduced to less than 20% with a dune class 1 (less than 1 meter high) and further to only 5% with a class 2 dune (Fig. 3.6). Therefore, colonizing or purposely planted species that immobilized these sand dunes helped to increase the defense against incoming waves. Policies that promote these types of plant-dune ecosystems should be promoted. These policies should evaluate the use of tree-crops that could provide direct revenue for local inhabitants, but also the possible use of agro-forestry systems with a permanent ground cover that immobilizes structures such as sand dunes. A well thought and locally adapted selection and combination of species could provide simultaneously direct benefits, e.g. products for consumption, as well as indirect services, i.e. landscaping increasing touristic attraction, becoming at the same time protection against incoming waves.

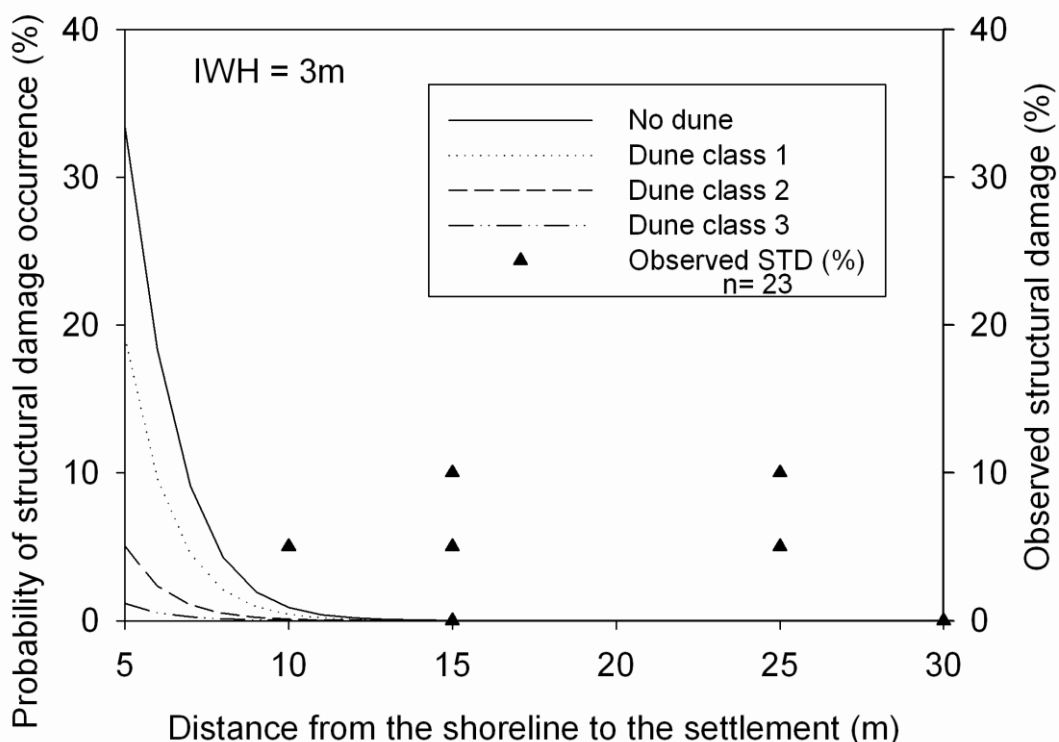


Figure 3.6. Probability of structural damage with distance from shoreline to settlement (D) (lines, **STD** model, Table 3.7) with different dune sizes. Symbols represent observed structural damage (%).

3.6.3. Additional factors influencing impact models

The 2004 tsunami effects on structural damage in the Seychelles with an average of 2% of damage to buildings in the affected area were much less severe than the average 78% of damage to buildings measured on the west coast of Aceh (Table 3.4). Apart from the above described effects of coastal vegetation, other factors such as offshore effects (IWH), distance from the settlement to the shoreline (D) and topography (E) had particular effects on the corresponding models:

With regards to offshore factors, the presence of reefs and the shallow near-shore bathymetry in the Seychelles, reflected by the low IWH, played a major role determining tsunami effects inland (Tables 3.6 and 3.7). The importance of these factors has also been previously established in other sites and referred to in several studies (Laso Bayas et al., 2011, Kurian *et al.* 2006, Chadha *et al.* 2005). In the area studied in Aceh, the absence of reefs left these places without a first line of defense against the waves that could have reduced the force of the incoming tsunami (Kunkel *et al.* 2006). In the current study, structural damage and maximum flood distance models selected initial water height at shoreline (IWH) as having a statistically positive and significant effect, i.e. the higher the initial wave the larger the flooding ($p = 0.023$) as well as the probability of more damage to buildings ($p < 0.001$) (Tables 3.6 and 3.7). When comparing these results with the case of Aceh, the maximum flood distance model for that area also selected IWH as a factor increasing maximum flood distance. This was not the case for structural damage, where IWH was not significant. This counter-intuitive effect occurred since in Aceh, the minimum IWH of 10 m (Table 3.4), was enough to cause total devastation of buildings close to the coast. The resulting structural damage for these areas was not significantly different from that produced by a 20 or 25 m wave.

Distance to the shoreline (D) was an important factor in the current research. The finding that the farther the buildings were located with regards to the shoreline the less damage they suffered was concurrent with the findings of the original model application in Aceh and other studies (Vermaat and Thampanya 2006).

Elevation (E): Generally speaking, when elevation increases, impact of a tsunami decrease, that is, places located on higher grounds are less likely to be affected than those on a lower elevation (Vermaat and Thampanya 2006, Kathiresan and Rajendran 2005). When comparing the current study to Aceh, where the tsunami energy was much higher (IWH average= 20 m, Table 3.4), the similar lack of topographical effect for the structural damage model could be because changes in elevation were small in the affected areas (Table 3.4). Nevertheless, for the maximum flood distance model, elevation changes in Aceh were more evident (Table 3.4), most likely due to the larger distance reached by the water (up to 4.4 km, Table 3.4). Because of these characteristics, in the maximum flood distance model for Aceh, elevation was selected as a significant factor reducing flood distance. Nevertheless, since in the Seychelles elevation changes were modest (Table 3.4) and there was a “funneling” effect in bay areas (Jackson *et al.* 2005, Gelfenbaum *et al.* 2011, Morton *et al.* 2011), flood distance showed a direct positive correlation with elevation (Table 3.6). It is precisely this “funneling” plus different offshore effects, e.g. reef distribution, wave arrival pattern and bathymetry (Jackson *et al.* 2005, Hagan *et al.* 2007), that made bay areas the most affected sites, suffering in the Seychelles an estimated total loss of USD 30

million (UNEP 2006). Embayment effects such as these were non evident on the sites selected in the Aceh study.

With regards to the observed positive correlation between elevation and maximum flood distance, this could be explained by differences between average and maximum flood distances reached by the tsunami event in the Seychelles. Maximum flood distances were 5 to 7 times farther than the observed average maximum flood distance (Table 3.2). The results suggest a funneling effect possibly due to embayment. Previous studies have reported that embayment amplifies the tsunami wave at the shoreline (Gelfenbaum *et al.* 2011, Morton *et al.* 2011). In the Seychelles these effects were noted by previous studies for the 2004 tsunami event (Jackson *et al.* 2005).

3.7. Conclusions and recommendations

Contrary to our observations for the high intensity tsunami event in Aceh, coastal vegetation did not have a significant direct effect in reducing tsunami impact in the Seychelles with its moderate tsunami event. The present study suggested however, that under low tsunami intensity scenarios such as the Seychelles, sand dunes reinforced by coastal vegetation provided additional protection to buildings and structures and should be therefore considered as an important feature with regards to coastal planning and communities' resilience. These structures could serve also as a complementary strategy to direct coastal vegetation protection, an effect not seen for this case (low intensity tsunami scenario) but a valuable investment for the case of possible higher intensity tsunami scenarios, as proven by the results in Aceh. Plant species supporting or in proximity of these dunes not only maintained these structures but also were used as landscaping features, attracting tourism and therefore becoming an important economic consideration given that tourism is one of the main income-generating activities of the islands. Coastal vegetation with high resistance coefficients located in between the sea-shore and the communities could also moderately reduce vulnerability of local inhabitants once tsunami intensities are higher, as seen on the case of Aceh, but dunes appeared to be more important against tsunami impacts when waves strength was lower. It must be noted though that dunes reduced the strength of the wave but not its extension, that is, they diminished the probability of occurrence of structural damage but did not affect maximum flood distance. Seawalls, on the contrary led to a significant reduction of the maximum flood distance, although an effect with regards to decreasing structural damage was not observed. As it was for the case of Aceh-Indonesia, distance from the settlement to the shoreline was in the Seychelles the most important factor to be considered in order to reduce tsunami impacts.

Being around 5000 km from the epicenter of the seaquake, the mere existence of damage and flooding served to prove the intensity of this tsunami event. This peculiarity provided a chance to test and adapt our model under low tsunami intensity. The models also showed that off-shore factors represented by the initial wave height (IWH) did play an important role exacerbating tsunami impacts, i.e. increasing maximum flood distance as well as structural damage.

Adequate coastal planning must ponder the location of the settlements (distance) with regards to the sea shore as the main factor to reduce tsunami impacts. Additionally,

such planning should determine the likelihood of different tsunami intensities in order to decide strategies that are better adapted and use synergetic strategies that could afford additionally some protection to local inhabitants. Tsunami education and disaster preparedness including proper warning systems, and the timely informing of governments and populations (Jin and Lin 2011) are additional important considerations on preparedness and resilience planning. Such planning and strategies should consider the inclusion and promotion of native coastal vegetation that stabilizes and supports physical defense structures such as dunes and beach berms. Such policies shall provide in the middle and long term a higher resilience against natural events such as tsunamis and storm generated waves.

**CHAPTER 4. Comparison of land cover roughness coefficients
derived from different imagery sources using tsunami impact models
from west Aceh, Indonesia**

4. Comparison of land cover roughness coefficients derived from different imagery sources using tsunami impact models from West Aceh, Indonesia³

Laso Bayas J.C.¹, Ekadinata A.², Widayati A.², Marohn C.¹, Cadisch G.¹

¹ *Institute of Plant Production and Agroecology in the Tropics and Subtropics, University of Hohenheim, 70593 Stuttgart, Germany*

² *World Agroforestry Centre (ICRAF), Southeast Asia Regional Program, P.O. Box 161, Bogor 16001, Indonesia*

4.1. Abstract

Land cover roughness coefficients (LCRs) have been used in multivariate spatial models to test the mitigation potential of coastal vegetation to reduce the 2004 tsunami impacts. Previously, a Landsat 2002 satellite imagery was employed to derive land cover maps which were then combined with vegetation characteristics, i.e. stand height, stem diameter and planting density to obtain the 2002 LCRs. The present study tested LCRs extracted from 2003 and 2004 Landsat (30 m) images as well as a combination of 2003 and 2004 higher resolution SPOT (10 m) imagery. Transects along the coast were used to extract land cover, whenever availability and visibility allowed. These new LCRs were used in previously developed tsunami impact models confirmed previous findings regarding distance to the shoreline as a main factor reducing tsunami impacts. Nevertheless, the models using the new LCRs did not perform better than the original one. Particularly casualties models using 2002 LCRs performed better ($\delta AIC > 2$) than the compared Landsat and SPOT counterparts. Adverse climatic conditions at image acquisition date for Landsat and low area coverage for SPOT images decreased statistical predictive power (fewer observations). The results suggested that due to the large spatial heterogeneity existing with regards to tsunami characteristics as well as topographic and land-use features on the area, it was more important to cover a larger number of transects. Nevertheless, if more land cover classes are referenced and high resolution imagery with low cloud cover is available, the full benefits of higher spatial resolution imagery used to extract more precise land use roughness coefficients could be exploited.

4.2. Keywords

Tsunami, West Aceh, GLIMMIX, Land Cover Roughness, Model selection, Landsat, SPOT

³ **A version of this chapter has been considered for publication as:**

Laso Bayas J.C., Ekadinata A., Widayati A., Marohn C., Cadisch G., Comparison of land cover roughness coefficients derived from different imagery sources using tsunami impact models from West Aceh, Indonesia. *Remote Sensing of Environment*. 2014.

4.3. Introduction

During the tsunami event of 2004 traditional land uses were damaged or permanently changed, e.g. large parts of coconut plantations were destroyed, and a major impact on rubber forests could be observed as well, in particular at sites close to the coast line (Szcucinski *et al.*, 2006). In Aceh, specifically in West Aceh, 40 – 60% of pre-tsunami economy relied on tree crops, such as coconut, rubber, coffee, cacao and oil palm (Joshi, 2006). Remote sensing was one of the key tools used by emergency agencies and scientific studies to determine the extent of the damage and its characteristics in order to channel emergency aid effectively and efficiently. Additionally, remote sensing is helping science to achieve research results avoiding long field data gathering campaigns. In some cases, simply due to the local conditions after such a catastrophe, e.g. inaccessible areas along the west coast of Aceh, intensive field studies were simply not possible. The study of Laso Bayas *et al.* (2011) combined the use of processed remote sensing data i.e., land cover maps, with a land cover roughness coefficient (LCR) and information provided by semi-structured field interviews with local inhabitants to develop spatial statistical models to assess the potential tsunami 2004 impact mitigation of coastal vegetation. Data from these interviews were cross-checked with field measurements and secondary governmental and non-governmental databases providing tsunami impact indicators, i.e. structural damages (STD), casualties (CASU), maximum distance reached by the flooding water (MD) as well as relative wave strength, i.e. height of the water at the shoreline (IWH). The developed models related tsunami strength (IWH), topography (E) and land uses existing in the area to the damage indicators, i.e. STD, CASU and MD. According to Laso Bayas *et al.* (2011), sites with coastal vegetation in front of communities showed significant tsunami impact damage mitigation, especially reducing casualties. Mapping assessments (Borrero *et al.* 2006, EC JRC, 2005; Laso Bayas *et al.*, 2007) indicated that along the coastline of Sumatra (Indonesia) major changes in land cover occurred at that time, possibly having a tsunami buffering action due to the presence of coastal vegetation. These facts raised awareness of the importance of sustainable management of the coastal areas including the development of vegetation barriers along the coastal zones (BRR, 2005). For the purpose of planning, the modelling of proneness to tsunami damage as depending on coastal vegetation needs to be more refined.

Based on results of Peltola *et al.* (2000) the relationship between the resistance of coastal vegetation against a pulling/pushing force (e.g. wind, flood, wave) and its plant characteristics, specifically the interaction between a tree diameter (measured at breast height) and its height, was adapted in order to extract land cover roughness coefficients (LCRs) by Laso Bayas *et al.* (2011). The study, based on the tsunami event of 2004, analysed a land cover map developed from a 2002 Landsat satellite image to extract the different land uses. By combining them with their respective characteristics i.e. stem diameter, height and planting density it was possible to obtain LCRs of the transects analysed. These factors represented the resistance that a combination of land uses offered to the advance of the wave and therefore were an important factor of the models.

In order to test if the previously estimated land cover roughness coefficients could be improved using satellite imagery closer to the tsunami date and with higher spatial resolution, the current study employed 4 additional satellite images, i.e. two mid-spatial resolution (Landsat 30 m) and two high spatial resolution (SPOT 10 m) images from 2003 and 2004. LCR coefficients extracted from these images were alternated on

the existing statistical models relating tsunami impacts and coastal vegetation. Land cover maps derived from imagery with a high spatial resolution (SPOT images - 10 m spatial resolution) were expected to show a higher accuracy (Moody and Woodcock, 1994) compared to those corresponding from lower resolution at similar years before the tsunami. In general, remote sensing of data with higher spatial resolution should increase the visual interpretation of the observed scene (Munehika *et al.*, 1993). However, constraints of a higher spatial resolution image are the increased data volume and the processing costs (Gao, 1999) and even so, sometimes they may not provide more accurate results (Takara and Kojima, 1996). In terms of land cover classification and imagery selection, a balance between data processing cost and highest information available per pixel is desired (Gao, 1999; Atkinson, 1997). Data processing costs for the current tsunami impact mitigation models include increased time for field measurements of parameters needed to construct LCR coefficients as well as land cover classes ground-truthing.

By using LCRs extracted from imagery coming from different sensors, the models were also comparing different spectral resolutions. The Landsat imagery used in this study had higher spectral resolution than SPOT imagery since it could separate fine wavelength breaks (Campbell, 1996), shown by the higher number of bands that it has compared to SPOT. Spectral resolution has made a difference in various studies that were able to better differentiate land uses with a higher spectral resolution image despite being of lower spatial resolution (Harvey and Hill; 2011, May *et al.*, 1997). Many studies have proposed different methods to combine these different sources of imagery in order to obtain a desired mix of spatial and spectral resolution (Chavez *et al.*, 1991; Yocky, 1996; Gao, 1999). Given the nature of the tsunami mitigation models, a fast, efficient and reliable source of imagery producing effective LCR coefficients should be recommended.

Nevertheless, since raster datasets were essential for the models used, propagation of errors had to be monitored as recommended by previous studies (Heuvelink *et al.* 1989). Uncertainty and sensitivity analyses check the validity of the model predictions and the usability of its results. They assess model responses looking at the uncertainties of its inputs allocating these to different sources of variation and explaining how the model depends on them (Crosetto *et al.* 2000). Some of the methodologies used for these assessments are Monte Carlo analysis, response surface methodology, and Fourier amplitude sensitivity test (Helton, 1993) as well as the Generalized Likelihood Uncertainty Estimation (Muleta and Nicklow, 2005). An additional sensitivity measure is given by the use of standardized regression coefficients (Hamby, 1995), currently employed in the models in this study.

The present study analysed possible combinations and constraints regarding the use of LCR coefficients, extracted from satellite imagery taken at different dates and by different sensors, for tsunami mitigation models (Laso Bayas *et al.*, 2011) in Aceh, Indonesia. The extracted LCR coefficients based on land use maps derived from SPOT imagery as well as those from Landsat imagery closer to the tsunami event of December 2004 were expected to produce better tsunami mitigation models than the previously used LS02 derived land cover maps. These models were compared through their relative goodness of fit using the Akaike Information Criterion (AIC) (Akaike, 1974).

An effective solution for risk mapping and coastal planning as well as a more generic and widely applicable tool, not only for the region but also globally, was the aim of the comparison.

4.4. Methodology

4.4.1. Impact mitigation models

The models previously developed by Laso Bayas *et al.* (2011), described the role of coastal vegetation in impact mitigation of a tsunami event. Those models statistically related tsunami impacts on land to several characteristics. Two of these models used offshore factors (IWH), distance from the community to the shoreline (D), topography (elevation m a.s.l., E) and overland roughness/resistance (mainly coastal vegetation, LCR) to explain number of casualties (CASU) as well as the maximum flood distance reached by the tsunami waves (MD) (eqs. 2.4 -2.5)

In the original study (Laso Bayas *et al.*, 2011), overland resistance was given mainly by coastal vegetation coverage existing before the tsunami event. For this, Landsat 2002 land use maps covering an area of more than 100 km along the Aceh coastline were used. The land use map was developed by the World Agroforestry Center (ICRAF)-South East Asia. Landsat 2002 was employed originally because it covered a larger section of the study area compared to those coming from different sensors. Additionally, by being free from cloud and haze it provided better image quality than newer Landsat images. The current study tested ways to improve the previously developed models by comparing them against additional ones built using land cover coefficients (LCRs) derived from imagery with higher resolution and dates closer to the tsunami event.

Once land cover was extracted from satellite images, it was transformed to vegetation resistance (VR) using a combination of their inherent characteristics, mainly height (H) and diameter at breast height (DBH), as determined by Peltola *et al.* (2000). By including planting density, the vegetation resistance coefficient (VR) at stand level was defined as seen on equation 2.1.

The VR coefficient allowed translating vegetation specific characteristics into an approximation of resistance of land uses against a moving force, at a landscape level. In the study of Laso Bayas *et al.* (2011) transects 550 m wide were used to extract the area covered by every land use and each of these areas was then multiplied with their corresponding vegetation resistance coefficient in order to obtain a cumulative land cover roughness (see eq. 2.2).

A corrected coefficient that acknowledged distance (intrinsically included in eq. 2.2), i.e. a weighted average land cover roughness coefficient 'LCR' was used in the impact models describing tsunami impact (see eq. 2.3).

Thus, LCR describes the resistance at landscape level of the combination of several different types of land uses in a transect. It is a volumetric resistance approximation that includes height, density and area covered by each of the land cover classes included on each transect. The total possible area to be compared in each of the considered models can be seen in Table 4.1. Land cover types identified in the study area for each of the satellite images classified (with their respective coefficients) are shown in Table 4.2. Additionally, as reported by community members and mentioned by Laso Bayas *et al.* (2011), the vegetation directly behind a settlement influenced the

tsunami impact they experienced. Therefore, as in the original models (eqs. 2.4-2.5), the land cover roughness of the first 500 m behind the settlement was also evaluated and added as a further predictor (LCR_{B5}) in the impact models.

Table 4.1. Summary of total possible areas to be compared using the tsunami impact models^a.

Detail	Landsat 2002	vs. LS03	vs. LS04	vs. SPOT^b
Area				
(pixels) ^c	257,585	136,601	106,334	125,880
Transects	180	84	63	109
Area (ha)	23,183	12,294	9,570	11,329
% of area vs. original model ^d		53	41	49

Notation: LS= LANDSAT; 02= 2002, 03= 2003, 04= 2004. ^a= Full available transects, from shoreline to maximum flood distance. ^b= Combination of available transects from 2003 and 2004 SPOT imagery (i.e. free of clouds/haze) ^c= Pixel size= 30 x 30 m (Landsat based) ^d= Tsunami mitigation model based on 180 transects overlaid on Landsat 2002 land cover map (Laso Bayas et al., 2011)

A spatially explicit statistical analysis employing generalized linear mixed models was used to evaluate the data (Schabenberger 2005). For the present study, two of the original three models employed by the authors (Laso Bayas et al., 2011) describing the relationships between estimated impact and factors were used. These models were selected because their relative goodness of fit was reported in terms of AIC. This particularity, added to the use of Maximum Likelihood (ML) instead of Restricted Maximum Likelihood (REML) as the estimation technique, allowing to perform model selection sequences comparing models with different predictors, i.e. LCRs coming from different imagery dates and sources.

Table 4.2. Land cover types, area covered, planting densities, and vegetation resistance coefficients (VR) in available study transects (T) from each of the satellite images considered^a. West coast of Aceh (Calang to south of Meulaboh). Ordered by VR. Adapted from (Laso Bayas et al., 2011)

Land-cover type (%)	LS02 T=180	LS03 T=84	LS04 T=63	SP03 T=71	SP04 T=70	Estimated planting density (stems ha ⁻¹)	VR (m ³ ha ⁻¹) ^b
Cleared land: Areas with no vegetation	0.63	3.37	0.20	5.82	2.94	0	0
River: Water areas including ponds and estuaries	3.33	4.41	3.64	3.39	3.73	0	0
Agriculture: Various crops, mostly vegetable plantations	0.03	0.00	0.00	0.00	0.00	31,250	13
Grass: Grasses growing on previously cleared areas or used for animal feed e.g. <i>Imperata spp.</i>	8.34	7.66	16.49	3.49	21.08	2,000,000	15
Rice field: Plantations of <i>Oriza sativa</i> , usually paddies	19.04	20.80	24.86	16.12	12.70	2,000,000	15
Shrub: Natural vegetation of 1 to 2 m height	0.01	0.82	5.38	7.32	2.27	4,445	150
Cocoa: Plantations of <i>Theobroma cacao</i>	1.99	0.00	0.00	0.00	0.00	1,111	156
Coconut: Plantations of <i>Cocos nucifera</i>	20.46	3.34	8.03	8.54	2.97	156	281
Oil palm: Plantations of <i>Elaeis guineensis</i>	4.45	0.00	0.00	0.00	0.00	156	366
Agroforest: Combination of different plant species with canopies at various levels e.g. mango (<i>Mangifera indica</i>), coffee (<i>Coffea arabica</i>), sugar cane (<i>Saccharum spp.</i>) and vegetables	6.34	33.24	22.88	25.21	31.57	625	844
Rubber: <i>Hevea brasiliensis</i> , mostly extensive jungle rubber	16.72	14.38	11.08	16.84	13.64	494	1,343
Forest: Local timber and non-timber species on protected and non-protected areas	0.24	0.00	1.74	0.00	0.00	494	2,099
Settlements	17.11	9.79	4.31	11.68	7.54	N/A	3,538

Notation: LS= LANDSAT; SP= SPOT; 02= 2002, 03= 2003, 04= 2004

Note: From the transects, given the quality of the image, (see Figs 4.1 and 4.2), there was still 1-4% of the area non-identifiable on satellite imagery (classified either as cloud, shadow or no data). Classification accuracy >75%. ^a= Transects shown here represent the total number of transects available on each image without any additional condition. ^b=‘m³ ha⁻¹’, refers to volume of plants (stems) resisting the force of water advancing per hectare. See eqs. 2.2-2.3.

4.4.2. Land cover classification

A general overview of how the transects were set is shown in Figures 4.1 and 4.2. Figure 2.2 shows a transect schematic with the parameters used in the current models.

Laso Bayas *et al.* (2011) extracted land cover roughness coefficients using land cover maps developed from Landsat imagery dated 14th of May, 2002. The image was chosen because it was the closest image to the tsunami event date that covered a large area with low or non-existent cloud cover. In the present study, two additional images from Landsat (30 m) dated 10th of February, 2003 and 12th of June, 2004 as well as two high-resolution (10 m) SPOT images dated from 18th July, 2003 and 10th of July, 2004, were considered to obtain additional LCR coefficients. Despite their increased cloud coverage, these images were chosen because they were closer to the tsunami event date but also to the acquisition month of Landsat 2002. This was done to minimize vegetation differences (wavelength reflection on different seasons), although availability and cloud coverage did not allow for an exact month-match. A hierarchical object-based classification procedure was executed for each of the four additional images using the software Definiens Developer® 7.0. The first level of the hierarchical segmentation defined major objects in the landscape, i.e. sea, land and major clouds/haze. The second level segmentation separated land into vegetation and non-vegetation. The third level divided vegetation into trees and non-trees and non-vegetation into rivers, smaller clouds/haze, cleared land and settlements, including roads and buildings. The fourth segmentation level separated trees into their final land uses, i.e. agroforests, cocoa, coconut, shrub, oil palm, rubber and forest; non trees included grass, rice and agriculture. Object sizes were decreasing at each segmentation level and were adapted to each type of sensor according to perceived visual accuracy. The final land cover classification used the same land cover classes as those employed by Laso Bayas *et al.* (2011) in the previously developed models (Table 2.1). In these models the Landsat 2002 land-cover classification was done using ground-truth GPS points taken after the tsunami on affected and non-affected areas at the west coast of Aceh. The same set of points and major land cover areas were employed in the classification of the new images.

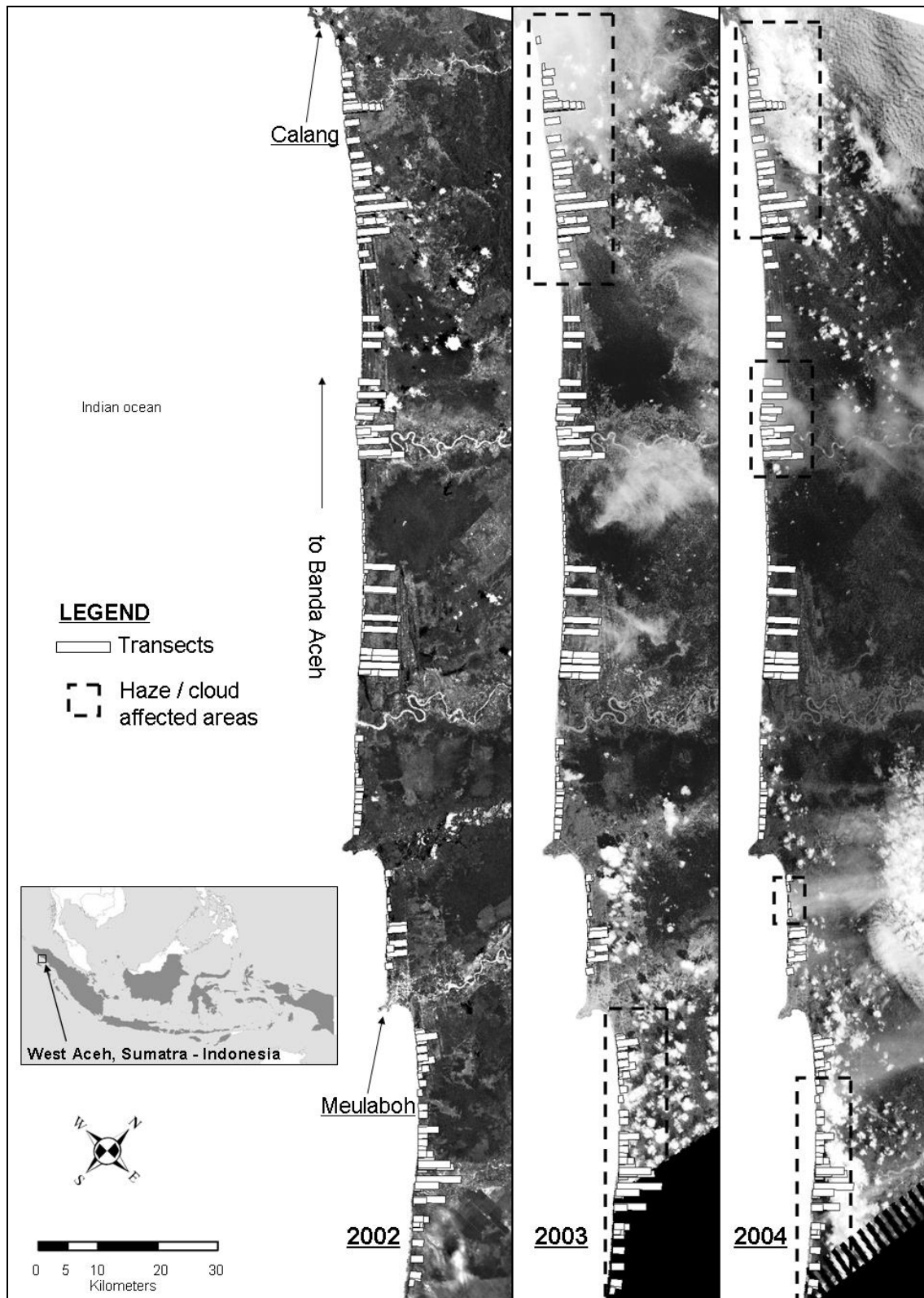


Figure 4.1. Study area showing Landsat® (ETM) imagery from three different years. Areas where cloud, haze or lack of data occurred shown in boxes.

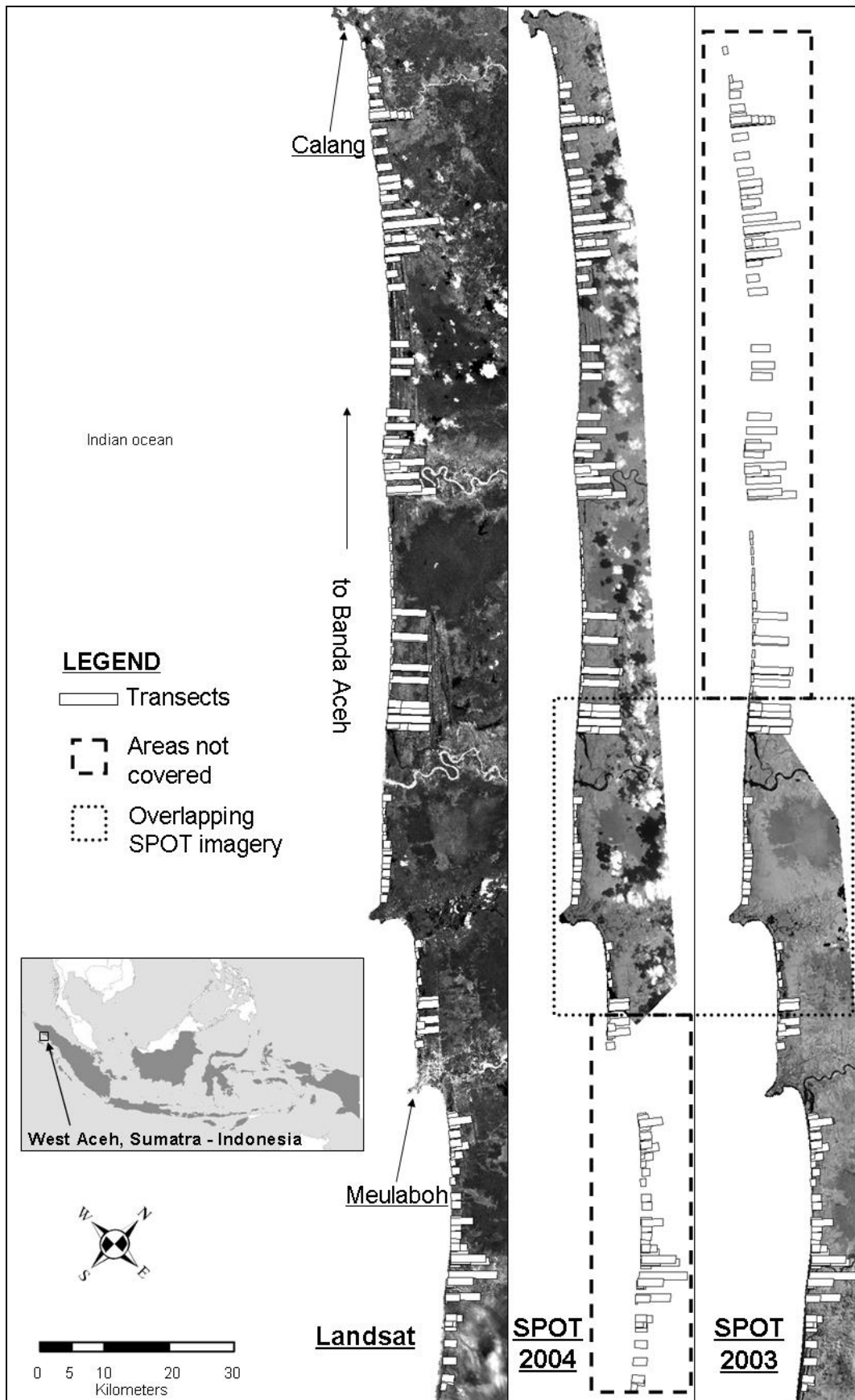


Figure 4.2. Study area showing the original 2002 Landsat® (ETM) image and the high resolution (10m) SPOT images. Areas where cloud, haze or lack of data occurred shown in boxes. Overlapping area of SPOT images is also shown.

To execute the procedure on SPOT imagery, in addition to the existing green, red and infrared bands (bands 1-3), enhanced ‘greenness’ and ‘brightness’ indices were used. These were adapted from the tasselled cap enhancement (Crist and Cicone 1984) and were used as additional parameters within the object-based classification. These combinations were:

$$\text{‘Greenness’} = - 0.30132 (\text{Band 1}) - 0.4321 (\text{Band 2}) + 0.86408 (\text{Band 3}) \quad (4.1)$$

and

$$\text{‘Brightness’} = 0.60539 (\text{Band 1}) + 0.61922 (\text{Band 2}) + 0.50008 (\text{Band 3}) \quad (4.2)$$

For Landsat imagery the visible bands 1-3 were used and additionally the infrared bands 4 and 5 as well as the mid-infrared band 7. A Normalized Difference Vegetation Index (NDVI) (Tucker 1979) was also developed and employed, obtained as:

$$\text{NDVI} = (\text{near IR band} - \text{red band}) / (\text{near IR band} + \text{red band}) \quad (4.3)$$

Afterwards, accuracy tests using the above mentioned ground-truth GPS points were performed for each image classification using a confusion matrix (Campbell 1996) to check overall and user accuracy. A minimum of 75% of accuracy on both ratings was used as benchmark. Cohen’s kappa statistics (ArcView® 3.2) was used to check accuracy (Cohen 1960). Additionally, consistency tests between images in a time sequence were performed using a matrix of change verifying the percentage of inconsistency and possible patterns (Congalton 2011). These checks involved individual land classes comparisons across years as well as ‘resistance’ comparisons, where land classes were grouped into high, medium and low resistance according to their VR values. Subsequent reclassifications and tests were made accordingly to obtain a satisfactory classification i.e. obtaining a minimum accuracy larger than 75%. Consistency changes of land cover classes as well as resistance levels from one year to another were verified on a matrix of change.

Each of these land cover classifications were then used to extract land cover types and their corresponding areas for each transect and these values were converted to land cover roughness coefficients (LCR_F , LCR_{B5} , and LCR_T) as explained in equations 2.1-2.3. These coefficients were pair-wise compared in each of the two impact models (eqs. 2.4-2.5). Only transects that were shared between the compared imagery were used as observations for the model. Nevertheless, each individual available SPOT image, i.e. 2003 as well as 2004 only covered a reduced area compared to Landsat (Fig. 4.2). Therefore, transects extracted from both SPOT images (2003 and 2004) were combined. Additionally, since both SPOT images had overlapping transects (Fig. 4.2) a combination that included all transects from SPOT 2003 plus additional ones from 2004 (SP3+) was selected. This increased the number of transects ($n=109$, Table 4.1) to compare against the model using LS02 derived coefficients, although not as many as in the original study ($n=180$).

AIC (δ AIC) was employed while comparing models to assess possible improvements given their different LCR sources. Standardized regression coefficients giving a measure of sensitivity to possible changes (Hamby, 1995) are shown for each of the comparisons.

4.5. Results

4.5.1. Image classification

The land cover classification was performed satisfactorily on the tested four additional images (Landsat and SPOT 2003 + 2004) with accuracies reaching levels above 85%. The major constraint for image classification was the existence of clouds and haze on the Landsat 2003 and 2004 images as well as lack of coverage in some areas. This reduced the number of transects and area covered by more than 50% for Landsat 2004 compared to those obtained from the Landsat 2002 image (Fig. 4.1, Table 4.1). Due to this decrease, the comparison of the original Landsat 2002 model was done only against Landsat 2003, which covered 50% of the original area and 47% of the transects from the original model.

Combining SPOT 2003 and 2004 images (SP3+) allowed to increase the area covered compensating for the reduced area coverage of the individual images (Fig. 4.2). Nevertheless a reduced overall area and number of transects to compare was unavoidable (Table 4.1). Despite this reduction, the SP3+ area compared was almost 50% of the original one (Landsat 2002) and the overlapping transects constituted 60% of the original model. Furthermore, consistency checks for resistance coefficients (LCR's) were successful for all the imagery used.

All the roughness coefficients data (LCR_F , LCR_{B5} , and LCR_T) for the newly classified images from Landsat as well as SPOT 2003 and 2004 showed similar patterns of distribution (Fig. 4.4). Compared to the previous study (Laso Bayas *et al.*, 2011), the indicators in the present research, especially LCR_F , showed mostly lower values of resistance. The tendency can be seen in Figure 4.5, where LCR_F total resistance estimates were lower using Landsat 2003 and SPOT imagery than Landsat 2002 by ca. 15% and 25% respectively.

When comparing the land cover changes in front and behind the settlements as well as along the whole transect (until maximum flood distance), the patterns for both comparisons were very similar (Fig. 4.5) with one exception. When comparing LS02 vs LS03, rice fields occupied more area in LS03 for all LCRs (~3-8%). The opposite is true when comparing LS02 vs SP3+, where all but LCR_{B5} have more rice area covered in LS02 than in SP3+ (~2-8%, Fig. 4.5). In general, land uses with low VR values seem to have a larger coverage in LS03 and SP3+ than in LS02. Agroforestry, with a large VR value ($844 \text{ m}^3 \text{ ha}^{-1}$), showed the same increased tendency (~28-31%, Fig. 4.5). Nevertheless, land uses with mid and high values of VR such as Coconut, Oilpalm, Rubber and Settlements showed a reduced percentage of coverage in LS03 and SP3+ vs. LS02 with values ranging from ~2% for settlements in LCR_T to ~28% for coconut in LCR_{B5} (Fig. 4.5).

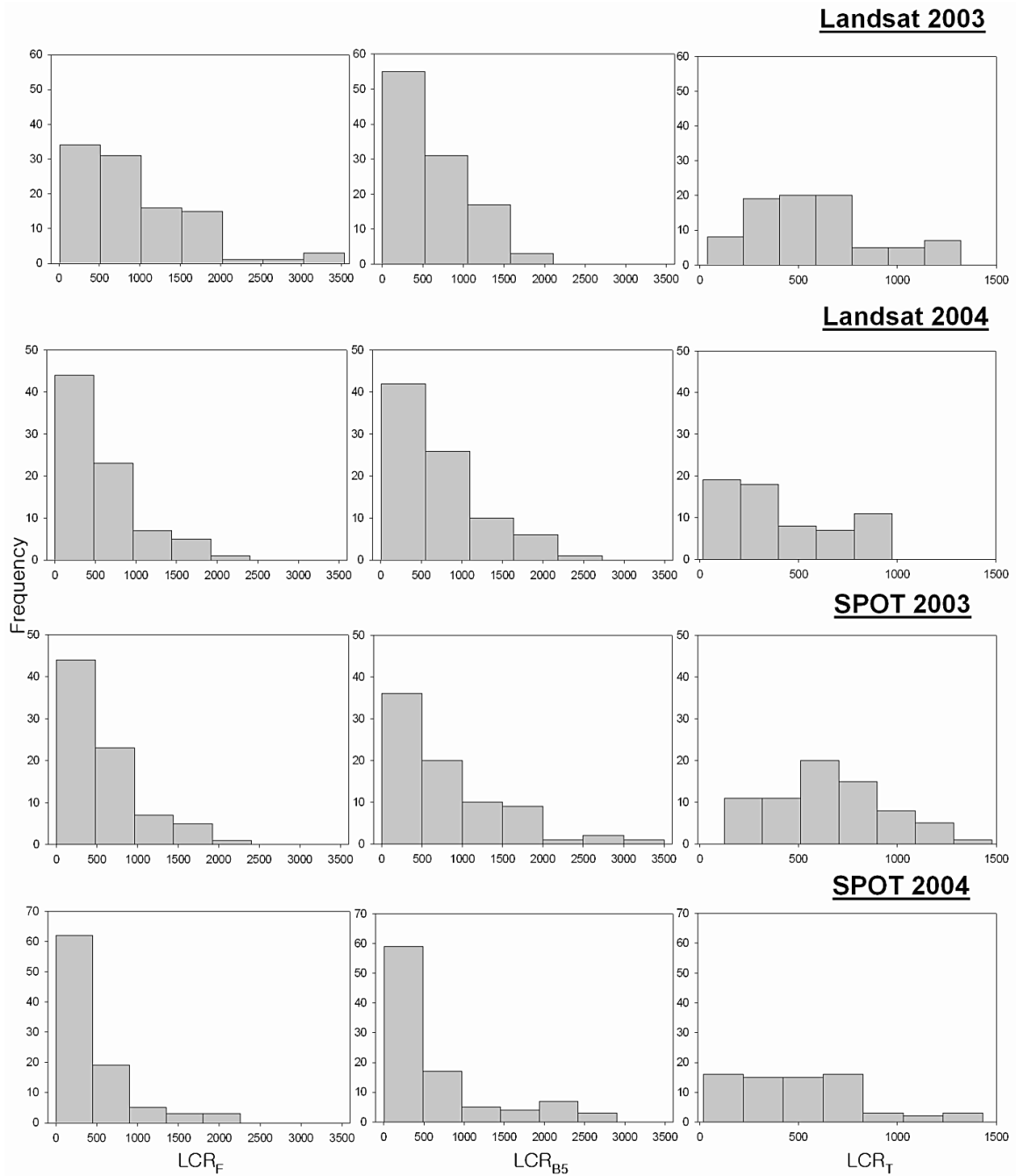


Figure 4.4. Histogram comparisons for weighted average land cover roughness in front of the settlement (LCR_F), weighted average land cover roughness from the settlement up to 500 m behind (LCR_{B5}) and weighted average land cover roughness in the transect (up to the maximum flood distance) (LCR_T).

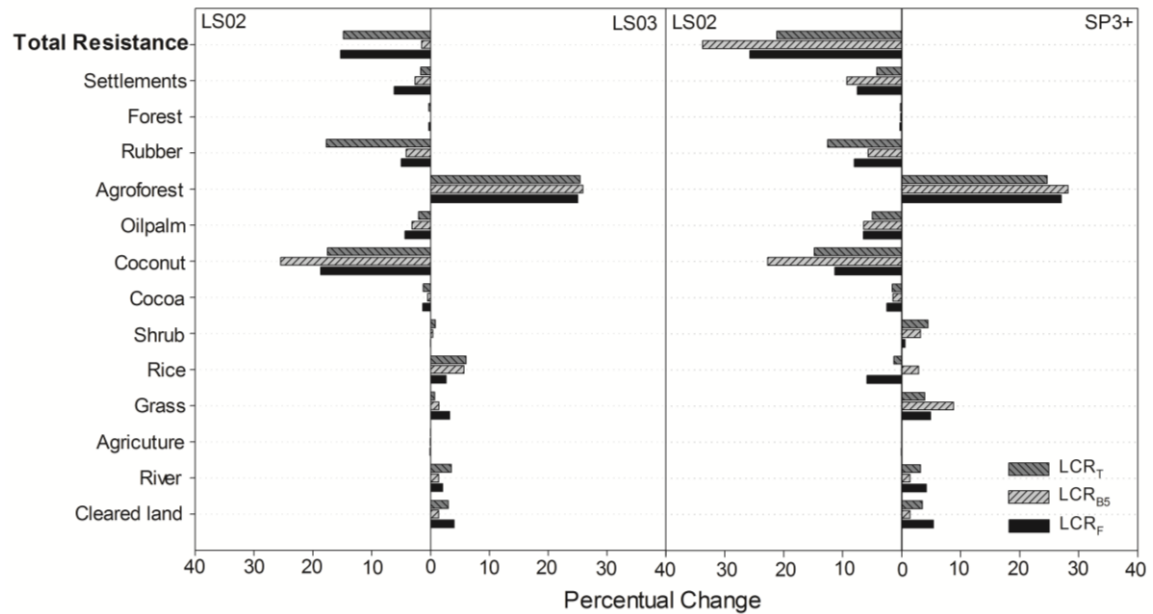


Figure 4.5. Change in total resistance and land cover roughness coefficients from Landsat 2002 (LS02) and SPOT imagery^a 2003-2004 (SP3+) with regards to Landsat 2002 (LS02). Transects selected overlap both imagery sources compared (see Fig. 4.2). West coast of Aceh (Calang to south of Meulaboh). Land uses ordered by vegetation resistance coefficients (VR).

Note: In order to obtain total resistance, each land cover percentage was multiplied by its VR then added up. From transects that overlapped each satellite image (given the quality of the image, see Figs 4.1 and 4.2), there was still 1-4% of the area non-identifiable on satellite imagery (classified either as cloud, shadow or no data).^a SP3+ = all transects from SPOT 2003 plus additional ones from SPOT 2004. LCR_F, LCR_{B5} and LCR_T = land cover roughness coefficients in front of the settlements, from the settlements up to 500 m behind and from shoreline to maximum flooded distance, respectively.

When comparing the land cover changes in front and behind the settlements as well as along the whole transect (until maximum flood distance), the patterns for both comparisons were very similar (Fig. 4.5) with one exception. When comparing LS02 vs LS03, rice fields occupied more area in LS03 for all LCRs (~3-8%). The opposite is true when comparing LS02 vs SP3+, where all but LCR_{B5} have more rice area covered in LS02 than in SP3+ (~2-8%, Fig. 4.5). In general, land uses with low VR values seem to have a larger coverage in LS03 and SP3+ than in LS02. Agroforestry, with a large VR value (844 m³ ha⁻¹), showed the same increased tendency (~28-31%, Fig. 4.5). Nevertheless, land uses with mid and high values of VR such as Coconut, Oilpalm, Rubber and Settlements showed a reduced percentage of coverage in LS03 and SP3+ vs. LS02 with values ranging from ~2% for settlements in LCR_T to ~28% for coconut in LCR_{B5} (Fig. 4.5).

In the previous research the factor LCR_F showed a more normally distributed frequency (Fig. 2.5) due to larger values of resistance compared to the current LCR_F values (Fig. 4.4).

4.5.2. Models comparison

Overall values of resistance measured through LCR_F , LCR_{B5} and LCR_T were higher using LS02 than LS03 or SP3+ images (Tables 4.3a-4.3b). For the casualties models, LCR_F was almost one third lower for LS03 and SP3+ than their LS02 counterpart (Table 4.3a). Also LCR_{B5} from LS02 was more than a quarter higher in both comparisons (Table 4.3a). In the maximum flood distance models (MD) LCR_T values from LS02 were more than 40% higher when comparing against LS03 and 20% higher when comparing against SP3+ (Table 4.3b).

Table 4.3a. Variables used in the casualties (CASU) models and their descriptive statistics showing mean (\pm standard deviation) and minimum-maximum values (in brackets). The land cover resistance factors (LCR_F , and LCR_{B5}) are specific to each satellite image whereas the other variables values are similar for each compared pair. Transects selected (N) overlap the compared imagery (see Figures 4.1 and 4.2). West coast of Aceh (Calang to south of Meulaboh).

N	Source	CASU (%)	IWH (m)	D (m)	E_F (m)	LCR_F	LCR_{B5}
88	LS02	47 ± 29 (0-95)	23 ± 2 (20-25)	1050 ± 1100 (50-3400)	12 ± 5 (6-47)	1334 ± 697 (70-3538)	827 ± 638 (6-2369)
	LS03					904 ± 657 (37-3538)	619 ± 483 (8-2106)
114	LS02	45 ± 29 (0-95)	21 ± 4 (10-25)	700 ± 550 (50-3000)	12 ± 3 (6-24)	1327 ± 687 (71-3538)	1015 ± 577 (0-2370)
	SP3+					896 ± 594 (49-2826)	759 ± 447 (15-2472)

Notation: LS= LANDSAT; SP3+= all transects from SPOT 2003 plus additional ones from SPOT 2004; 02= 2002, 03= 2003. IWH = initial water height (m), D = distance from the shoreline to the settlement (m), E_F = Maximum elevation at the settlement level (m), LCR_F = weighted average land cover roughness in front of the settlement, and LCR_{B5} = weighted average land cover roughness up to 500 m behind the settlement.

Table 4.3b. Variables used in the maximum flood distance (MD) models and their descriptive statistics showing mean (\pm standard deviation) and minimum-maximum values (in brackets). The land cover resistance factor (LCR_T) is specific to each satellite image whereas the other variables values are similar for each compared pair. Transects selected (N) overlap the compared imagery (see Figures 4.1 and 4.2). West coast of Aceh (Calang to south of Meulaboh).

N	Source	MD (m)	IWH (m)	E_T (m)	LCR_T
84	LS02	2600 ± 750	23 ± 2	18 ± 5	1020 ± 304 (208-1899)
	LS03	(1550-4250)	(20-25)	(12-47)	579 ± 310 (37-1321)
109	LS02	1950 ± 600	21 ± 4	20 ± 9	1030 ± 308 (208-1899)
	SP3+	(800-3950)	(10-25)	(12-74)	814 ± 268 (240-1632)

Notation: LS= LANDSAT; SP3+= all transects from SPOT 2003 plus additional ones from SPOT 2004; 02= 2002, 03= 2003. IWH = initial water height (m), E_T = maximum elevation over the whole transect (m), LCR_T = weighted average land cover roughness in the transect.

Overall, the casualties (CASU) model based on Landsat 2002 performed better ($\delta AIC > 2$) than the one based on Landsat 2003 (Table 4.4a). No ranking difference ($\delta AIC < 2$) was seen for any of the other models (Tables 4.4a-4.4b)

Table 4.4a. Selected models for the casualties (CASU) models using the roughness coefficients derived from different satellite imagery. Standardized regression coefficients (\pm standard error) and their corresponding p value as well as incremental AIC (δ AIC) indicating better fit are shown. Transects selected (N) overlap the imagery compared (see Figures 4.1 and 4.2). Generalized linear mixed model using a spatial variance-covariance model fitted by a random term. Estimation technique used: Maximum likelihood (ML). West coast of Aceh (Calang to south of Meulaboh).

N	Source	Intercept	IWH-s	D-s	E _F -s	LCR _F -s	LCR _{B5} -s	δ AIC
88	LS02	0.47 \pm 0.04 (<i>p</i> <0.001)	-0.23 \pm 0.31 (<i>p</i> =0.472)	-2.35 \pm 0.31 (<i>p</i> <0.001)	-0.45 \pm 0.23 (<i>p</i> =0.053)	-0.75 \pm 0.22 (<i>p</i> =0.001)	0.24 \pm 0.18 (<i>p</i> =0.183)	8.85
		LS03	0.47 \pm 0.04 (<i>p</i> <0.001)	-0.12 \pm 0.36 (<i>p</i> =0.740)	-2.37 \pm 0.33 (<i>p</i> <0.001)	-0.44 \pm 0.24 (<i>p</i> =0.077)	-0.31 \pm 0.19 (<i>p</i> =0.103)	
114	LS02		0.08 \pm 0.59 (<i>p</i> <0.889)	0.11 \pm 0.21 (<i>p</i> =0.597)	-0.57 \pm 0.10 (<i>p</i> <0.001)	-0.08 \pm 0.08 (<i>p</i> =0.283)	-0.17 \pm 0.07 (<i>p</i> =0.018)	0.04 \pm 0.06 (<i>p</i> =0.432)
		SP3+	0.13 \pm 0.48 (<i>p</i> =0.7937)	0.12 \pm 0.20 (<i>p</i> =0.548)	-0.57 \pm 0.10 (<i>p</i> <0.001)	-0.08 \pm 0.08 (<i>p</i> =0.282)	-0.14 \pm 0.06 (<i>p</i> =0.030)	-0.06 \pm 0.06 (<i>p</i> =0.281)

Notation: LS= LANDSAT; SP3+= all transects from SPOT 2003 plus additional ones from SPOT 2004; 02= 2002, 03= 2003. IWH-s = initial water height, D-s = distance from the shoreline to the settlement, E_F-s = Maximum elevation at the settlement level, LCR_F-s = weighted average land cover roughness in front of the settlement, and LCR_{B5}-s = weighted average land cover roughness up to 500 m behind the settlement. All independent variables used in the models were standardized (suffix “-s”) to variance = 1, mean = 0. *Akaike information criterion. A difference larger than 2 points (δ AIC) is considered as a sufficient threshold to rank models (Burham and Anderson, 2002)

Distance from the shoreline to the settlement (D) remained as the most important factor decreasing casualties (*p*<0.01) and weighted average land cover roughness in front of the settlement (LCR_F) also appeared to significantly decrease casualties in all models at α = 0.1 (Table 4.4a). The original model used 180 transects whereas the current LS02 CASU and LS02 MD models used 88 and 84 transects respectively when compared to models employing Landsat 2003; the same models use 114 and 109 transects respectively when compared to models using SPOT imagery (Tables 4.4a-4.4b).

Table 4.4b. Selected models for the maximum flood distance (MD) models using the roughness coefficients derived from different satellite imagery. Standardized regression coefficients (\pm standard error) and their corresponding p value as well as incremental AIC (δ AIC) indicating better fit are shown. Transects selected (N) overlap the imagery compared (see Figures 4.1 and 4.2). Generalized linear mixed model using a spatial variance-covariance model fitted by a random term. Estimation technique used: Maximum likelihood (ML). West coast of Aceh (Calang to south of Meulaboh).

N	Source	Intercept	IWH-s	E _T -s	LCR _T -s	δ AIC
84	LS02	0.54 \pm 0.13 (<i>p</i> =0.148)	0.13 \pm 0.17 (<i>p</i> =0.448)	-0.04 \pm 0.06 (<i>p</i> =0.481)	0.03 \pm 0.07 (<i>p</i> =0.716)	0.45
	LS03	0.54 \pm 0.13 (<i>p</i> =0.154)	0.12 \pm 0.17 (<i>p</i> =0.477)	0.04 \pm 0.06 (<i>p</i> =0.500)	0.03 \pm 0.08 (<i>p</i> =0.758)	
109	LS02	0.52 \pm 0.05 (<i>p</i> <0.001)	0.01 \pm 0.02 (<i>p</i> =0.625)	-0.02 \pm 0.01 (<i>p</i> =0.045)	0.01 \pm 0.01 (<i>p</i> =0.224)	1.28
	SP3+	0.53 \pm 0.05 (<i>p</i> <0.001)	0.01 \pm 0.02 (<i>p</i> =0.669)	-0.02 \pm 0.01 (<i>p</i> =0.043)	0.00 \pm 0.01 (<i>p</i> =0.654)	

Notation: LS= LANDSAT; SP3+= all transects from SPOT 2003 plus additional ones from SPOT 2004; 02= 2002, 03= 2003. IWH-s = initial water height, E_T-s = maximum elevation over the whole transect, LCR_T-s = weighted average land cover roughness in the transect. All independent variables used in the models were standardized (suffix “-s”) to variance = 1, mean = 0. *Akaike information criterion. A difference larger than 2 points (δ AIC) is considered as a sufficient threshold to rank models (Burham and Anderson, 2002)

4.5.3. Parameter performance across models

D: In all the model comparisons, distance to the shoreline (D) was the most important and significant factor reducing casualties (Table 4.4a).

IWH: Initial water height did not show any significant effect either increasing or decreasing casualties or maximum flooded distance in any of the comparisons. (Tables 4.4a-4.4b).

E: Elevation showed to be a significant factor reducing casualties for the comparisons amongst Landsat imagery but not when comparing LS02 to SP3+ (at α = 0.1, Table 4.4a). In the maximum flooded distance models elevation significantly decreased MD only when comparing LS02 to SP3+ models (α = 0.05, Fig 4.4b). No significant effect was detected for the models comparing LS02 to LS03.

LCR_T: No significance in any of the pair-wise comparisons for the maximum flood distance models was observed (α = 0.1, Table 4.4b). This result is in agreement with the findings of the original model,

LCR_F: The previous study by the authors also determined that vegetation in between the coast and the settlement (LCR_F) significantly decreased casualties. This assertion was maintained in all comparisons at a level of α = 0.05, except at the model using LS03 (*p* = 0.1, Table 4.4a).

LCR_{B5}: Vegetation behind the settlements (LCR_{B5}) did not show significant effects for any of the pair-wise comparisons ($\alpha=0.1$, Table 4.4a).

4.6. Discussion

Overall, although no apparent improvement by the use of higher resolution imagery and/or imagery closer to the tsunami event was seen ($\delta AIC < 2$), the MD model using SPOT imagery displayed higher AIC than the one using LS02 ($\delta AIC = 1.28$, Table 4.4b), showing promise for a better performance using high resolution imagery.

The comparisons made on this study maintain the same trends seen in the original model (Laso Bayas et al., 2011), namely that D and LCR_F are key variables reducing casualties. With regards to the other parameters, IWH and LCR_{B5} were not selected as significant variables, as it was the case for the original model. This could be explained by observing the different means (\pm standard deviations) and ranges of these variables in the current study (Table 4.3a) with regards to those from the original model (Table 2.2). Particularly, the maximum value LCR_{B5} in the current comparisons is about 2472 m³ ha⁻¹ (Table 4.3a) when in the original model it reached up to 3444 m³ ha⁻¹ (Table 2.2). This translates into a 30% less vegetation resistance which is in fact in agreement with the conclusions of the original model (Laso Bayas et al., 2011) where vegetation with low resistance is recommended to be allocated behind the settlements to avoid trapping people escaping a tsunami. In the current models the lower vegetation resistance is due to the lack of availability of all transects used on the original model, mainly, for the case of LCR_{B5}, due to the presence of clouds in the areas behind the settlements (away from the shoreline) (Figs. 4.1-4.2).

Nevertheless, despite the drastic overall reduction of transects (~40-50%) between the original (with 180 transects) and the current models, the statistical decrease of casualties explained by D and, most importantly, by LCR_F, shows the robustness of the developed models and their land cover resistance coefficients.

In order to fully utilize the increased resolution of SPOT vs. Landsat imagery, a more specific land use classification would be desired. Nevertheless, in the current study budget constraints did not allow an additional field campaign. This would be required in order to obtain more specific ground-truth points for new land use classes to determine their specific vegetation characteristics. Despite this lack of additional information, we postulated that model differences would still be expected, favouring higher spatial resolution imagery. The following discussion about the differences existing with the models using diverse imagery sources might shine a light on what factors should be considered as priorities when developing more accurate tsunami impact mitigation models.

4.6.1. Impacts of differences in land cover maps on LCRs

The land cover roughness coefficients (LCRs) extracted from each transect are formed by a weighted average of all the different land uses that compose such a transect. As explained above, different land uses have specific characteristics, i.e. specific stem height, stem diameter and planting density. When a land cover classification of a satellite image is developed, any possible accuracy errors, i.e. mistakenly allocating a

land cover type to an area that contains a different type of vegetation, will be reflected in the LCR of the transect. Nevertheless, most of the errors made in land cover allocation occurred between land use types that have similar characteristics i.e. similar VR. For example, an increased rubber area, resulting in an overall higher LCR, may be counter-weighted by the decrease of agroforest area, a land use that had a similar reflectance as rubber and almost similar VR.

Most of the errors of land cover classification from a satellite image derive from difficulties separating different land uses that have similar reflectance characteristics. In the current study the land cover classes “rubber”, “coconut” and “agroforestry” were some of the groups prone to such errors. Nevertheless, a close analysis of the differences produced in the classification showed that such errors were mostly outweighed by the different proportions of contrasting land uses and their specific characteristics. For example, when comparing the Landsat satellite images from 2002 and 2003 (Fig. 4.5), LCR_{B5} obtained from the 2003 image showed 25% more agroforestry than its counterpart. Nevertheless, once all the land uses were combined, the difference in terms of total resistance index was reduced to only a 2% less than the total resistance of 2002. Similar changes for agroforestry (approx. 25%) occurred in the LCR_F and LCR_T coefficients of the same comparison but in these cases the offset on the total resistance reduction with regards to 2002 was 18% and 16%, respectively. A similar case occurs with the comparison of LS02 against SPOT imagery but in this case, the values observed for settlements are larger (~4-9%) and in favour of LS02. Since this is not fully compensated by the agroforestry values in favour of SP3+, higher total resistance of all LCR coefficients derived from LS02 is observed (Fig. 4.5).

4.6.2. *Model dependence on spatial and temporal resolution*

Overall, the tendency observed in the pair-wise comparisons as well as the model rankings (Tables 4a-4b) seemed to indicate that no major improvement ($\delta AIC > 2$) was achieved neither by the use of imagery closer to the event date and/or of higher spatial resolution. The larger spectral resolution of Landsat seemed to have compensated for its lower spatial resolution. According to the results, a well classified Landsat image covering a larger stretch of coastal area (e.g. Landsat 2002) provided a better input for the current statistical models producing results with high credibility.

Given that the model was used across a large part of the coast and the roughness coefficient was developed as a landscape-wise resistance approximation, results seem to indicate that a highly precise (in terms of spatial resolution) land cover classification may not be required. Our model comparisons suggested that reliable information on coastal vegetation and land cover effects on a tsunami event can be modelled using mid resolution imagery. Nevertheless some considerations must be acknowledged:

- 1) The current analysis classified Landsat and SPOT satellite imagery using the same land cover classes for both type of images, i.e. cleared land, river, agriculture, grass, rice, shrub, cocoa, coconut, oilpalm, agroforest, rubber, forest and settlements (Table 4.2). These classes were employed in the initial study (Table 2.1) and were considered the starting point to compare imagery using “similar” conditions. Nevertheless, a satellite image that has a higher resolution should allow separating a larger variety of

land cover classes and therefore providing a larger amount of data. This information may provide a more representative picture of the real forces opposing resistance to the advance of the wave. A disadvantage of such detailed classification would be that it requires a more accurate ground-truth procedure, which may not be possible as an ex-post activity and may also reduce the speed of the overall processing and modelling. Each new land use class would require knowledge about its field characteristics i.e. height, diameter, and density of each of these new classes in order to construct a resistance coefficient to be used under the current modelling conditions.

2) For the area analysed, good quality satellite imagery (low percentage of clouds) from before the tsunami event was unfortunately not available. This hindered the possibilities of extracting LCRs from a larger number of transects to compare amongst different sources. The presence of haze on the available imagery also reduced dramatically the available transects, therefore reducing the predicting power of the tested models.

3) Higher resolution imagery, despite the increased amount of information it provides per area covered, it also inherently has a reduced total area of coverage per image. More images would then be required for this task further reducing the number of possible transects per available image. New technologies, e.g. more satellites and sensors, as well as increased image capture frequency are making imagery availability a problem of the past although increased costs remain an issue.

4) Ground truth points used for the allocation of classes on all the images were taken from the ones collected initially by the ICRAF team that visited the area in 2005. Due to the tsunami event and the socio-politic characteristics of the area before the event i.e., presence of guerrilla movements (GAM-Aceh) and governmental restrictions to movement in the province, earlier ground truth points were not available. An ideal way of reducing the error of classification would be to have more time-accurate ground truth points to be used for each of the images to be classified.

5) Object based classification software such as the one employed in this study (Definiens® developer v7.0) is becoming more and more accessible to the end users but they are still privative in terms of budget. An interesting comparison could be done by obtaining LCR coefficients through the use of different types of classifications, including pixel based supervised and unsupervised classifications as well as object based, and using these on the tsunami impact models developed by the authors.

4.7. Conclusions and recommendations

For the current research, area coverage became a critical requirement, selecting only those models that had the largest number of transects possible in order to mimic the conditions of the original study (Laso Bayas et al., 2011). This allowed increasing statistical predictive power and including different areas with dissimilar tsunami conditions. The use of mid resolution imagery could result in reduced costs, making coastal planning more feasible for local governments and decision makers. This would allow time and budget allocation to education and awareness plans as well as developing and coordinating even better early warning systems. These systems have been proven as effective means for casualty reduction, as tested on the Tohuko-Oki

seaquake in the east coast of Japan on March 2011 (Heki 2011), although many lives were still lost. Additional to early warning systems, sustainable mitigation and coastal development plans that encompass local communities and their livelihood must be prioritized. As often mentioned by several authors (Laso Bayas et al., 2011, Ziegler A.D. *et al.* 2009, Pomeroy *et al.* 2006, Cochard 2011) such planning must consider local needs and customs to obtain not only a more sustainable protection against tsunami events but also tangible benefits for the local populations depending on coastal vegetation in the short and midterm.

For future applications of the model, we believe there are several important factors that should be pondered prior to the decision of which satellite imagery should be used, as well as how it could be employed:

- 1) If higher spatial resolution imagery is used, larger number of land cover classes should be used, therefore time and resources required for this task should also be acknowledged.
- 2) Image quality (low cloud coverage) allows for larger number of observational units to be considered, increasing the predictive power of the models.
- 3) Image frequency of acquisition and costs should be considered.
- 4) Ground truthing with GPS points closer to the time of imagery data acquisition may improve sample selection and land cover classification accuracy.
- 5) Tests between land cover classification methods i.e., object vs. pixel based for the same imagery source may provide more insight on the procedures needed to process satellite imagery and produce reliable LCR coefficients.

CHAPTER 5. General Discussion

Chapter 5. General Discussion

5.1. Is coastal vegetation protecting communities?

The ongoing discussion of vegetation protecting communities or diminishing inland tsunami damage has been hindered by a lack of empirical data, both for and against a “protective” effect of coastal vegetation. In the case of mangrove forests, these have been proved as effective barriers reducing wave amplitude and its energy (Mazda 1997). Nevertheless few studies have dealt with locally existing vegetation, especially on areas where such mangrove forests did not exist. The main cases dealt with in this study refer to the west coast of Aceh and the Seychelles where, given the relative homogeneous coastal geomorphology in one case and the esthetical value of open beaches for touristic purposes, mangroves were absent. Mangrove forests exist mainly on more protected areas, e.g. coastlines with lower wave energy, which is the case for several coastlines but not for many populated areas. In areas where, either due to natural non-occurrence of mangroves or human-induced land cover change (e.g. shrimp farms and touristic beach front), the only coastal vegetation that could offer an effect against an advancing wave are the existing local land uses. These land uses comprise a mixture of tree crops such as rubber, coconut, cacao, oil palm; agricultural crops including paddy rice, agroforestry or home gardens. Home gardens include different species of fruit and timber trees, perennial and annual crops all covering different canopy layers across the planted area. Sometimes these types of vegetation may also be an association of the previously mentioned species plus forested areas with timber and non timber forest products and grasslands. These last ones could be naturally occurring or resulting from land cover changes, usually the destruction of forests in order to open cropping land. In the case of Aceh, the creation of oil palm plantations was one of the reasons for the clearing of forests, opening of new areas of which some became subsequently temporary grasslands, as observed during the course of the study.

Thus, for the current research, the question “is coastal vegetation protecting communities?” had to consider the absence of mangrove vegetation and be put in the context of livelihood and food security. This means that the coastal vegetation existent at the moment the tsunami stroke was a combination of several different species used by the local population in order to sustain their way of life, either by their products or their services such as esthetic value. The research showed that on one hand, in the case of Aceh, direct effects of vegetation providing protection against the incoming wave occurred. The existence of vegetation between the sea and the community produced a sort of “buffer effect”, allowing people to escape. Coastal vegetation reduced casualties by up to 8% when e.g. forests, were in front of settlements. Other types of tree based vegetation like agroforestry and rubber also reduced casualties by around 5%. Since no changes existed regarding the maximum distance the water reached inland, the reduction of casualties was most likely achieved through a buffer effect given by coastal vegetation. Such an effect provided time for people to escape the incoming waves. Nevertheless, when such coarse vegetation was allocated right behind these settlements then it became a trap, complicating or blocking the escape mostly by debris brought by the backwash, increasing therefore casualties and damage to buildings and structures. In the low intensity case from the Seychelles, no direct effect of vegetation was found but a hint of an indirect action of coastal vegetation shielding communities was observed. Sand dunes created and maintained by coastal

vegetation, such as *Ipomea sp.* as well as roots of different trees and plants including coconut trees, reduced the damage to buildings. The scale of destruction in both areas was completely different, with waves reaching a maximum of 25 meters in the study zone in Aceh but only 3 m on the Seychelles. This fact allowed, in the case of the Seychelles, to include additional factors such as dunes and seawalls. Seawalls showed to decrease maximum flooded distance but overall, neither a direct nor an indirect effect of vegetation was observed in the Seychelles or in Aceh regarding how far the water advanced inland. This relationship, additionally to the ones regarding vegetation effects on casualties and structural damages, shows just how much energy a tsunami carries, as explained by several authors (Annunziato and Best 2005; Geist *et al.* 2006; Stein and Okal 2006). This energy gets dissipated advancing inland through mainly gravity or built structures such as seawalls. In the case of the present study, empirical data showed vegetation having direct and indirect effects on local communities, on their members and their properties, and that is an important factor to be considered in coastal planning. The model results with regards to coastal vegetation, especially for the case of Aceh but also in the Seychelles, are quite robust. A large dataset and the use of multivariate methods considering at the same time the spatial distribution of the observations are clear advantages of the methodology used in the present study. The results observed in the current research show clearly the potential effects of coastal vegetation as possible buffer in front of communities close to the sea, but also, if located behind communities, their hindering effects for people escaping from a tsunami as well as the damage they may cause to property. Local coastal vegetation is also of paramount importance to the daily survival of the populations living and thriving on coastal areas. Consequently, planning should consider allocation of settlements with regards to the sea and their coastal vegetation in order to provide livelihood and income sources as well as mitigation and resilience in case of tsunami events.

5.2. How was the effect of coastal vegetation acknowledged?

The models used in the current research attempt to determine if coastal vegetation, being one of the forces interacting with the tsunami once the wave reaches the shore, has any measurable significant effect. The concept of gravity and friction opposing resistance to an incoming force (Shuto 1987) was used as one of the bases of the study. The effect of gravity was represented by elevation (meters above sea level) and as such was a straightforward factor to fit into the model. On the other hand friction, containing usually several factors, was mainly described by land cover resistance, chiefly given by coastal vegetation present at the moment of the tsunami. This meant that any other resistance, e.g. provided by soil friction or other factors, was incorporated as part of the friction produced by each land-use in the area it occupied inside each transect.

The possible resistance of trees and vegetation on the coast has been dubbed as generating a false sense of security (Kerr and Baird 2007) or as negligible due to the immense force that the tsunami water exerts on its advance. For the current study, a sense of proportionality rather than an accurate physical force measurement of the resistance that each land use provided was the most important factor to be considered. This meant acknowledging the existence of coastal vegetation resistance as an

additional factor influencing the effects of the tsunami, i.e. maximum flooded distance, casualties and structural damage.

In order to acknowledge efficiently plant characteristics into resistance at a landscape level an initial approach used an “ad-hoc” coefficient (Table 5.1) called the “Land Use Green Roughness” (LUGR). This coefficient was derived by comparing and combining different land uses characteristics, namely their height, branching and planting density on a relative scale from 1 to 5 (Laso Bayas 2007). Nevertheless, despite being a good starting point, the expected differences amongst different land uses were arbitrary and not quantitatively measurable, therefore not representing well enough the proportional resistance exerted by different types of vegetation.

Table 5.1. “Green Roughness” characteristics forming the Land Use Green Roughness (LUGR). Units are relative between land uses and therefore dimensionless. (From Laso Bayas 2007)

Land cover	Height	Branching	Density	LUGR
Cleared land	0	0	0	0.000
Coconut	5	1	1	0.040
Oil Palm	4	2	2	0.128
Grass	1	4	5	0.160
Rice	1	4	5	0.160
Cacao	2	3	4	0.192
Settlement	3	5	2	0.240
Shrub	2	4	4	0.256
Home Garden	4	4	4	0.512
Forest	5	4	4	0.640
Rubber	5	4	4	0.640

Consequently, for the present research a combination of easily measured field characteristics, i.e. stem height, planting density and stem diameter (shown on Eq. 2.1) yielded a better sense of proportional resistance amongst different land uses. This is due to the high correlation these vegetation characteristics have with the bending moment and consequently with the modulus of elasticity of specific materials, i.e. the force that e.g. a tree opposes to a pulling or pushing force (Peltola *et al.* 2000). Therefore, besides using field measurements that could be easily obtained, an additional advantage of this resistance measurement was that it could be used to compare against the force exerted by fixed structures e.g. settlements, through the existing relationship between modulus of elasticity and concrete compressive strength (Tomosawa and Noguchi 1993). A comparison of several values of Modulus of Elasticity (MOE) of wood, concrete and grasses reported in various studies (Peltola *et al.* 2000; Chan *et al.* 1999; Oladokun 2006, Toledo and Rincón 1997; Tomosawa and Noguchi 1993; Boen 2006) was used. A resistance coefficient using the same units as the ones reported for vegetation, i.e. $\text{m}^3 \text{ha}^{-1}$, was then derived for each of the land cover classes used in the models. Practically, this meant that buildings offered a resistance to the flow about 1.7 times higher than forests.

The use of transects as the study units in both research areas allowed for the extraction of elevation, from digital elevation models (DEM), and land cover types at the same

time. The area covered by each land use was multiplied by its specific stem height, squared stem diameter and planting density. In the case of Aceh these characteristic values were assigned specifically to each land use, no matter where these were located, due to the coarse land use maps available and the lack of more detailed pre-tsunami information. For the Seychelles, freely available high resolution pre-tsunami imagery was found using Google Earth®. Over these images, visual recognition paired with field visits, GPS points and pictures allowed for a more precise determination of the characteristics for each land use, so the values were variable depending on each location.

In the case of Aceh, faster model processing was possible due to the available land use maps and their “uniformity” of characteristics, whereas in Seychelles a more precise allocation resulted in a slower data allocation but a more precise one. In order to compare the effects of such possible “increase” of precision, more pre-tsunami satellite images were compiled and processed into land cover maps from which land cover resistance coefficients (LCRs) were extracted. The maps covered albeit only parts of the original research area in the west coast of Aceh because the higher the resolution of a sensor the lower the coverage per image. Despite the attempted enhancement, the results from Chapter 4 showed that the use of these new LCRs against the ones used originally, did not improve the tsunami prediction models. Nevertheless, the considerations mentioned, i.e. 1) use of same land cover classes independently of the sensor; 2) quality (cloud and haze cover); 3) area coverage and imagery acquisition frequency; 4) use of GPS ground truth points close to the image acquisition date; 5) software and procedures compared, must be acknowledged before stating differences on coastal vegetation resistance as observed from different sensors and at different pre-tsunami times.

5.3. What is the effect of coastal vegetation under different tsunami intensities?

Overall it could be said that coastal vegetation effects under different tsunami intensities was observed on the current research in two ways: Coastal vegetation had direct positive and negative effects depending on its location with regards to the sea and the settlement in the case of a high intensity tsunami.

In the case of a low intensity tsunami, coastal vegetation had an indirect positive effect given by physical structures (dunes) created or maintained by the plant species on the shoreline. In practical terms this may be applied as separated alternatives for each area:

For a highly exposed area, close to tsunamigenic factors such as those countries located in the Pacific “ring of fire” attention should be put with regards as to where are the settlements located, what kind of defenses exist (e.g. physical barriers, vegetation) between them and the shoreline but also how easy can the population of these communities escape. Coastal planning for these areas should emphasize then the existence of coarser vegetation in front of the settlements (e.g. agroforests). Behind these communities vegetation with a lower VR value (e.g. grasslands, agriculture, cacao) should be promoted.

For areas located farther from a tsunami generating tectonic area, e.g. the Seychelles, where tourism is an important source of income for local communities, a promotion of programs that maintain and promote the conservation of ecological niches allowing for the existence of dunes is recommended.

Nevertheless, it has to be taken into consideration that in both areas where the research was carried on, Seychelles and Aceh, distance of the settlement to the shoreline was considered as the most important factor to avoid casualties (in the case of Aceh) and structural damages (Aceh and the Seychelles) caused by the tsunami. Also, in both types of scenarios, these planning activities must be in the frame of a larger education and early warning systems, capable of alerting local population quickly and effectively.

5.4. What are the most important factors influencing the damages made by a tsunami?

In order to separate the vegetation effect from other factors, multivariate approaches were employed. These included several other variables such as topography and distance from the shoreline to the settlements.

Initial water height, i.e. the height the wave reached at the shoreline, represented all the offshore factors that shaped the tsunami energy up to its arrival to the shoreline. In all the models tested (with exception of the structural damage model in Aceh) was considered as a main factor. It was the driver of all the impacts of the tsunami inland. In the case of Aceh, it was not selected as a significant factor just because the damage was so strong on the communities close to the shore that no differences were observed.

Coastal vegetation protected but also endangered lives in Aceh depending on its location with regards to the settlement and the sea as explained before. Nevertheless, the study also showed that the main factor affecting the damages caused by the tsunami was how far the settlements were located with regards to the shoreline. For the case of Seychelles and Aceh, the closer a village was to the sea-shore, the higher the damage to buildings was. Additionally in the case of Aceh, the closer the settlement to the sea the higher the casualties were.

Topography did not have an important role in Aceh except for the maximum flooded distance model where it showed an inverse relationship. In the case of the Seychelles, the relationship was direct but this was mainly due to the funneling effect of bays that increased the maximum flooded distance reached in these areas.

Indirect effects of vegetation, i.e. dunes created and or maintained by plants roots, were not observed in Aceh. This was due mainly to the scale at which the events and land cover was considered in the models. On the contrary, in the Seychelles, where more subtle differences were visually appraised, dunes and seawalls were added as additional factors. These two factors decreased structural damages and maximum flooded distance respectively.

5.5. Do images with higher resolution and/or closest to the tsunami event provide a more accurate vegetation resistance approximation?

One of the additional efforts to fine-tune the models was the use of satellite imagery proceeding from dates closer to the tsunami event but also from a higher resolution sensor (SPOT® 10 m resolution). Given the advantages seen in the Seychelles by the use of Google Earth® imagery which allowed for a more precise allocation of vegetation resistance, it was expected that imagery from higher resolution sensors and/or closer to the event would provide a more accurate reflection of the situation in Aceh before the tsunami. The results of the models comparison were nevertheless not conclusive as discussed in chapter 4. In principle, no evidence suggesting an improvement or a better goodness of fit of the models using the new coefficients derived from the added imagery was obtained albeit a promising result for the model employing SPOT imagery was observed.

The conditions prevailing for the image acquisition from before the tsunami were less than optimal. On one hand, an almost permanent existence of cloud coverage and or haze seriously diminished the possibilities of classifying larger areas on the Landsat® 2003 and 2004 images. On the other hand, the available SPOT® 2003 and 2004 images covered only a fraction of the initial area covered by Landsat® 2002 and their overlap was even further reduced, as shown on Figures 4.1 and 4.2. Land cover classification differences also account for these problems. Despite all images being controlled for accuracy and consistency, existing differences in land uses between different years added to the problems, hindering the selection of a better model. Nevertheless, since these tests were passed, it was possible to state that the current use of mid-resolution imagery was sufficient in order to derive resistance coefficients that could account for the general resistance that vegetation opposed to the incoming water.

Given the chance of more imagery available, more observational units (transects) could have been laid, increasing the model predictive power, as recommended on chapter 4. This nevertheless, would mean more costs in terms of budget and time and therefore should be considered when applying the models on different areas. Given the results shown on chapter 4, more area covered is preferred to more spatial accuracy.

5.6. What are the advantages and disadvantages of the current developed approaches?

The study used an important combination of factors and techniques. This combination allowed developing solid statistical prediction models able to produce robust analysis.

One of the important factors was the search for adequate coefficients that could show proportional resistance between different land uses present in the transects. The currently used land cover resistance coefficients were adapted and calibrated to local vegetation existing on the area according the land use classes determined on chapter 2. These vegetation resistance coefficients employed factors measured on the field such as diameter, height and density. They provided a good yet quick idea of measurable resistance offered by different land uses present at a given time before a

tsunami event. Nevertheless, the quick response of the model sacrifices accuracy when compared to models that employ drag effects such as Darcy Weisbach and Manning's coefficients which describe more in detail all the forces interacting against a moving fluid (Freeman *et al.* 2000; Järvelä 2004). Despite the loss in accuracy, the load of data that should be collected from the field using the settings of the current study is reduced. An interesting comparison would be to incorporate the drag coefficients mentioned on the studies cited above, into the tsunami mitigation models developed on the current study and compare the model predictions and goodness of fit as to determine if a significant improvement occurs.

Another interesting factor to analyze would be the inclusion of different vegetation types. This would require also the determination of their particular resistance coefficient. For example, in the areas studied by the current research, no mangroves were found and therefore their effects as mentioned in several studies (Mazda *et al.* 1997; Kar and Kar 2005; Vermaat and Thampanya 2006; Das and Vincent 2009), did not apply to the models. The selection of different areas with different tsunami intensities and a coastal geomorphology allowing for the creation and maintenance of mangrove forests could be an interesting test for the models.

In the current study, an important step in order to develop a correct analysis of the data was to determine the most adequate type of statistical procedure to be followed. The data collected in Aceh showed several characteristics that limited the development of a traditional linear analysis: First, an initial exploratory analysis showed no indications of a non-linear tendency of the data. Second, the use of percentages of casualties derived from counts and reports from local people resulted in data distributions that followed if not a perfect, a pretty normal distribution. Nevertheless, given the strength of the tsunami, the destruction of buildings that was accounted for by the variable structural damage showed a more binomial distribution, i.e. full destruction or not destroyed. Additionally, given the nature of how the data was collected, i.e. via the use of transects laid alongside each other, spatial autocorrelation had to be considered.

Consequently the multivariate approach selected, i.e. GLIMMIX acknowledged several factors that were neglected by previous studies (Kaplan *et al.* 2009) or were reported as confused or missing by others (Kerr and Baird 2007). The approach also allowed to understand the data from a spatial point of view and to acknowledge the effect of all these factors from a sum of forces point of view (Shuto 1987). The use of a spatial variance covariance matrix included in the GLIMMIX framework allowed to use adjacent transects that, although given continuous information over neighboring straits of coast, were unavoidably related and therefore useless without such an adjustment as done in the applied models. A possible drawback in the models is the lack of inclusion of socio-economic variables as compiled in other studies (Das and Vincent 2009). These may affect for example income levels, which usually relate to the location of the settlement and often to the building structural quality. Therefore any structural damages might be influenced by these and other factors. Nevertheless, at least in the case of Aceh, a mixture of types of buildings was present when the tsunami arrived (Boen 2006) and these were acknowledged through the land cover class settlement, its resistance derived from the relationship between compressive strength and concrete (chapter 2).

An additional advantage of the currently developed models is the use of a large amount of empirical evidence, data collected from different field campaigns and sites, granting a high statistical prediction power which resulted on reliable predictions and results from the models, especially in the Aceh case (see note on appendix B). In cases where the data was reduced (chapter 3) the predictive power was notably reduced and the conclusions as well as model fits become more difficult to compare. An important consideration nevertheless, is that the significance at which the vegetation effects were selected was moderate ($\alpha=0.1$), therefore extrapolations to different areas must consider each case factors specifically and adapt the models to each circumstance, as was the case for the Seychelles (chapter 3).

In the case of the Seychelles, since dense vegetation was scarce in the affected areas, the indirect effect of vegetation reflected on the sand dunes maintained by coastal vegetation was an important added factor that further fine-tuned the model. Nevertheless, this could lead to confusion when no clear separation is done between higher resolution elevation models and the existence of sand dunes, since the latter become a part of such changes in elevation. In the case of Aceh, all topographical changes were acknowledged by the digital elevation models whereas in the Seychelles dunes were set as an additional factor.

5.7. Planning effective tsunami impact mitigation measures

Tsunami effects inland, especially casualties, were caused in the case of the event of 2004 mainly due to lack of public awareness and warning systems. A tsunami event of such a magnitude is not an everyday event (Monecke *et al.* 2008) but tsunamis like the one in March of 2011 in Japan or the one in February 2010 showed that these events can and will continue occurring. Giving the steadily growing population over the world, especially in coastal cities and towns, the danger to human life is perhaps the most important factor to be considered. Therefore, the main priority should be education campaigns that teach how to act when an earthquake occurs or when tsunami signs are visible. As show by the example from the inhabitants of the Simeulue island, knowledge saves lives. Awareness of the possibility of such an event should be the main concern of local and central governments. At the moment several campaigns of education have started in many coastal areas of the world including drills and practice on how to react when such an event occurs.

Warning systems that were triggered after this decisive event, especially in areas of the Indian Ocean where no warning system was installed are also important factors to be considered and maintained. As mentioned by Jin and Lin (2011), the warning systems must be accurate and timely, informing governments and more importantly passing the message quickly to populations at risk. These systems must be accompanied by clear signaling and evacuation routes as well as the existence of tall buildings that could withstand the waves in case higher ground is not reachable in time. Additionally, and given the low recurrence of these events, a long time planning that considers local needs and customs becomes an urgent task.

In high risk areas, like the case of countries fronting directly a fault capable of producing a big tsunami, the location of the settlements with regards to the sea should be the main priority in any coastal plan. Nevertheless, this must be weighed against

coastal vegetation and its uses. Location with regards to the sea determines access to resources such as fisheries and tourism but also coastal vegetation is a source of income, food and other goods and services. As such, coastal planning must take into consideration that the effects of different types of coastal vegetation as described on the study are highly depending on its location. Consequently, settlements should encourage the planting and maintenance of vegetation with a high resistance coefficient in between them and the shoreline, being an example agroforestry and, like in the case of Aceh, rubber plantations. They must also allow for an easy escape in case of an incoming tsunami, either through grasslands, coconut or similar low resistance vegetation located behind the settlements.

In cases where the risk of tsunami damages is limited, like it was for the 2004 event in the Seychelles, the preservation of dunes and the vegetation that maintains them should be incorporated as an asset for the tourism business, not as a problem. Places that boast natural defenses that are also esthetically nice could promote their locations as beautiful and safe. These measures however cannot be apart from proper education and population awareness, and they certainly should not have higher priority than a properly working warning system as suggested initially by some authors (Dahdouh-Guebas *et al.* 2005).

Overall, any type of land use planning should aim for sustainability in the longer term. This kind of sustainability is only obtained when the people that inhabit and use the areas and resources existing on the coast can be involved in the planning of their future villages. Such a planning should provide options for short and mid term income generation but also sudden buffering of tsunami events. At this point, the use of local species versus introduced ones may become a debate point. Nevertheless, local vegetation under a well programmed spatial arrangement provides not only an effective albeit limited buffer against a tsunami as shown in the current study, but also they offer income and subsistence means especially for communities with low income per capita. Introduced species, e.g. *Casuarina sp.* and *Pandanus sp.* could be as good as the visible short and mid-term benefits they may provide to local inhabitants. Additionally, in terms of ecological impact, the introduction of species is a difficult task and usually not a recommendable action since it may affect local food chains and ecosystems. If these species fail to provide benefits, socially, ecologically and financially, their sustainability will most likely be short lived. Most importantly, it will be taking away the opportunity of building a longer lasting spatial arrangement using local species with proven benefits for the communities where they are located.

In summary, a good planning should consider not only settlements allocation with regards to the sea but also the allocation of coastal vegetation around them. This allocation must consider its limited effect as tsunami impact buffer but also its function as livelihood provider. Such a planning should allow coastal communities to achieve higher resilience. Together with an efficient early warning system these populations will not only thrive but also recover more quickly after a tsunami and any other natural disaster affecting their cities and towns.

CHAPTER 6. References

Chapter 6. References

- Akaike, H., 1974. A new look at the statistical model identification. *IEEE Trans Automat Contr* 19, 716-723.
- Annunziato, A., Best, C., 2005. The tsunami event analysis and models. Report for the Institute for the Protection and Security of the Citizen - Joint Research Centre - European Commission, p. 42.
- Atkinson, P.M., 1997. Selecting the spatial resolution of airborne MSS imagery for small-scale agricultural mapping. *Int. J. Remote Sens.* 18, 1903-1917.
- Baird, A., Kerr, A., 2008. Landscape analysis and tsunami damage in Aceh: comment on Iverson and Prasad (2007). *Landscape Ecol.* 23, 3-5.
- Baird, A.H., Bhalla, R.S., Kerr, A.M., Pelkey, N.W., Srinivas, V., 2009. Do mangroves provide an effective barrier to storm surges? *Proc. Natl. Acad. Sci. USA* 106, E111-E111.
- Barbier, E.B., 2006. Natural barriers to natural disasters: Replanting mangroves after the tsunami. *Front. Ecol. Environ.* 4, 124-131.
- Boen, T., 2006. Observed Reconstruction of Houses in Aceh Seven Months after the Great Sumatra Earthquake and Indian Ocean Tsunami of December 2004. *Earthquake Spectra* 22, S803-S818.
- Borrero, J.C., Sieh, K., Chlieh, M., Synolakis, C.E., 2006. Tsunami inundation modeling for western Sumatra. *Proc. Natl. Acad. Sci. USA* 103, 19673-19677.
- BRR, 2005. Aceh and Nias One Year after the Tsunami: The recovery effort and way forward. Reconstruction and Rehabilitation Agency (BRR). Jakarta, Indonesia. 205 pp.
- Burnham, K.P., Anderson, D.R., 2002. Model selection and multimodel inference. A practical information theoretic approach. Springer-Verlag, New York.
- Campbell, J.B., 1996. Introduction to remote sensing. (2nd ed.). Taylor and Francis, London.
- Cazes-Duvat, V., 2001. Évaluation de la vulnérabilité des plages à l'érosion : application à l'archipel des Seychelles / A beach vulnerability index and its implementation in the islands of Seychelles. *Géomorphologie : relief, processus, environnement*, 31-40.
- Chadha, R.K., Latha, G., Yeh, H., Peterson, C., Katada, T., 2005. The tsunami of the great Sumatra earthquake of M 9.0 on 26 December 2004 - Impact on the east coast of India. *Curr. Sci.* 88, 1297-1301.

Chan, T.K., Lim, S.H., Tan, H.T.W., Lim, C.P., 1999. Variation of bending capacity along the lamina length of a grass, *Imperata cylindrica* var. *major* (Gramineae). *Ann. Bot.* 84, 703-703.

Chandrasekar, N., Immanuel, J.L., Sahayam, J.D., Rajamanickam, M., Saravanan, S., 2007. Appraisal of tsunami inundation and run-up along the coast of Kanyakumari District, India - GIS analysis. *Oceanologia* 49, 397-412.

Chatenoux, B., Peduzzi, P., 2007. Impacts from the 2004 Indian Ocean Tsunami: Analyzing the potential protecting role of environmental features. *Nat Hazards* 40, 289-304.

Chavez, P.S., Sides, S.C., Anderson, J.A., 1991. Comparison of three different methods to merge multiresolution and multispectral data- Landsat TM and SPOT panchromatic. *Photogramm. Eng. Remote Sensing* 57, 295-303.

Choi, B.H., Hong, S.J., Pelinovsky, E., 2006. Distribution of runup heights of the December 26, 2004 tsunami in the Indian Ocean. *Geophys. Res. Lett.* 33, L13601-L13601.

Cochard, R., Ranamukhaarachchi, S.L., Shivakoti, G.P., Shipin, O.V., Edwards, P.J., Seeland, K.T., 2008. The 2004 tsunami in Aceh and Southern Thailand: A review on coastal ecosystems, wave hazards and vulnerability. *Perspect. Plant Ecol. Evol. Syst.* 10, 3-40.

Cochard, R., 2011. On the strengths and drawbacks of tsunami-buffer forests. *Proceedings of the National Academy of Sciences* 108, 18571-18572.

Cohen, J., 1960. A Coefficient of Agreement for Nominal Scales. *Educational and Psychological Measurement* 20, 37-46.

Congalton, R.G., 2001. Accuracy assessment and validation of remotely sensed and other spatial information. *Int. J. Wildland Fire* 10, 321-328.

Crist, E.P., Cicone, R.C., 1984. A physically-based transformation of Thematic Mapper data---The TM Tasseled Cap. *IEEE Trans Geosci Remote Sens*, 256-263.

Crosetto, M., Tarantola, S., Saltelli, A., 2000. Sensitivity and uncertainty analysis in spatial modelling based on GIS. *Agric., Ecosyst. Environ.* 81, 71-79.

Dahdouh-Guebas, F., Jayatissa, L.P., Di Nitto, D., Bosire, J.O., Seen, D.L., Koedam, N., 2005. How effective were mangroves as a defense against the recent tsunami? *Curr. Biol.* 15, R443-R447.

Danielsen, F., Sørensen, M.K., Olwig, M.F., Selvam, V., Parish, F., Burgess, N.D., Hiraiishi, T., Karunakaran, V.M., Rasmussen, M.S., Hansen, L.B., Quarto, A., Suryadiputra, N., 2005. The Asian tsunami: A protective role for coastal vegetation. *Science* 310, 643.

- Das, S., Vincent, J.R., 2009. Mangroves protected villages and reduced death toll during Indian super cyclone. *Proceedings of the National Academy of Sciences* 106, 7357-7360.
- Dengler, L., Preuss, J., 2003. Mitigation lessons from the July 17, 1998 Papua New Guinea tsunami. *Pure and Applied Geophysics* 160, 2001-2031.
- Devall, M.S., 1992. The Biological Flora of Coastal Dunes and Wetlands. 2. *Ipomoea Pes-Caprae* (L.) Roth. *J. Coast. Res.* 8, 442-456.
- Dominey-Howes, D., Cummins, P., Burbidge, D., 2007. Historic records of teletsunami in the Indian Ocean and insights from numerical modelling. *Nat Hazards* 42, 1-17.
- EC JRC, 2005. Mapping severe damage to S.E. Asia's land cover following the Tsunami. European Commission Joint Research Centre
http://tsunami.jrc.it/Reports/Tsunami_land_cover_change.pdf. Accessed 26 June 2012
- Fleischmann, K., Héritier, P., Meuwly, C., Küffer, C., Edwards, P.J., 2003. Virtual gallery of the vegetation and flora of the Seychelles. *Bull. Geobot. Inst. ETH* 69, 57-64.
- Freeman, G.E., Rahmeyer, W.H., Copeland, R.R., 2000. Determination of resistance due to shrubs and woody vegetation. ERDC/CHLTR-00-25, U.S. Army Eng. Res. Devpt. Center, Vicksburg, MS.
- Fritz, H.M., Borrero, J.C., 2006. Somalia field survey after the December 2004 Indian Ocean tsunami. *Earthquake Spectra* 22, S219-S233.
- Gao, J., 1999. A comparative study on spatial and spectral resolutions of satellite data in mapping mangrove forests. *Int. J. Remote Sens.* 20, 2823-2833.
- Garcés, M., Caron, P., Hetzer, C., Le Pichon, A., Bass, H., Drob, D., Bhattacharyya, J., 2005. Deep infrasound radiated by the Sumatra earthquake and tsunami. *Eos, Transactions American Geophysical Union* 86, 317-317.
- Geist, E.L., Titov, V.V., Synolakis, C.E., 2006. Tsunami: Wave of Change. *Sci. Am.* 294, 56-63.
- Hagan, A.B., Spencer, T., Stoddart, D.R., Loustau-Lalanne, M., Renaud, R., 2007. Tsunami impacts in the Republic of Seychelles, Western Indian Ocean. *Atoll Res. Bull.*, 149-162.
- Hamby, D.M., 1995. A comparison of sensitivity analysis techniques. *Health Phys.* 68, 195-204.
- Hart, D.E., Knight, G.A., 2009. Geographic information system assessment of tsunami vulnerability on a dune coast. *J. Coast. Res.* 25, 131-141.

Harvey, K.R., Hill, G.J.E., 2001. Vegetation mapping of a tropical freshwater swamp in the Northern Territory, Australia: a comparison of aerial photography, Landsat TM and SPOT satellite imagery. *Int. J. Remote Sens.* 22, 2911-2925.

Heki, K., 2011. A tale of two earthquakes. *Science* 332, 1390.

Helton, J.C., 1993. Uncertainty and sensitivity analysis techniques for use in performance assessment for radioactive waste disposal. *Reliab. Eng. Syst. Saf.* 42, 327-367.

Heuvelink, G.B.M., Peter, A.B., Stein, A., 1989. Propagation of errors in spatial modelling with GIS. *Int J Geogr Inf Syst* 3, 303-322.

Iverson, L.R., Prasad, A.M., 2007a. Modeling tsunami damage in Aceh: a reply. *Landscape Ecol.* 23, 7-10.

Iverson, L.R., Prasad, A.M., 2007b. Using landscape analysis to assess and model tsunami damage in Aceh province, Sumatra. *Landscape Ecol.* 22, 323-331.

Jackson, L.E., Barrie, J.V., Forbes, D.L., Shaw, J., Mawson, G.K., Schmidt, M., 2005. Effects of the 26 December 2004 Indian Ocean tsunami in the Republic of Seychelles. *Eos. Trans. Amer. Geophys. Un.* 86, F6-F7.

Jankaew, K., Atwater, B.F., Sawai, Y., Choowong, M., Charoentitirat, T., Martin, M.E., Prendergast, A., 2008. Medieval forewarning of the 2004 Indian Ocean tsunami in Thailand. *Nature* 455, 1228-1231.

Järvelä, J., 2004. Determination of flow resistance caused by non-submerged woody vegetation. *International Journal of River Basin Management* 2, 61-70.

Jin, D., Lin, J., 2011. Managing tsunamis through early warning systems: A multidisciplinary approach. *Ocean & Coastal Management* 54, 189-199.

Joshi, L., 2006. Tree crops for environmental protection and livelihood enhancement in the tsunami-affected coastal zone in West Aceh, Indonesia, in: Broadhead, J.S., Leslie, R.N. (Eds.), *Workshop on coastal area planning and management in Asian tsunami-affected countries*. RAP publication, Bangkok, Thailand, pp. 317-318.

Kaplan, M., Renaud, F.G., Lüchters, G., 2009. Vulnerability assessment and protective effects of coastal vegetation during the 2004 Tsunami in Sri Lanka. *Nat. Hazards Earth Syst. Sci* 9, 1479-1494-1479-1494.

Kar, R., Kar, R.K., 2005. Mangroves can check the wrath of tsunami. *Curr. Sci.* 88, 675-675.

Kathiresan, K., Rajendran, N., 2005. Coastal mangrove forests mitigated tsunami. *Estuar. Coast. Shelf Sci.* 65, 601-606.

Kerr, A.M., Baird, A.H., 2007. Natural barriers to natural disasters. *Bioscience* 57, 102-103.

- Keys, A., Masterman-Smith, H., Cottle, D., 2006. The political economy of a natural disaster: The Boxing Day tsunami, 2004. *Antipode* 38, 195-204.
- Kurian, N.P., Pillai, A.P., Rajith, K., Murali Krishnan, B.T., Kalaiarasan, P., 2006. Inundation characteristics and geomorphological impacts of December 2004 tsunami on Kerala coast. *Curr. Sci.* 90, 240-249.
- Laso Bayas, J.C., 2007. Assessment of physical mitigation provided by tree crops in the 2004 Tsunami event in West Aceh-Indonesia. MSc. Thesis, Universität Hohenheim, pp. 66.
- Laso Bayas, J.C., Marohn, C., Dercon, G., Dewi, S., Piepho, H.P., Joshi, L., van Noordwijk, M., Cadisch, G., 2011. Influence of coastal vegetation on the 2004 tsunami wave impact in west Aceh. *Proc. Natl. Acad. Sci. USA* 108, 18612-18617.
- Laso Bayas J.C., Marohn C., Cadisch G., 2013. Tsunami in the Seychelles: Assessing mitigation mechanisms. *Ocean Coast Manage.* 86, pp. 42–52.
- Latief, H., Hadi, S., Braatz, S., Fortuna, S., Broadhead, J., Leslie, R., 2007. The role of forests and trees in protecting coastal areas against tsunamis, in: Braatz, S., Fortuna, S., Broadhead, J. (Eds.), *Regional Technical Workshop on Coastal Protection in the Aftermath of the Indian Ocean Tsunami What Role for Forests Trees?* FAO, Rome, pp. 5-32.
- Lay, T., Kanamori, H., Ammon, C.J., Nettles, M., Ward, S.N., Aster, R.C., Beck, S.L., Bilek, S.L., Brudzinski, M.R., Butler, R., Deshon, H.R., Ekstrom, G., Satake, K., Sipkin, S., 2005. The great Sumatra-Andaman earthquake of 26 December 2004. *Science* 308, 1127-1133.
- Liu, P.L.F., Lynett, P., Fernando, H., Jaffe, B.E., Fritz, H., Higman, B., Morton, R., Goff, J., Synolakis, C., 2005. Observations by the International Tsunami Survey Team in Sri Lanka. *Science* 308, 1595.
- Mascarenhas, A., Jayakumar, S., 2008. An environmental perspective of the post-tsunami scenario along the coast of Tamil Nadu, India: Role of sand dunes and forests. *J. Environ. Manage.* 89, 24-34.
- May, A.M.B., Pinder Iii, J.E., Kroh, G.C., 1997. A comparison of Landsat Thematic Mapper and SPOT multi-spectral imagery for the classification of shrub and meadow vegetation in northern California, USA. *Int. J. Remote Sens.* 18, 3719-3728.
- Mazda, Y., Magi, M., Kogo, M., Phan Nguyen, H., 1997. Mangroves as a coastal protection from waves in the Tong King Delta, Vietnam. *Mangroves Salt Marshes* 1, 127-135.
- McAdoo, B.G., Dengler, L., Prasetya, G., Titov, V., 2006. [bold Smong]: How an Oral History Saved Thousands on Indonesia's Simeulue Island during the December 2004 and March 2005 Tsunamis. *Earthquake Spectra* 22, S661.

- Menke, W., Abend, H., Bach, D., Newman, K., Levin, V., 2006. Review of the source characteristics of the Great Sumatra-Andaman Islands earthquake of 2004. *Surveys in geophysics* 27, 603-613.
- Monecke, K., Finger, W., Klarer, D., Kongko, W., McAdoo, B.G., Moore, A.L., Sudrajat, S.U., 2008. A 1,000-year sediment record of tsunami recurrence in northern Sumatra. *Nature* 455, 1232-1234.
- Moody, A., Woodcock, C.E., 1994. Scale-dependent errors in the estimation of land-cover proportions: Implications for global land-cover datasets. *Photogramm. Eng. Remote Sensing* 60, 585-596.
- Muleta, M.K., Nicklow, J.W., 2005. Sensitivity and uncertainty analysis coupled with automatic calibration for a distributed watershed model. *Journal of Hydrology* 306, 127-145.
- Munichika, C.K., Warnick, J.S., Salvaggio, C., Schott, J.R., 1993. Resolution enhancement of multispectral image data to improve classification accuracy. *Photogramm. Eng. Remote Sensing* 59, 67-72.
- Obura, D., 2006. Impacts of the 26 December 2004 tsunami in Eastern Africa. *Ocean & Coastal Management* 49, 873-888.
- Obura, D., Abdulla, A., 2005. Assessment of Tsunami Impacts on the Marine Environment of the Seychelles. IUCN/UNEP, pp. 1-17.
- Okal, E.A., Synolakis, C.E., 2008. Far-field tsunami hazard from mega-thrust earthquakes in the Indian Ocean. *Geophys. J. Int.* 172, 995-1015.
- Oladokun, M., 2006. Structural development and stability of rice *Oryza sativa* L. var. Nerica 1. *J. Exp. Bot.* 57, 3123-3130.
- Olwig, M.F., Sørensen, M.K., Rasmussen, M.S., Danielsen, F., Selvam, V., Hansen, L.B., Nyborg, L., Vestergaard, K.B., Parish, F., Karunakaran, V.M., 2007. Using remote sensing to assess the protective role of coastal woody vegetation against tsunami waves. *Int. J. Remote Sens.* 28, 3153-3169.
- Paul, A., Rahman, M., 2006. Cyclone Mitigation Perspectives in the Islands of Bangladesh: A Case of Sandwip and Hatia Islands. *Coast. Manage.* 34, 199 - 215.
- Peltola, H., Kellomäki, S., Hassinen, A., Granander, M., 2000. Mechanical stability of Scots pine, Norway spruce and birch: an analysis of tree-pulling experiments in Finland. *For. Ecol. Manage.* 135, 143-153.
- Pomeroy, R.S., Ratner, B.D., Hall, S.J., Pimoljinda, J., Vivekanandan, V., 2006. Coping with disaster: Rehabilitating coastal livelihoods and communities. *Mar. Policy* 30, 786-793.

Schabenberger, O., 2005. Introducing the GLIMMIX procedure for generalized linear mixed models, Proceedings of the Thirtieth Annual SAS Users Group International Conference. Cary, NC: SAS Institute Inc.

Shuto, N., 1987. The effectiveness and limits of tsunami control forests. *Coast. Eng. Jpn.* 30, 143-153.

Small, C., Nicholls, R.J., 2003. A global analysis of human settlement in coastal zones. *J. Coast. Res.*, 584-599.

Stein, S., Okal, E.A., 2005. Speed and size of the Sumatra earthquake. *Nature* 434, 581-582.

Synolakis, C.E., Bernard, E.N., 2006. Tsunami science before and beyond Boxing Day 2004. *Philosophical Transactions of the Royal Society A: Mathematical, Physical and Engineering Sciences* 364, 2231-2265.

Szczucinski, W., Chaimanee, N., Niedzielski, P., Rachlewicz, G., Saisuttichai, D., Tepsuwan, T., Lorenc, S., Siepak, J., 2006. Environmental and geological impacts of the 26 December 2004 tsunami in coastal zone of Thailand - Overview of short and long-term effects. *Pol. J. Environ. Stud* 15, 793-810.

Takara, K., Kojima, T., 1996. GIS-aided land cover classification assessment based on remote sensing images with different spatial resolutions. *IAHS Publications-Series of Proceedings and Reports-Intern Assoc Hydrological Sciences* 235, 659-668.

Tanaka, N., 2009. Vegetation bioshields for tsunami mitigation: review of effectiveness, limitations, construction, and sustainable management. *Landsc. Ecol. Eng.* 5, 71-79.

Tanaka, N., Sasaki, Y., Mowjood, M.I.M., Jinadasa, K.B.S.N., Homchuen, S., 2007. Coastal vegetation structures and their functions in tsunami protection: Experience of the recent Indian Ocean tsunami. *Landsc. Ecol. Eng.* 3, 33-45.

Titov, V., Rabinovich, A.B., Mofjeld, H.O., Thomson, R.E., González, F.I., 2005. The global reach of the 26 December 2004 Sumatra tsunami. *Science* 309, 2045-2048.

Toledo, E., Rincón, C., 1997. Utilización industrial de nuevas especies forestales en Perú. *Revista Forestal Centroamericana* 21, 31-36.

Tomosawa, F., Noguchi, T., 1993. Relationship between compressive strength and modulus of elasticity of high-strength concrete, Proceedings of the Third International Symposium on Utilization of High-Strength Concrete, pp. 1247-1254.

Tucker, C.J., 1979. Red and photographic infrared linear combinations for monitoring vegetation. *Remote Sens. Environ.* 8, 127-150.

UNEP, 2005. After the tsunami: rapid environmental assessment report. United Nations Environment Programme, Nairobi, Kenya, p. 140.

Vermaat, J.E., Thampanya, U., 2006. Mangroves mitigate tsunami damage: a further response. *Estuar. Coast. Shelf Sci.* 69, 1–3–1–3.

Yocky, D.A., 1996. Multiresolution Wavelet Decomposition Image Merger of Landsat Thematic Mapper and SPOT Panchromatic Data. *Photogramm. Eng. Remote Sensing* 62, 1067-1074.

Young, E., 2006. Is replanting coasts the way to protect against tsunamis? *New Sci.* 189, 14-14.

Ziegler, A.D., Wong, P.P., Grundy-Warr, C., 2009. Still Vulnerable to Killer Tsunamis. *Science* 326, 1188-1189.

Summary

A tsunami causes several effects once it reaches inland. Infrastructure damage and casualties are two of its most severe consequences being mostly determined by seaquake intensity and offshore properties. Nevertheless, once on land, the energy of the wave is attenuated by gravity (elevation) and friction (land cover). Despite being promoted as 'bio-shields' against wave impact, proposed tree-belt effects lacked quantitative evidence of their performance in such extreme events, and have been criticized for creating a false sense of security. The current study analyzed some of the land uses in sites affected by the 2004 tsunami event, especially in coastal areas close to the coast of Indonesia, more specifically on the west coast of Aceh, Sumatra as well as on the Seychelles. Using transects perpendicular to the coast, the influence of coastal vegetation on the impact of the 2004 tsunami, particularly cultivated trees, was modeled. A spatial statistical model using a land cover roughness coefficient to account for the resistance offered by different land uses to the wave advance was developed. The coefficient was built using land cover maps, land use characteristics (stem diameter, height, and planting density), as well as a literature review. The spatial generalized linear mixed models used showed that while distance to coast was the dominant determinant of impact (casualties and infrastructure damage), the existing coastal vegetation in front of settlements also significantly reduced casualties, in the case of Aceh, by an average of 5%. Despite this positive effect of coastal vegetation in front of a settlement, it was also found that dense vegetation behind villages endangered human lives and increased structural damage in the same case, most likely due to debris carried by the backwash. The models initially developed in Aceh were adapted and tested for the effects that the same tsunami event caused in the Seychelles, where the intensity of the event was a tenth of that in Aceh. These new models suggested no direct effect of coastal vegetation, but they indicated that vegetation maintained dunes decreased the probability of structural damage. Additionally, using satellite imagery with higher resolution than that of the first study and/or from different years before the tsunami, corresponding land roughness coefficients were developed and tested with the existing models. The new models showed no signs of further increase of goodness of fit (AIC). Nevertheless, weather conditions at the acquisition dates as well as coverage and lack of image availability diminished the predictive power of these models. Overall, more than advocating for or against tree belts, a sustainable and effective coastal risk management should be promoted. This planning should acknowledge the location (relative to the sea) of settlements as the most important factor for future coastal arrangements. Nevertheless, it should also consider the possible direct and indirect roles of coastal vegetation, determined by its spatial arrangement as shown in the study models. Sustainability of these measures would only occur when coastal vegetation is regarded as a livelihood provider rather than just as a bio-shield. Practical examples could include, e.g. rubber plantations or home gardens in front of settlements, while leaving escape routes or grasslands and coconut plantations behind these. Therefore, the enforcement of educational programs, the setup and maintenance of effective warning systems and the adequate spatial allocation of coastal vegetation bringing tangible short and mid term benefits for local communities, as well as its adaption to local customs should be considered.

Zusammenfassung

Tsunamis können beim Erreichen besiedelter Landflächen schwerste Schäden an Menschen und Infrastruktur verursachen. Die Intensität eines Tsunamis an der Küstenlinie wird wesentlich von der Stärke des verursachenden Seebebens und der Bathimetrie des Meeresgrunds beeinflusst. An Land wird die Intensität der Wellen dann im Wesentlichen durch die Schwerkraft (als Funktion der Topographie) und Reibung (Funktion der Vegetation) abgeschwächt. Folglich wird die Pflanzung von Baumgürteln als Schutzschild gegen Tsunamis vielerorts gefördert, obwohl bisher keine quantitativen Belege für ihren tatsächlichen Nutzen bei großen Tsunamis vorliegen. In diesem Fall könnten Baumpflanzungen Bewohnern von Küstengegenden sogar ein trügerisches Gefühl von Sicherheit vermitteln. In der vorliegenden Arbeit wurden die Auswirkungen verschiedener Landnutzungen auf Tsunamischäden an einigen durch den großen Tsunami von 2004 betroffenen Orten an der Westküste von Aceh, Sumatra, Indonesien, und den Seychellen untersucht. Mit Hilfe von orthogonal zur Küste verlaufenden Transekten wurde der Einfluss der Küstenvegetation, insbesondere von Bäumen, auf die Auswirkungen des Tsunamis 2004 modelliert. Geostatistische Modelle (generalised linear mixed models - GLMM) wurden entwickelt, um den Einfluss verschiedener Vegetationstypen auf die Reichweite der Welle, sowie Opferzahlen und Schäden an Wohngebäuden, zu schätzen. In die Modelle flossen Topographie, Landnutzung und Werte des Reibungswiderstands verschiedener Landnutzungen, geschätzt aus Stammdurchmesser, Höhe und Planzdichte, ein. Mittels der GLMM wurde die Entfernung einer Siedlung zur Küste als wichtigster determinierender Faktor für Todesfälle und Schäden an Gebäuden durch den Tsunami ermittelt. Daneben zeigte sich jedoch auch, dass dichte Küstenvegetation zwischen Siedlungen und der Küste in Aceh die Anzahl der Todesfälle signifikant (im Durchschnitt um 5%) reduzierte. Im Gegensatz zu dem positiven Effekt der Küstenvegetation zwischen Siedlungen und der Küstenlinie wurden bei dichter Vegetation landeinwärts der Siedlungen erhöhte Opferzahlen und Schäden an Gebäuden festgestellt, was vermutlich auf den Transport von Trümmern in den ins Meer zurückströmenden Wellen zurückzuführen ist. Die Modelle, ursprünglich entwickelt für Aceh, wurden im Folgenden angepasst und auf die Auswirkungen desselben Tsunamis in den Seychellen getestet. Dort betrug die Intensität der Wellen ein Zehntel derer in Aceh und küstennahe Schutzwälle sowie Dünen verminderten die Auswirkungen des Tsunamis. Die angepassten Modelle ergaben keine direkten Auswirkungen der Küstenvegetation auf Tsunamischäden in den Seychellen, allerdings deuten die Ergebnisse darauf hin, dass Schäden an Gebäuden durch Dünen reduziert werden konnten. Da die Dünen durch Vegetation wesentlich vor Erosion geschützt werden, besteht hier zumindest eine indirekte Auswirkung der Pflanzendecke. Zusätzlich wurde für die Modelle im Fall Aceh ein weiterer Verbesserungsansatz getestet. Mit Hilfe hochauflösender Satellitenbilder aus verschiedenen Jahren vor dem Tsunami konnten verbesserte Reibungswiderstands-Koeffizienten entwickelt und anhand der existierenden Modelle getestet werden. Die neuen Koeffizienten führten allerdings nicht zu einer signifikanten Verbesserung der Vorhersagegenauigkeit der Modelle, was jedoch teilweise auch ungünstigen Wetterverhältnissen zum Zeitpunkt der Luftaufnahmen und lückenhafter Datenlage geschuldet war.

Die Ergebnisse der vorliegenden Arbeit legen nahe, dass nachhaltige und effektive Maßnahmen zur Risikoverminderung in gefährdeten Küstenregionen verstärkt werden sollten. Dabei sollte die Entfernung der Siedlungen zum Meer als wichtigster Faktor

für zukünftige Küstenschutzmaßnahmen berücksichtigt werden. Zusätzlich sollten mögliche direkte und indirekte Auswirkungen der küstennahen Vegetation berücksichtigt werden. Die Akzeptanz und Nachhaltigkeit solcher Maßnahmen kann nur erreicht werden, wenn Küstenvegetation nicht ausschließlich als Schutzschild, sondern als Teil der Lebensgrundlage der Bevölkerung dient. In der Praxis könnten zum Beispiel Kautschukplantagen oder Hausgärten zwischen Siedlungen und Küste angelegt werden, während hinter den Siedlungen Fluchtwege, Weiden und Kokosnussplantagen integriert werden könnten. Die Förderung von Schulungsprogrammen für die Bevölkerung, die Entwicklung effektiver Warnsysteme, und eine den örtlichen Begebenheiten angepasste räumliche Anordnung der Küstenvegetation können konkrete kurz- und mittelfristige Vorteile für die lokale Bevölkerung bringen.

Resumen

Cuando un tsunami llega a la costa produce varias secuelas. Víctimas y daños materiales son dos de estas consecuencias, determinadas principalmente por la intensidad del maremoto y las características específicas del fondo oceánico. Sin embargo, una vez que las olas están en tierra firme, su energía es atenuada por la fuerza de gravedad (altura sobre el nivel del mar) y la fricción (usos del suelo). Franjas costeras plantadas con árboles han sido propuestas como “bio-escudos” protegiendo a las comunidades detrás de ellas de los efectos de un tsunami. Tales planes han sido criticados por algunos autores debido a que no existe evidencia cuantitativa sobre su desempeño en casos tan extremos y por ende, puede estar creando una falsa sensación de seguridad. El presente estudio analizó algunos de los usos del suelo en áreas costeras afectadas por el tsunami ocurrido en el 2004 en el océano Índico, especialmente en la costa oeste de la provincia de Aceh, en el norte de Sumatra, Indonesia, así como en las principales islas de la nación archipiélago de las Seychelles. Se desarrolló un modelo estadístico espacial que considerara la influencia de la vegetación costera, particularmente plantaciones arbóreas, en el impacto del tsunami. El modelo utilizó transectos perpendiculares a la línea costera para extraer coeficientes de resistencia al avance de las olas, específicos para cada uso del suelo. Estos coeficientes fueron construidos utilizando mapas de uso del suelo, características específicas de cada tipo de cobertura del suelo (diámetro del tallo/tronco, altura y densidad de siembra) así como una revisión de literatura. Los modelos lineales generalizados espaciales utilizados para el análisis de los datos mostraron que, a pesar de que la distancia entre la costa y la población fue el factor más determinante en los daños causados por el tsunami, la vegetación costera redujo en promedio 5% de las víctimas fatales en el caso de Aceh. A pesar de que la vegetación ubicada entre la costa y la población mostrara este efecto positivo, la vegetación existente en los primeros 500 m detrás de las poblaciones analizadas puso en riesgo vidas humanas e incrementó los daños materiales a viviendas y estructuras. Esto debido lo más probablemente a la generación de escombros que fueron llevados por la resaca. Los modelos desarrollados originalmente en Aceh fueron adaptados y aplicados a los efectos causados por el mismo tsunami en las Seychelles, donde su intensidad fue diez veces menor que en Aceh. Estos nuevos modelos indicaron que no existió ningún efecto directo de la vegetación costera, sin embargo, también mostraron que las dunas mantenidas y/o creadas por la vegetación costera redujeron las probabilidades de daños materiales. Adicionalmente, y mediante el uso de imágenes de satélite de mayor resolución espacial que la de la imagen utilizada inicialmente así como procedentes de fechas más próximas al tsunami del 2004, se desarrollaron nuevos coeficientes de resistencia para cada uno de los distintos usos del suelo para el caso de Aceh. Estos coeficientes fueron introducidos en los modelos existentes para su análisis mas no se observó ninguna señal de mejora en el grado de ajuste (AIC). Sin embargo, el poder predictivo de los modelos se redujo sustancialmente debido a la reducción de observaciones. Esta reducción se dio por las condiciones climáticas reinantes al momento de la adquisición de las imágenes de satélite así como la poca disponibilidad de imágenes de este período y, en el caso de las imágenes de alta resolución espacial, la reducida cobertura de área que provee cada imagen. En conjunto, más que promover o no el uso de franjas arbóreas se debe promover el manejo y la planeación de riesgos costeros. Este tipo de planes debe considerar la distancia a la cual las poblaciones se encuentran con relación al mar pero también el rol directo o indirecto que juega la vegetación costera, dependiendo de su

ubicación con respecto a la población considerada. Además, la sostenibilidad de cualquier plan que determine la ubicación de estos recursos costeros dependerá de que se considere a la vegetación costera no solamente como protección costera limitada sino también como proveedora de bienes y servicios para el sustento de las poblaciones locales. Un ejemplo práctico podría incluir, como en el caso de Aceh, plantaciones de caucho o sistemas agroforestales localizados en frente de las poblaciones en riesgo y simultáneamente la existencia de rutas de escape detrás de estas facilitadas por usos del suelo como pastizales, agricultura y plantaciones de coco. Consecuentemente se debe considerar la instalación de programas de concientización y educación, el establecimiento y mantenimiento de sistemas de alerta temprana efectivos así como la ubicación espacial adecuada de la vegetación costera adaptada a las costumbres locales y beneficiosa a corto y mediano plazo.

Appendix A: Supplementary information for chapter 2

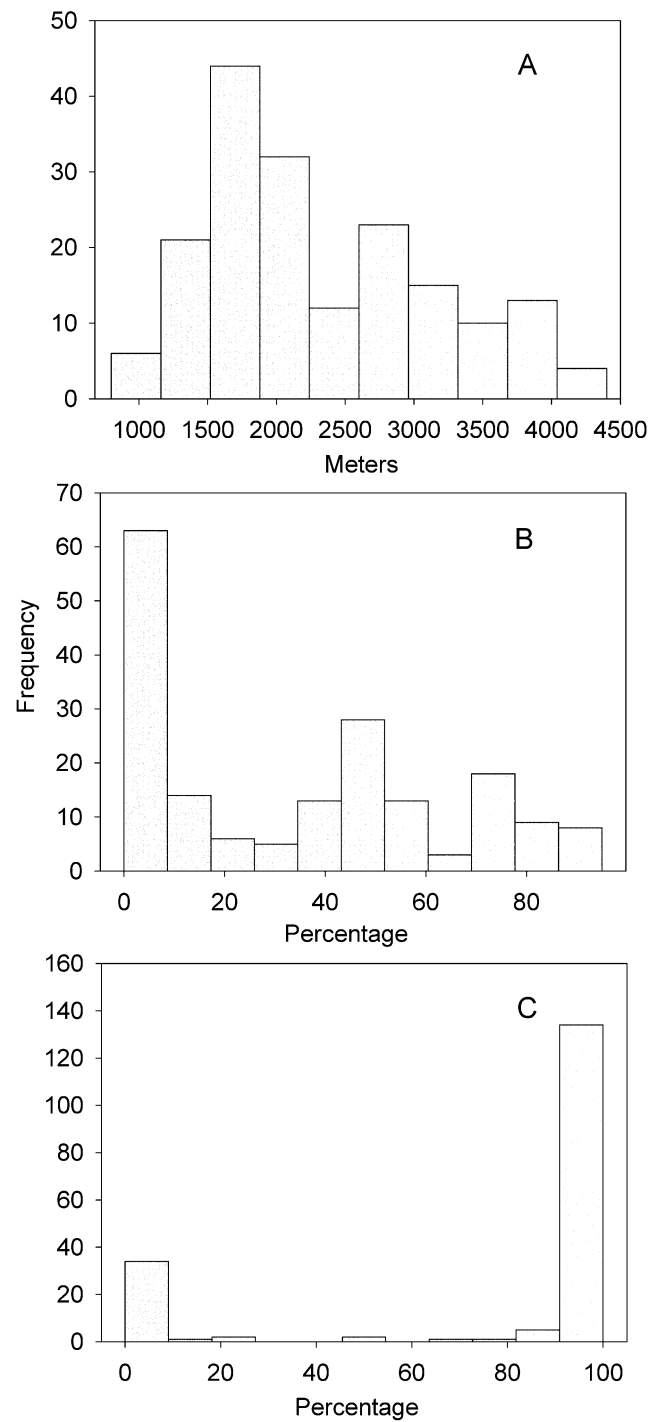


Figure A1. Data distribution for the dependent variables (A) maximum flood distance (MD), (B) casualties (CASU) and (C) structural damage (STD)

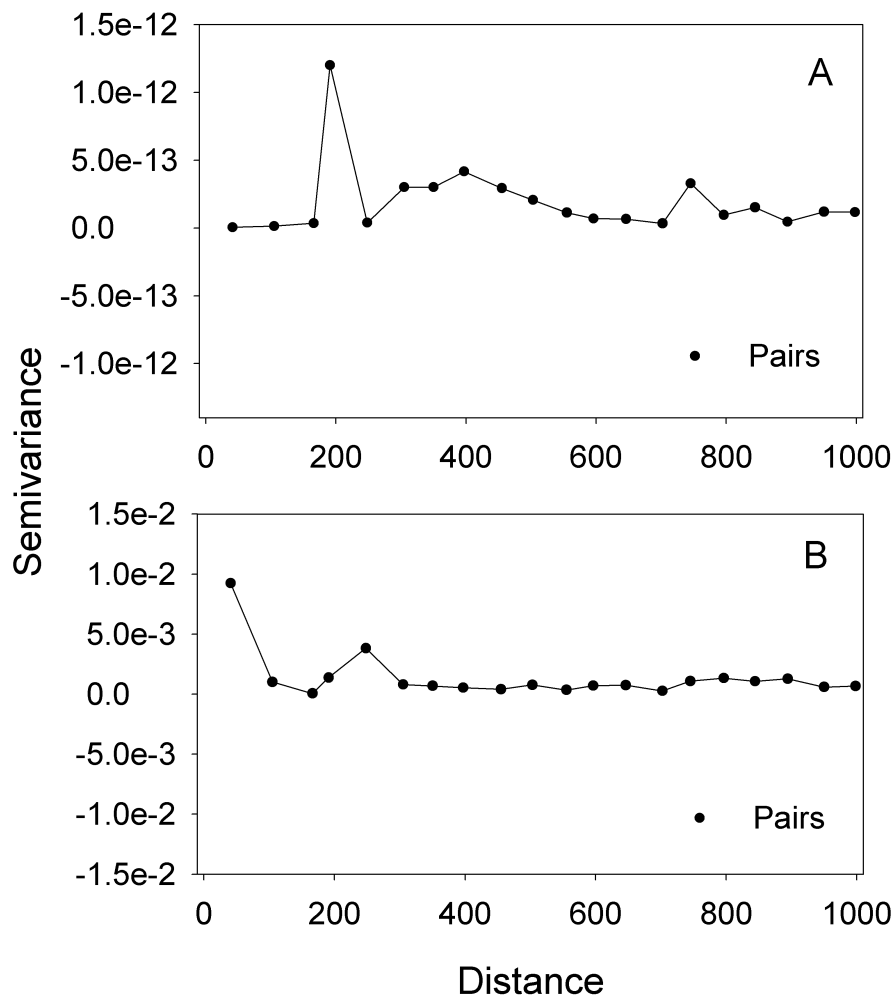


Figure A2. Experimental semi-variograms for the (A) maximum flood distance (MD01) and (B) casualties (CASU01) models (Pairs > 30).

Table A1. Casualties models (CASU) showing standardized regression coefficients and their corresponding p values. Generalized linear mixed model using a spatial variance-covariance matrix as a random term. Estimation technique: Maximum Likelihood (ML). N=180.

Intercept	IWH-s	E_F-s	D-s	LCR_F-s	LCR_{B5}-s	AIC*
0.35 ± 0.05 (<i>p</i> <0.001)						-75.1
0.38 ± 0.03 (<i>p</i> <0.001)	1.10 ± 0.41 (<i>p</i> =0.009)	-0.19 ± 0.21 (<i>p</i> =0.354)	-2.40 ± 0.34 (<i>p</i> <0.001)			-116.1
0.38 ± 0.03 (<i>p</i> <0.001)	1.18 ± 0.41 (<i>p</i> =0.006)	-0.23 ± 0.21 (<i>p</i> =0.265)	-2.40 ± 0.34 (<i>p</i> <0.001)	-0.35 ± 0.21 (<i>p</i> =0.096)		-116.8
0.38 ± 0.04 (<i>p</i> <0.001)	1.14 ± 0.46 (<i>p</i> =0.018)	-0.19 ± 0.21 (<i>p</i> =0.368)	-2.40 ± 0.36 (<i>p</i> <0.001)	-0.38 ± 0.21 (<i>p</i> =0.067)	0.28 ± 0.17 (<i>p</i> =0.101)	-117.3

Notes: Independent variables used in the models were standardized (suffix ‘-s’) to variance=1, mean=0.

IWH-s = initial water height (standardized), **E_F-s** = maximum elevation at the settlement level (standardized), **D-s** = distance from the shoreline to the settlement (standardized) **LCR_F-s** = weighted average land cover roughness in front of the settlement (standardized) and **LCR_{B5}-s** = weighted average land cover roughness from the settlement up to 500 m behind (standardized).

*= Akaike Information Criterion: lower value = better fit.

Table A2. Structural damage models (STD) showing standardized regression coefficients and their corresponding p values. Generalized linear mixed model using a spatial variance-covariance matrix as a random term. Estimation technique: Pseudo Likelihood (PL). N=180.

Intercept	IWH-s	E_F-s	D-s	LCR_F-s	LCR_{B5}-s	X²/Df*
2.58 ± 0.38 (<i>p</i> <0.001)	3.15 ± 3.68 (<i>p</i> =0.394)	-5.02 ± 3.18 (<i>p</i> =0.119)	-23.72 ± 4.34 (<i>p</i> <0.001)			0.98
2.58 ± 0.39 (<i>p</i> <0.001)	3.14 ± 3.68 (<i>p</i> =0.395)	-5.03 ± 3.19 (<i>p</i> =0.119)	-23.74 ± 4.37 (<i>p</i> <0.001)	-0.25 ± 5.30 (<i>p</i> =0.963)		0.99
2.66 ± 0.41 (<i>p</i> <0.001)	3.45 ± 3.73 (<i>p</i> =0.358)	-4.95 ± 3.35 (<i>p</i> =0.143)	-22.42 ± 4.40 (<i>p</i> <0.001)	0.13 ± 5.14 (<i>p</i> =0.981)	6.90 ± 3.62 (<i>p</i> =0.061)	1.07

Notes: Independent variables used in the models were standardized (suffix ‘-s’) to variance=1, mean=0.

IWH-s = initial water height (standardized), **E_F-s** = maximum elevation at the settlement level (standardized), **D-s** = distance from the shoreline to the settlement (standardized) **LCR_F-s** = weighted average land cover roughness in front of the settlement (standardized) and **LCR_{B5}-s** = weighted average land cover roughness from the settlement up to 500 m behind (standardized).

*= Chi square / degrees of freedom

Table A3. Individual explanatory power of the variables used in the maximum flood distance model (MD). Generalized linear mixed procedure using a spatial spherical covariance matrix as a random term. Estimation technique: Maximum Likelihood (ML). N=180.

Variable	Std. Reg. Coeff.	p value	AIC*
IWH-s - Initial water height at shoreline	0.61 ± 0.31	0.054	-494.2
E_T-s - Maximum elevation over the whole transect	-0.32 ± 0.09	0.001	-499.4
LCR_T-s – Weighted average land cover roughness in the transect (up to maximum flood distance)	0.05 ± 0.06	0.429	-484.9

Notes: Independent variables used in the models were standardized (suffix ‘-s’) to variance=1, mean=0.

*=Akaike Information Criterion: lower value = better fit

Table A4. Individual explanatory power of the variables used in the casualties model (CASU). Generalized linear mixed procedure using a spatial spherical covariance matrix as a random term. Estimation technique: Maximum Likelihood (ML). N=180.

Variable	Std. Reg. Coeff.	p value	AIC*
IWH-s - Initial water height at shoreline	1.03 ± 0.59	0.098	-76.0
D-s - Distance from the shoreline to the settlement	-2.73 ± 0.38	<0.001	-115.0
E_F-s - Maximum elevation at the settlement level	-0.41 ± 0.22	0.072	-76.5
LCR_F-s – Weighted average land cover Roughness in front of the settlement	-0.36 ± 0.23	0.115	-75.6
LCR_{B5}-s – Weighted average land cover roughness from the settlement up to 500 m behind	0.43 ± 0.19	0.027	-78.3

Notes: Independent variables used in the models were standardized (suffix ‘-s’) to variance=1, mean=0.

*=Akaike Information Criterion: lower value = better fit

Appendix B: Supplementary information for chapter 3



Figure B1. Vegetation maintained sand dunes along the coastline Left: Small dune (less than 1 meter, class 1), lower levels at both sides (front and behind) of it. Right: No dune area (class 0), road at the same height as the end of the beach.



Figure B2. Example of beach vegetation creating/maintaining dunes: (1) Bois Blanc (*Herrnandia sinora*), (2) Takamaka (*Calophyllum inophyllum*), (3) Coconut trees (*Cocos nucifera*), and (4) Beach Morning glories (*Ipomoea pes-caprae*). Anse Kerlan, Praslin.



Figure B3. Example of beach vegetation creating/maintaining dunes and surrounding: (1) Bois Blanc (*Herrnandia sinora*), (2) Mango trees (*Mangifera indica*), and (3) Voloutye (*Scaevola sericea*). Anse aux Pins, Mahé.



Figure B4. Example of beach vegetation creating/maintaining dunes: (1) Casuarina (*Casuarina equisetifolia*), (2) young Coconut trees (*Cocos nucifera*), and (3) Voloutye (*Scaevola sericea*). Grand Anse, Praslin.